EVALUATION OF GEOLOGICAL CONDITIONS ALONG THE PROPOSED NORTHERN COLLECTOR TUNNEL USING ELECTRICAL RESISTIVITY TOMOGRAPHY METHOD IN GATANGA, KENYA.

By:
Kamau Samuel Runo
I56/80912/2012

This dissertation has been submitted to the Department of Geology in partial fulfillment of the requirements for the Degree of Master of Science in Engineering Geology, the University of Nairobi

August 2015

DECLARATION

I hereby declare that the thesis is my original work under the supervision of Dr. Zacharia Kuria and Dr. Edwin Dindi, Department of Geology, University of Nairobi during the year 2015 as part of Masters of Science program in Engineering Geology. I further declare that this work has not been submitted to any other university or institution for the award of any degree or diploma and all sources of material used for the thesis have been duly acknowledged.

Kamau Samuel Runo.
I56/80912/2012

Signature…… Date.....

This desertation has been submited for examination with our knowledge as university supervisors

Supervisors

Dr.Zacharia Njuguna Kuria
Senior lecturer,
Department of Geology,School of Physical Sciences,
University of Nairobi

Signature..... Date.....

Dr. Edwin W. Dindi
Senior lecturer,
Department of Geology, School of Physical Sciences,
University of Nairobi

Signature..... Date.....

PLAGIARISM

This dissertation is the result of desktop data analysis of previous work done and field investigation carried out in Gatanga area between 2013 and 2015. Where other peoples work has been used, they have been acknowledged and cited in the reference section.

DEDICATION

To all my family members.

ABSTRACT

The proposed Northern collector Tunnel is located in Gatanga area within the southern slopes of the Abardare ranges in Kenya. Geologically, the area is composed of volcanic rocks comprising of the basalts and the pyroclastics. The mode of formation and deposition of these rocks make them prone to changes due to the dynamics of the earth and therefore influence on their mechanical behavior. Success of any tunnel project during implementation and after commissioning is influenced by the geological conditions. This study set out to investigate the geological conditions at the proposed tunnel location, 800 m length ERT Profile was carried out along the tunnel and supported by other short profiles at the valleys in each site and the results analyzed. The choice of ERT method was dictated by its widely known applicability in investigation of buried objects and structures, and also in exploration for underground water. The results of the study have shown that the upper most rocks have weathered to red brown soils. The basaltic agglomerates are the main rocks in the area and are overlain by pyroclastic rocks of varying thickness.

Although no geological structures that are clearly observed at the earth's surface the resistivity contrast between the rocks and the results from drill core logs reveals highly fractured rocks under the ground and these fractures are traced to correspond to the steep slopes at some sections along the tunnel route. The study also revealed ground water occurrence in all sections of the tunnel. The study recommends for the mitigation measures through pre-installation of horizontal drainage pipes below the adits to invert pore water pressures reducing seepage ingress and maintenance of relatively low hydraulic gradient compared with critical gradient for piping failure.

ACKNOWLEDGEMENT

I would like to especially thank my supervisors, Dr. Zacharia Njuguna Kuria and Dr. Edwin W. Dindi, for their encouragement and very helpful advice to me throughout my research. I have been very fortunate that they were my supervisors, and have learned many lessons in working under their guidance and leadership that I will remember for an extremely long time.

Special thanks to the entire staff in the department of Geology under the chairmanship of Dr. Ichangi, they ensured the environment was good for the research and were ready to assist when called upon.

I also acknowledge with gratitude the support of Engineers Kamau and Kiprono of Athi Water Service Board and Madam Lucy of Water Resources Management Authority (Murang'a Sub-region) for their co-operation and input during data collection.

I also owe a lot of thanks to my fellow classmates, Mr. Julius Odida and Mr. Leslie Dullo for the comradeship we experienced and for the countless useful conversations we had, often as we solved problems together.

Finally I would like to thank all my friends and family for their support and kindness to me throughout my research and during the writing this dissertation. There is one person to whom I am eternally grateful. She stayed with me throughout and her love and encouragement for me never stopped. We started as firm friends and she became my wife. To her I dedicate this dissertation. Thank you Mary.

TABLE OF CONTENT

LIST OF FIGURES

LIST OF TABLES

LIST OF ABBREVIATIONS

1- D - One Dimension

2-D - Two Dimension

AD - After death

ASL - Above sea level

ALT - Altitude

BC - Before Christ

Bgl - Below ground Level

CVES - Continuous Vertical Electrical Sounding

DC - Direct Current

ERT - Electrical Resistivity Tomography

HS - Horizontal Scale

ITCZ - Inter tropical Convergent Zone

KNBS - Kenya National Bureau of Statistics

Kms - Kilometers

Kshs - Kenya Shillings

MWI - Ministry of Water and Irrigation

NEMA - National Environment Management Authority

RI - Resistivity Imaging

TBM - Tunnel boring Machine

VES - Vertical Electrical Sounding

VS - Vertical Scale

WRMA - Water Resource Management Authority

WSP - Water Service Providers

WSL - Water Struck Level

WRL - Water Rest Level

Ωm - Ohm metre

GLOSSARY OF TERMS

Aquifer A geological formation which can store and transmit water.

Fault A large fracture at the earth where displacement has taken place.

Gradient The rate of change of total head per unit distance, which causes flow to the direction of lowest head.

Porosity The portion of bulk volume in a rock or sediment that is occupied by openings, whether isolated or connected.

Recharge General term applied to the passage of water from surface or subsurface sources (e.g. rivers, rainfall, lateral groundwater flow) to the aquifer zones.

Regolith General term for the layer of weathered, fragmented and unconsolidated rock material that overlies the fresh bedrock.

Traverse A straight line where investigation has been undertaken.

CHAPTER 1: INTRODUCTION

1.1 Background

Tunneling is increasingly being seen as an environmentally and a cost effective means of providing water in hilly and rugged terrain; this is where gravity and pumping systems are not economically viable. Tunnels of two meters diameter and upwards are usually constructed by Tunnel Boring Machines (TBM)), depending on the precise ground conditions.

This study was undertaken at the proposed 12 km Northern collector Tunnel (NCT) running from Mathioya River to Ndakaini Dam. The Tunnel is planned to collect raw water from several streams in the Aberdares ranges to Ndakaini Dam which is a major source of water supply to the city of Nairobi.

Understanding the geological conditions of an area plays a major role in successful design and construction of underground tunnels. Some of the geological factors of major concern include presence of ground, rock type, nature of rock, structures and structural orientation and the nature of the overburden. Inadequate information on these factors leads to structural failure and at times loss of life and equipment.

Electrical Resistivity Tomography (ERT) methods have been extensively used in a number of subsurface explorations since the first application in 1930 (Parasins, 1962). This includes groundwater exploration, mapping surface structures, geotechnical and engineering site investigations, mapping soil and groundwater contamination. Most of the early explorations made use of 1-D (VES) method until lately when VES changed greatly into a new technology namely Resistivity Imaging (RI) or Electrical Resistivity. Imaging (ERT) with 2-D and 3-D data interpretations (Shevinin et, al 2006) with new advancement, surface characteristics which enhances better understanding of geologic conditions at the time of the survey are revealed.

1.2 The Problem Statement

Tunneling is one of the most dangerous and expensive activity in engineering and construction works. The process of construction of a tunnel involves extensive research and surveying before the excavation stage of a project; this allows for proper project design to mitigate against disasters and unnecessary costs.

Rocks are quite unpredictable when excavating through them. Even solid rocks may contain cracks, folds, faults and other discontinuities which when triggered may cause collapse of the tunnel (Matsumoto and Nishioka, 1991).

Other rock conditions such as weathering, deterioration of rocks, number and type of rock layers, overburden, strikes, dips and underground water all determine the stability of a tunnel during and after construction.

Several methods for subsurface investigation are available, they include, Direct coring, Back hoe test pits and Trenching. These methods are point sources of investigation that are limited in depth and extent of coverage and also causes disturbance to the ground. Geophysical methods are able to give accurate ground conditions without interruption, and also cover a large area of investigation.

Athi Water Services Board employed coring method at seven borehole sites along the proposed tunnel to investigate the prevailing geological conditions. The method covers specific points of interest, is expensive and in some cases core recovery is poor.

This research employed ERT method at Maragua, Irate, Kaanja and Makomboki sites along the proposed tunnel. The method involves passing of electric current into the bedrock and measurement of the intensity of electric resistivity of the rock. Basically, it gives us information on electric resistivity properties of a material as a result of passing electrical current through them. This method is relatively simple and time effective, covers a large area and is able to probe deep into the ground.

1.3 Objectives of the Study

1.3.1 Main Objective

The main aim of the study is to use ERT method in carrying out geophysical survey to evaluate the geological conditions along Maragua, Gikigie, Irate, Kaanja and Makomboki sites.

1.3.2 Specific objectives

The study seeks to achieve the following objectives:

i. To establish the type of rock and weathering intensity along the pre-selected sites
ii. To investigate occurrence of geological structures; faults, joints and fractures along the proposed tunnel section.
iii. To determine the occurrence and distribution of ground water within the proposed tunnel section

1.4 Scope of the Research

The research involved desk studies as well as field studies along selected sections of the 10.8 kilometers of the proposed tunnel between Maragua River and Makomboki outfalls near Ndakaini Dam. The field study evaluated the actual geological conditions which may affect the construction of the tunnel. The conditions includes the soils, type of rocks and their characteristics, depth of the over burden and the occurrence of groundwater.

1.5 Justification and Significance of the Study

The tremendous increase in population and industrial growth in Nairobi County has led to increased pressure to the available water resources. The groundwater has been over exploited and the available surface water resources has been highly polluted from both domestic and industrial pollutants.

The need for increased supply has led the authority to look for the water from the surrounding areas. The Aberdares forms the major catchment areas for water supply to the city, with Ndakaini dam as the major storage. The increased outflow compared to the inflow to the dam has led to introduction of rationing programs to avoid drying the only rivers flowing into the dam. To increase the volume, more water has to be imported from the neighboring rivers. Most boreholes drilled within the Aberdares have low yields (appendix 2) and therefore the need to exploit the numerous rivers in the area.

Most of the rivers in the area flow along valleys within mountain ridges, this makes connection through pipe network not only difficult but expensive, and tunneling

makes it easier to pass the pipe network under the ridges and allows the water to flow under the influence of gravity.

Tunneling is known to have several effects on the environment. During construction stage it can cause stress to the surrounding rocks, ground vibration may trigger landslides, while groundwater regime may be affected both in short term and long term.

Findings from this study are expected give insights to the geological conditions at the proposed tunnel section. The research covers the ground surface where the main engineering structures will be constructed and probes deeper at the ground where the tunnel boring activity will interact with the prevailing ground conditions. The findings will complement other studies carried in the area for proper design and implementation of the tunnel project and any other future studies.

ERT method analyzes and images the subsurface, giving the relative resistivity of various formations. The method is able to show various layer of the rocks and underground structures; rock conditions, and can probe at deeper depths. Unlike other methods; the method is cost effective, require few machinery and staff, it also causes minimum disturbance to the area being investigated.

1.6 The Study area

1.6.1 Geographical setting

The study area is located within the Murang'a County of Kenya and lies within longitudes $36^{o}47'0''$and $36^{o}53'0''$ to the East and latitude $0^{o}40'0''$ and $0^{o}48'0''$ to the South. Maragua, Gikigie and Irate lies within topographic sheet (1-50000) 134/2 Maragua and Kaanja, Makomboki sites lying within topographic sheet 134/4 Mangu (1.50,000).

The study area is accessible through a series of well maintained all weathered roads connected to Thika - Kangema. Murang'a Town houses the county administration offices.

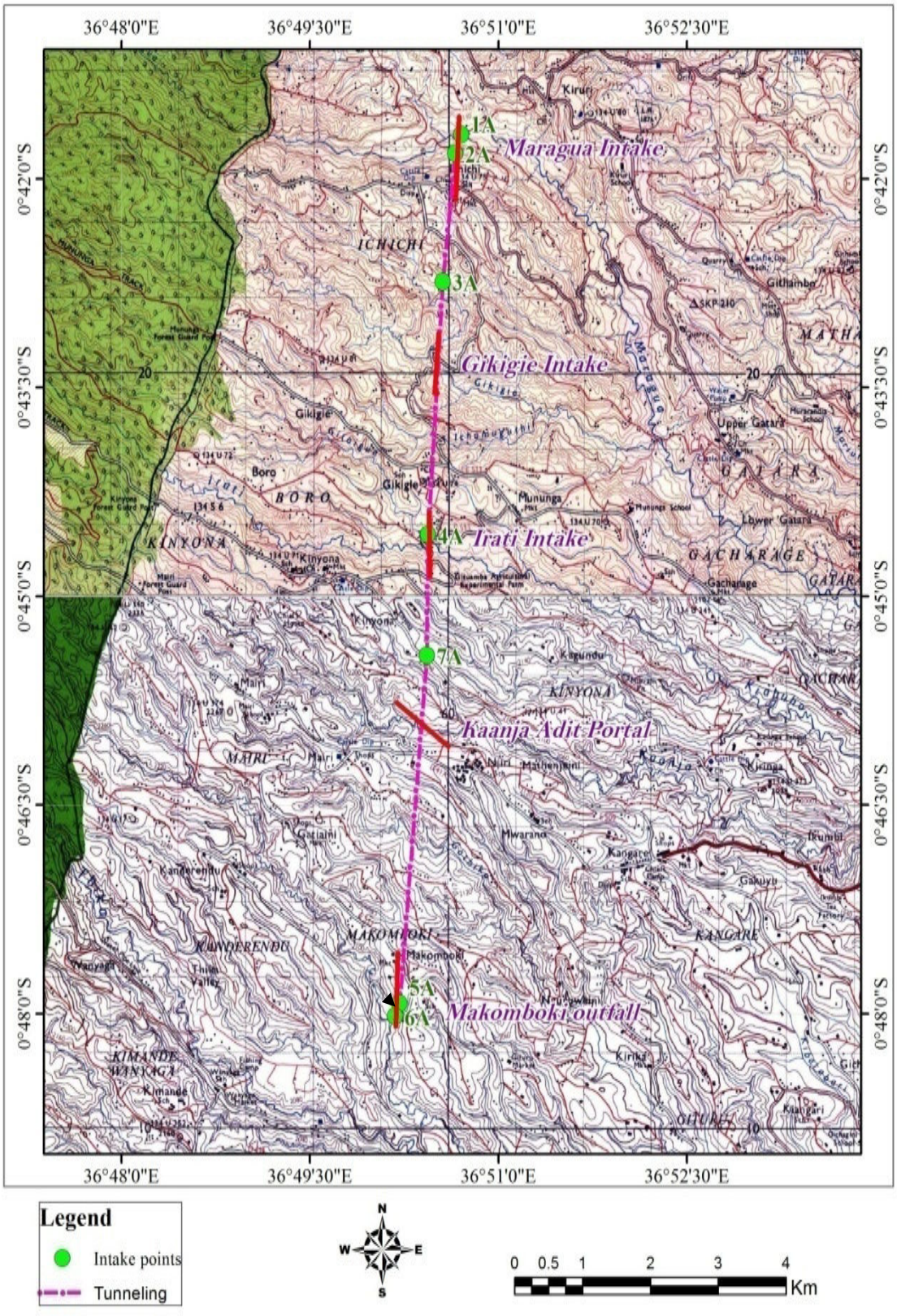

Figure 1.1 Map showing the study area, the intake points and the proposed tunnel route. (Adapted from Kijabe and Mangu topographical sheets 134/2 and 134/4 Survey of Kenya)

1.6.2 Climate and Drainage

The area experiences two rainfall seasons (bimodal) due to the influence of the Intertropical convergence Zone (ITCZ) of the Southern and the Northern Hemisphere. This gives rise to the short rains (October –November) and long rains (March-May), a minimum temperature of 6^{o}c and an average temperature of 18^{o}c (Table 1.1),

The area experience parallel type of drainage system which is highly influence by topography and radiating from the Aberdares mountains. The main rivers draining the area includes the Mathioya, Irate and Gikigie. Small springs forms in the unconformities between the basement and the volcanic.

Table 1.1 Climatic conditions, Fort Hall based on records for 50 years.

(Adapted from Kenya Meteorological Department, 2001)

Month	Average Rainfall (mm)	Mean relative humidity (%) 9.00 am	Mean relative humidity (%) 3.00 pm	Bright sunshine (average hours per day)
January	48	79	45	9
February	48	74	37	10
March	115	82	43	9
April	195	86	53	7
May	137	85	55	6
June	42	85	59	6
July	15	83	53	4
August	21	85	53	4
September	24	82	50	6
October	52	80	47	7
November	114	81	57	7
December	77	83	54	8
Year	74	78	51	7

1.6.3 Soil and Vegetation

Generally the soils in the study area have developed in highly undulating ridges cut by numerous steep sided valleys. These soils are red-brown with high humic content. These soils have developed above deeply weathered volcanic rocks to a considerable depth and are widely cultivated. Most of the natural vegetation comprising of indigenous trees and shrubs in the area have been cleared for agricultural development and human settlements. Eucalyptus tree have been planted for energy production in tea factories (Fig 1.2 and 1.3a, shows tea plantation with eucalyptus at the background). Thick bushes are common along the river valleys as indicated in Figure 1.3b.

Figure 1.2 Section of the Kaanja area showing the general topography and vegetation (Photo taken facing South East)

Figure 1.3 a Maragua site showing the general topography and 1.3 b basaltic boulders along Irate river.

1.6.4 Surface and Groundwater Resource

Most of the rivers radiate from the Aberdares, they tend to follow the topography and therefore form a parallel type of drainage system (Figure 1.4). Small permanent springs are common along the valleys, occurring at the unconformity between the basement systems and the overlying volcanic formations in the greater fort hall area. Shallow wells are common in unconsolidated and weathered formations within the area.

The presence of many surface water resources within this area has led to limited use of underground water. Most of the boreholes sited are within basaltic agglomerates and trachytic tuffs and yields vary between 1 and 5m^3/hr (Fairburn, 1963) and therefore uneconomical for large scale production.

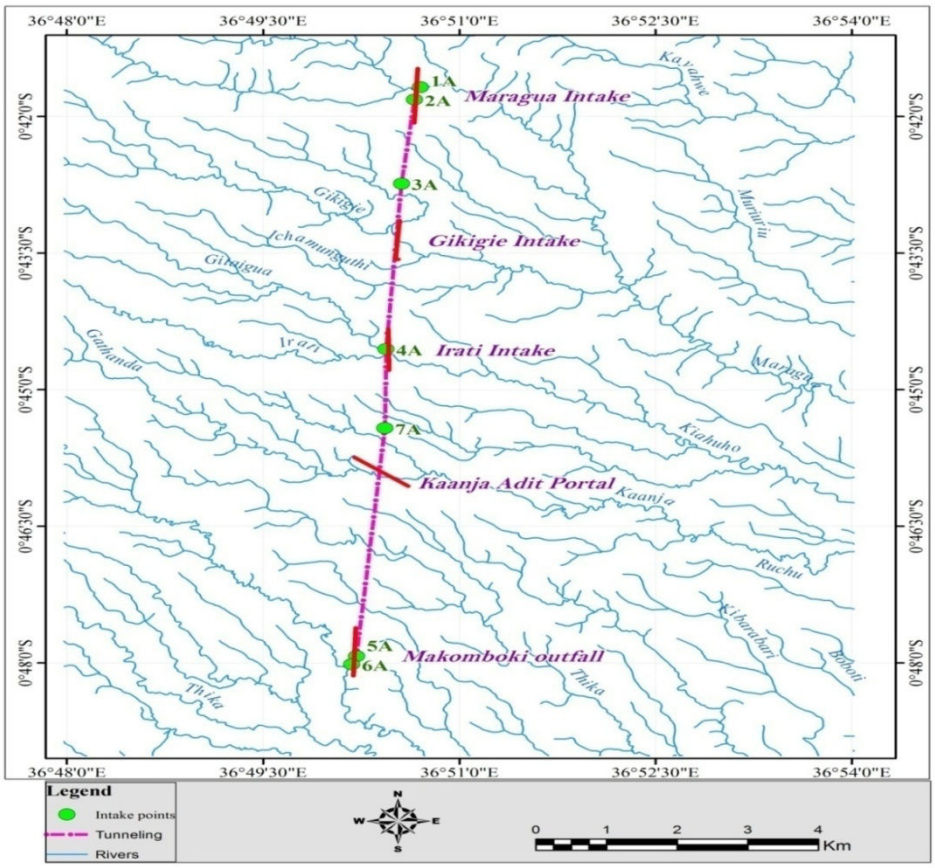

Figure 1.4 Major drainage systems within the study area(Adapted from Kijabe and Mangu topographical sheets 134/2 and 134/4 Survey of Kenya)

CHAPTER 2: LITERATURE REVIEW

According to World Bank report number 28398-KE (2004), Kenya is classified as chronically water - scarce in absolute and relative terms. The natural endowment of renewable freshwater is currently 647 m^3 per capita per annum. By 2025, Kenya is projected to have renewable freshwater supply of 235 m^3 per capita per year (Ministry of Water and Irrigation, 2007).

Like any other city in the world, Nairobi is faced with the problem of ever growing population; in 2010 Kenya National Bureau of Standards (KNBS) reported the population of the city to be 3,138,369. The high population has led to straining of the available water resources in this city. The city suffered severe drought in 2009 due to delayed 2008 October-December rains. The drought led to falling of water level in major dams like Sasumua and Ndakaini Dams, these are the major water storage facilities for the city. In order to alleviate the water shortage, the Government of Kenya drilled about fifty (50) boreholes in Nairobi to increase water supply.

The Ministry of Nairobi Metropolitan Development (2008) projected that the domestic water demand will be about 915.47 million cubic metres by 2030 (Figure 2.1), this calls for increase in research for more water sources to meet the increasing demand.

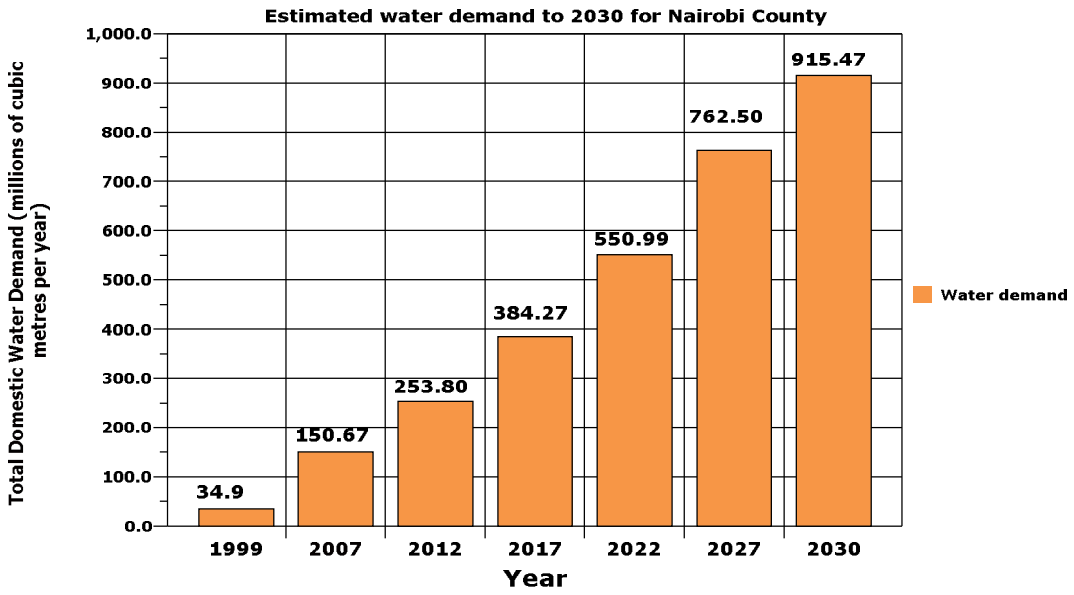

Figure 2.1 Estimated Water demand to 2030 (Adapted from Ministry of Nairobi Metropolitan Development, 2008)

The proposed Northern collector tunnel lies within Gatanga district in Murang'a County.

Several of the earliest travelers in Kenya passed through Fort hall area, particularly those on expedition to Mount Kenya, paying attention to physiography and the volcanic activity and gave their report on the geology of the area.

Gregory gave the earliest geological account for the area; on his return journey to Machakos from Lake Baringo and Mt Kenya in 1893 passed east of TumuTumu Hills to the lava plains north of Tana. A full account of the geology was published in 1921 and included geological information obtained from his second survey of 1919 and established the geological succession in the area.

Prior to publication of Gregory's work in 1921, Muff had given a brief description of geology in the Fort Hall and the phonolites forming the Kapiti and Athi plains (Muff, 1908).

Sikes (1934) described the conditions which water was likely to be encountered on the Kinangop area, he dealt with the rock in relation to their water bearing properties.

In 1936, Bullard established a gravity station in Fort Hall and carried out gravity survey in the area. Shackleton (1945) gave a further description of geology between Nyeri and Fort Hall.

Thomsons in 1964 distinguished the principal rocks in the Kijabe area to consist of the basalts, the basaltic agglomerates, the pyroclastic rocks and the lacustrine deposits. He tabulated the sequence in which these rocks are laid.

Ministry of works hydrogeological report gives groundwater data for area between Nairobi and Fort hall (Gevaerts 1964) it also includes a map of 124 square miles of volcanic rocks between Mitubiri and Makuyu in the south of Fort Hall area.

Ngecu and Ichang'i (1999) identified that the land sliding at Maringa, occurred when the weathered pyroclastic regolith becomes saturated after a heavy rainstorm on high mechanically unstable slope which slid over the more stable basalts. Over-saturation of clay soils (andesol) which were also derived from weathering of pyroclastic rocks contributed to the slope failure.

Turn O-metal (2013) carried out geological coring within the area at specific sites within the proposed tunnel and did the core analysis to a depth of 80m (Appendix 5,6 and 7), although the raw data was available for analysis the result remain undocumented.

Walhstron 1973 describes a tunnel as a long, narrow and essentially linear excavated underground opening, the length of which greatly exceeds its width or height. In contrast, a cavern is an underground opening whose length and width are roughly similar. These two types of excavations are end-members, and every underground excavation undertaken by mankind can be looked upon as a combination of the two. A shaft can simply be thought of as a tunnel which is vertical rather than horizontal.

For centuries, tunnels in rock were driven by building fires against the rock faces, which would cause expansion and spalling, often accelerated by dousing the hot rock with water, then picking the fractured rock away with picks and wedges (Wahlstrom, 1973). Egyptian and Roman mines were worked to depths of approximately 200 meters (Mahtab and Grasso, 1992). It has been estimated that the advance rate of a hand-worked tunnel in hard rock was perhaps 9 meters per year (Beall, 1973).

Today, nearly three thousand years later, the advance rate in a given excavation is increased over that by two or three orders of magnitude (Mahtab and Grasso, 1992). The advent of explosives, first black powder, then nitroglycerine and dynamite, issued in a new age of excavation. Not just that the rates of excavation improved but through improved methods of design and construction, the dimensions of underground workings have increased.

The process of digging a tunnel in rock, however, is not simply a case of deciding where the tunnel is to go and then blasting one's way through. Rock is a very treacherous medium through which to travel. Even "solid" rock often contains innumerable cracks, faults, folds, and discontinuities, the activation of any of which may become a trigger to a collapse of the tunnel. The design and construction of a tunnel must account for the mechanical properties of the surrounding rock, which includes not only the aforementioned cracks and discontinuities, but also the weathering and deterioration of the rock, the number and type of layers in the rock, strike and dip of these layers, underground water level, overburden, and the list goes

on and on (Matsumoto and Nishioka, 1991). For this reason, the principles of mechanics are used to determine the feasibility, methods of design and construction, and the stability of the tunnel once it is excavated.

Bickel, et al. (1996) describes a number of general uncertainties and unknowns when dealing with the underground. These variables can range from minor inconveniences to major challenges to the designers of the tunnel. A short list of some of these concerns consists of:

1. The overriding uncertainty when dealing with any underground project. The geology of the area will determine the feasibility and the cost of the undertaking.
2. Engineering properties of rock may change, sometimes drastically, with a wide range of conditions, notably time, season, rate and direction of loading.
3. Groundwater is the most difficult parameter to predict and the most troublesome during construction.
4. Drilling core, the most common method of determining underground conditions, only recovers less than 0.0005% of the excavated volume of the tunnel on a typical project in the most exhaustive survey, which leaves a great deal of room for uncertainty.

Electrical Resistivity (ER) surveying is a geophysical prospecting method which produces ER cross sections of shallow earth structure on the order of 10s of meters of depth. Electrical resistivity surveys have been used since the 1920s in hydrogeological, mining, and environmental investigations [Telford et al., 1990]. Among its many applications, it has been used to characterize aquifers, which are underground layers of permeable rock from which drinking water can be extracted. It has also been used in the monitoring of groundwater pollution and in the investigation of the earth's upper crust, and in the delineation of the structural setting of volcanic areas (Moukadaki et al., 2007).

CHAPTER 3: GEOLOGY

3.1 General Geology

Geology of the study area as described by Fairburn (1963) in his geological report No.73 "The geology of Fort hall" consists of Younger Pleistocene volcanics and Holocene sediments, trachytes rocks of the Younger Aberdare vents, Kijabe-type Basalts, Sattima Series and Laikpian Lavas and Simbara Series. No intrusive rocks are found in the district. The volcanic rocks occupy the western part of the district bordering the Aberdares while the rock of the Basement System occupies the eastern portion of the district.

Thomsons (1964) classifies the geological succession of the region into the following broad divisions;

3.1.1 Simbara Series

These are believed to be the oldest lavas in the area consisting of basalts and basaltic agglomerate. The lavas are probably Miocene in age, compose the high peaks of the Aberdares range and form the mountainous region as well as lower slopes. Both lavas and particularly the agglomerates were subsequently deeply dissected and with later lava flows of rift valley pyroclastics deposited on uneven surface.

3.1.2 Sattima Series and Laikipia Lavas

These rocks overlie the Simbara basalts and are recognized as Rift Valley trachyte, phonolites, basalts and pyroclastics. The trachytes and phonolites are in some areas intercalated within pyroclastic rocks. The pyroclastics often fill hollows in the eroded basaltic agglomerates of the Simbara Series in Muranga and Nyeri and frequently form thick deposits on the Kinangop and on scarps on the flank of Rift Valley as well as in Kiambu.

3.1.3 The Kijabe-type Basalts

These rocks are assigned Lower Pleistocene age and are found beneath a series of pyroclastics rocks. They also overlie Trachytes intercalated in the same series of pyroclastics and sediments. They are younger than the Simbara basalts.

3.1.4 Trachytic rocks of the Younger Aberdare Vents

These rocks are found on rounded hills in the forest reserve and at Karima hill in Nyeri probably as remnants of volcanic vents.

3.1.5 Younger Pleistocene Volcanic Rocks and Holocene Sediments

These rocks includes welded tuffs, agglomerate, coarse pumice and ashy beds. The sediments are composed mainly of pyroclastics materials though some were deposited subaqueously. The nodular laterite is also found and overlaps vesicular trachytes onto underlying agglomerate. They were believed to have been deposited in lower Middle Pleistocene times.

3.2 Lithological Units at the Study Area

The study area is dominated by two geological units as shown in Figure 3.1 namely; .

i. Basalts and agglomerates
ii. The Pyroclastic rocks

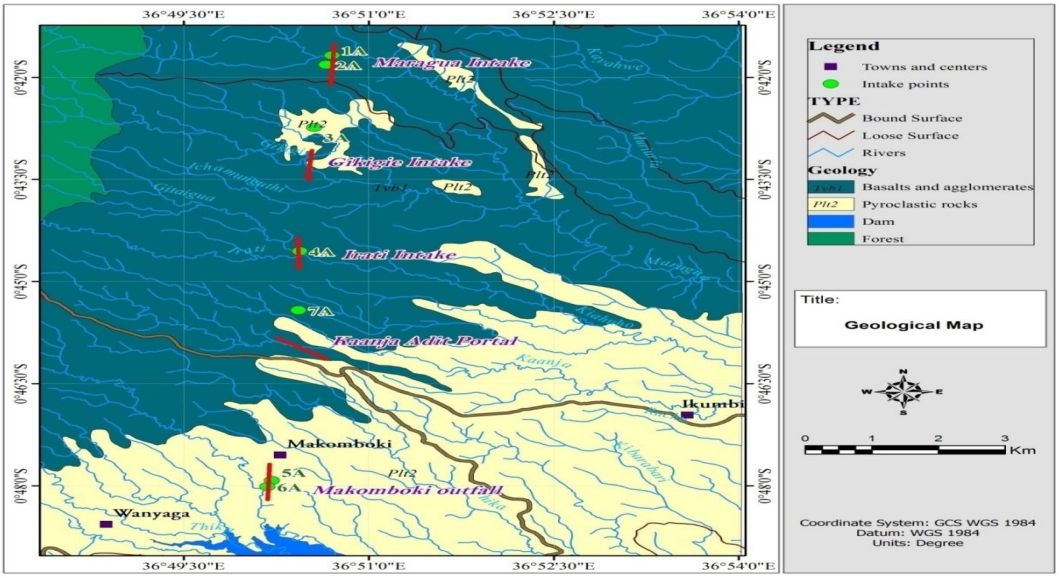

Figure 3.1 Geology of the study area (Modified from Thomsons 1964)

3.2.1 Maragua, Gikigie and Irate intakes

The geology in these areas is dominated by basalts and agglomerates of Simbara series with minor pyroclastic material, the basalts have weathered into deep column of red soil along the slope, eroded and deposited in the valleys. In some areas, effects of high rainfall to the volcanic soils have triggered landslides i.e. Figure 3.2 shows a relic of a landslide at Irate site which occurred in 1978, the land slide is said to have move down slope destroying a house and killing two people. Analysis of the

geological conditions reveals a thick layer of clay soil over a compact zone of pyroclastic rock, the swells under water conditions, and under the influence of gravity it broke at weak points and moved down slope.

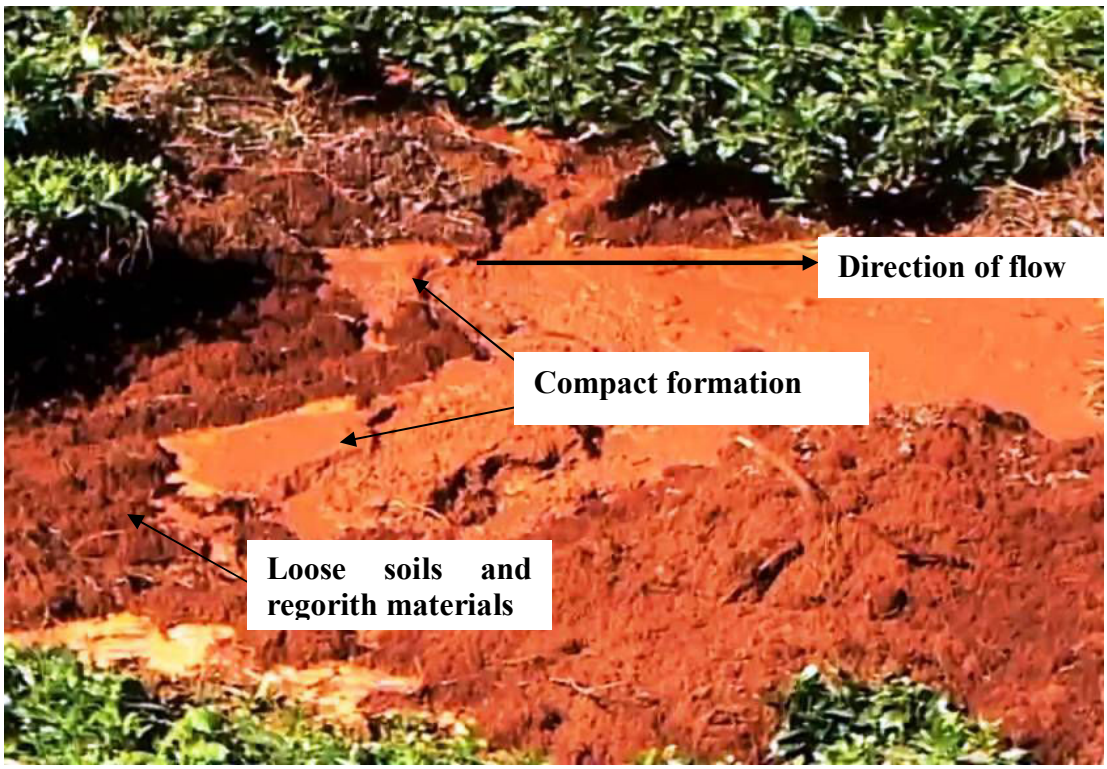

Figure 3.2 Section of a Landslide at Irate site

Very few outcrops can be observed in this section and majority of the rock are floats which have been transported to the area. Along Maragua River phonolite boulders from the Aberdares have been deposited, the diameter ranges between 3cm to 5cm Figure 3.3. The phonolites are dark coloured, fine crystalline groundmass dominated by sanidine and nepheline.

Figure 3.3 Maragua River, phonolite deposit are seen at the foreground

3.2.2 Makomboki and Kaanja intakes

The area consists of volcanic formation composed of the pyroclastic rocks and basaltic agglomerates. Few basaltic boulders are exposed along eroded section at the bottom of Makomboki valley, and also at an abandoned tuff quarry covered by thick under growth. The basaltic agglomerates of the Simbara Series and pyroclastic rocks intercalated Laikipian type basalt are also common at Kaanja site.

At the bottom of the valley few basaltic floats are exposed by erosion. They occur within the layer of soil and are dark coloured fine grained mass. The basaltic float consist of Olivine's and feldspars mineral, Figure 3.4 shows an exposed basaltic boulder at Gathika valley (259279.2, 990301).

The pyroclastic rocks as described by Shackleton (1945) include the basaltic Lava flows. They occur as soft light coloured tuffs which vary in composition. Relics of tuffs were observed at an abandoned quarry at the Gathika river valley.

Figure 3.4 Basaltic agglomerate exposed at a road cut in Makomboki.

3.3.1 Engineering Characteristics of rocks in the study area.

Basalts are dark coloured and fine grained rocks, under unweathered conditions the rocks have high strength and forms good foundation base, their hard and crystalline nature makes them hard to excavate.

Thomsons (1964) describes the mineralogical composition of these rocks in fort hall area to consist of phenocrysts of augite, olivine and plagioclase in a ground mass of the same minerals. These mineral when exposed to hydro climatic conditions weathers to red volcanic clay soils, some clays such as montimorillonites are known to swells and limit advancing of a tunnel.

Weathering is one of important principle process in formation of secondary porosity in basalt. Porosity governs physical attributes such as strength, deformation and hydraulic conductivity of a rock. Terzaghi (1958) describes the soil in this area to contain large portions of clays which consist of hallosite and considerable portions of iron oxide. The clay content of these soils and their plastic limits are abnormally high and dry density at maximum moisture low the ground becomes unstable for structural support.

According to Thomsons (1964), the pyroclastic rocks consists of mainly welded tuff which has been highly weathered and eroded along the slopes and deposited at the dissected valleys. The rock consists of welded tuffs which are soft and are easily eroded, the rocks forms stable grounds for structures and combines readily with cement.

Loose pyroclastic rocks have a low compaction and strength and therefore highly erodible, Thomsons (1964) describes weathering of the pyroclast in this area to form red soils. The soils are eroded along the slopes and deposited in the valley forming thick layer of soil on top of the unweathered rocks. The large column of soil has made it difficult to economically exploit the tuffs.

Tunnel engineers generally classify rock on the basis of resistance to deformation (strength), amount of weathering and general resistance to weathering Parker (1996). Terzaghi (1946) classified rock mass into seven divisions;

Intact rock: Intact rock contains neither joints nor hair cracks, and thus breaks across sound rock. Spalling conditions, which is when thin slabs of rock fall off the roof or walls of the tunnel, and popping conditions, where rock slabs on the sides or roof of the tunnel spontaneously and violently detach, may occur for several hours or days after blasting.

Stratified rock: Stratified rock consists of individual strata with little or no resistance against separation along strata boundaries. Spalling conditions are quite common.

Moderately jointed rock: Moderately jointed rock contains joints and hair cracks, but blocks between the joints are locally grown together or so intimately interlocked that vertical walls do not require lateral support. Again, spalling and popping conditions may be encountered.

Blocky and seamy rock: This consists of chemically intact or nearly intact rock fragments which are entirely separated from each other and imperfectly interlocked. The vertical walls of the tunnel may require support.

Crushed rock: Crushed rock is chemically intact, but extensively fractured. If the crushed rock is small-grained and below the water table, it will exhibit the properties of a water-bearing sand.

Squeezing rock: Squeezing rock slowly advances into the tunnel without a perceptible volume increase. This condition requires a very high percentage of microscopic and submicroscopic micaceous minerals or clay minerals with a low swelling capacity.

Swelling rock: Swelling rock advances into the tunnel primarily by the expansion of the rock itself. This condition seems to be limited to rocks containing clays, such as montimorillonite, which have a high capacity to swell when hydrated.

3.3.2 Effects of Geological structures to tunnel excavation

- **Effect of soil layers:** horizontal, vertical and inclined layers have different kinds of loading conditions for tunnels.
- **Tunnel excavations in the slopes:** the discontinuities (layers, fissures) inclined inside or outside of the slope are very important regarding the stress and strength of the tunnel.
- **Effect of the folds:** While tunnel is excavated in an area that contains folded rocks, different stresses and conditions may occur depending on the fold type. Fold axis and the tunnel direction is vertical, fold axis and the tunnel direction is parallel.

CHAPTER 4: METHODOLOGY

4.1 Geophysical Methods

Geophysical methods assist engineers in solving geotechnical problems through detection of different physical characteristics of the ground. Electrical Resistivity Tomography (ERT) techniques detect and characterize layers by exploiting resistivity contrast between different layers using electrical current.

The present study at the proposed tunnel construction site employs Electrical Resistivity Tomography (ERT), to evaluate the nature of the subsurface formation at five pre-selected sites to determine, the nature of rock, degree of rock weathering and establishing the presence of geological structures along the tunnel section.

The study employs the under mentioned multi-step approach during the site investigation:

a) A desk study and data-acquisition phase: Review of existing data, topographical maps, existing studies and borehole site investigations in the Murang'a area, geological reports and maps, borehole records, etc.

b) Geophysical fieldwork: Inspection of geological, geomorphological and structural characteristics of the investigated area, verification of existing data and findings.

c) Analysis of geophysical data.

e) Compilation, analysis, and evaluation of the gathered data and information.

f) Reporting.

Available geological data from reports and geologic maps were supplemented by field data collected from August to October 2013.

The data collection involved a reconnaissance survey to establish the sites and meet the land owners to explain the purpose of the study. This was followed by actual profiling where Electrical Resistivity Tomography method was employed a total of 27 profiles were carried out within five selected sites.

4.2 Electrical Resistivity method (DC resistivity technique)

This method measures the earth's resistivity by driving a direct current (DC) signal into the ground and measuring the resulting potentials (voltages) created in the earth. From that data the electrical properties of the earth (the geo-electric section) can be derived and thereby the geologic properties inferred.

4.3 Basic Principles of Electrical Resistivity Method

The electrical properties of rocks in the upper part of the earth's crust are dependent upon the lithology, porosity, and the degree of pore space saturation and the salinity of the water. It is imperative to note that:

1. Saturated rocks have lower resistivity than unsaturated and dry rocks.
2. The higher the porosity of the saturated rock, the lower its resistivity.
3. The higher the salinity of the saturating fluids, the lower resistivity of the host media.
4. Clays and conductive minerals also reduce the resistivity of the rock.

The resistivity of earth materials can be studied by measuring the electrical potential distribution produced at the earth's surface by an electric current that is passed through the earth.

(Telford et al, 1990) describes the resistance R of a material to be directly proportional to its length L and cross-sectional area A, expressed as:

$$R = \rho * L/A \quad \text{(Ohm)} \qquad (4.1)$$

Where ρ is known as the specific resistivity, characteristic of the material and independent of its shape or size. With Ohm's Law,

$$R = dV/I \quad \text{(Ohm)} \qquad (4.2)$$

Where dV is the potential difference across the resistor and I is the electric current through the resistor, the specific resistivity may be determined by:

$$\rho = (A/L) * (dV/I) \quad \text{(Ohm.m)} \qquad (4.3)$$

It is not possible to identify rock type solely on resistivity data rather resistivity data may be used to supplement other type of data and reduce the uncertainty of interpretation.

The diagram below illustrates the basic electrical array for that measurement.

Figure 4.1 illustrates the basic principle of DC resistivity measurements. Two short metallic stakes/current electrodes (AB) are driven about 0.3 m into the earth to apply the current to the ground. Two additional potential electrodes (MN) are used to measure the earth voltage (or electrical potential) generated by the current. Depth of investigation is a function of the distance of current electrodes.

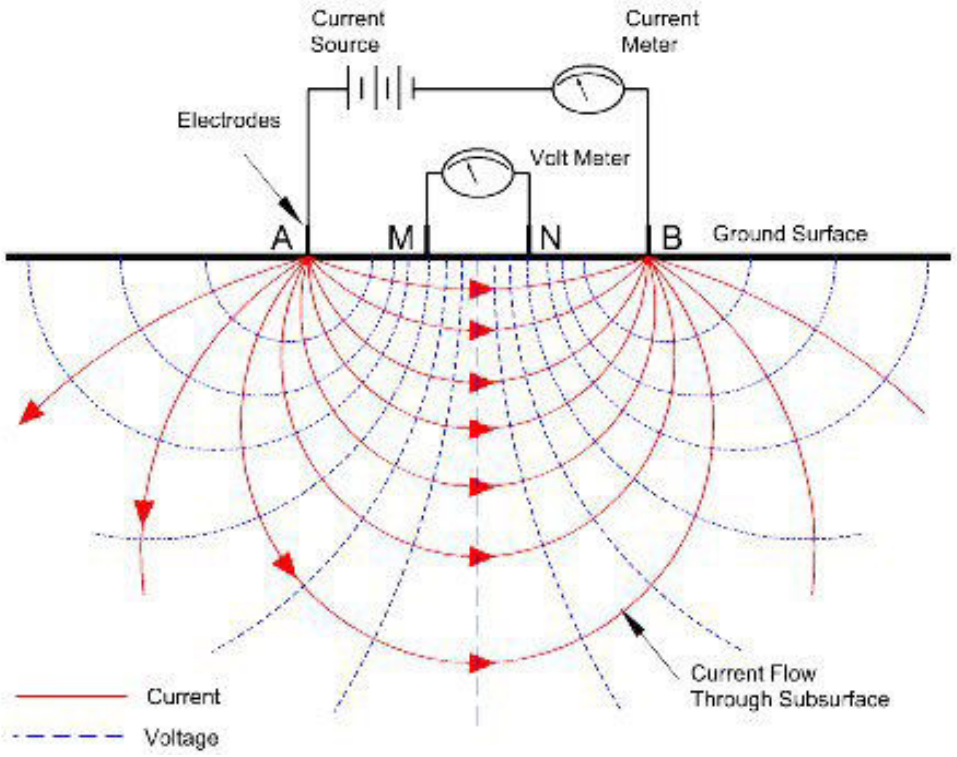

Figure 4.1: Qualitative distribution of current flow lines on homogeneous surface (After Hemeda, 2013)

In this method an electric current is passed into the ground and the potential difference measured to get the resistivity of the underlying layers. Common array systems include Wenner electrode system, Schlumberger system and Dipole-Dipole system.

Resistivity of water lies between 10 to 100 Ωm, increasing saturation, salinity, porosity of rock and the number of water filled fracture tend to decrease resistivity (figure 4.2).

Resistivity of igneous and metamorphic rocks lies between 10^3 and 10^4 Ωm.

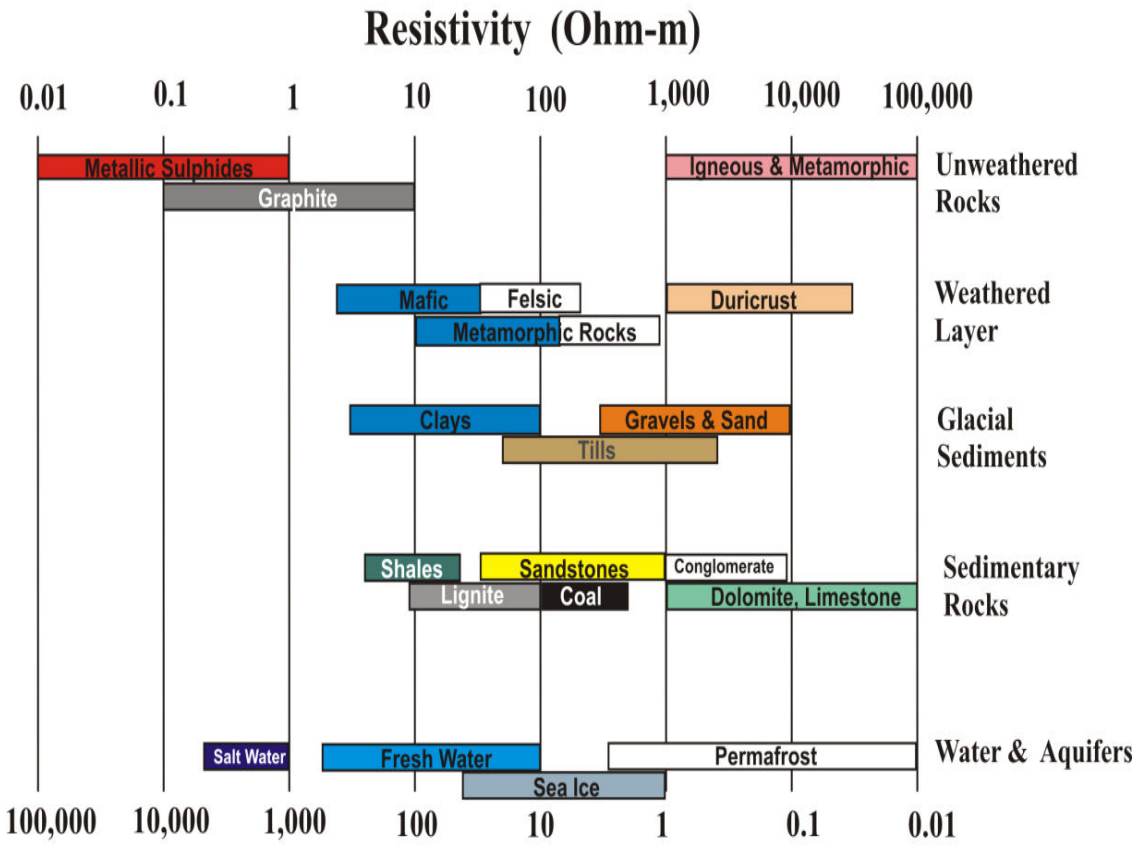

Figure 4.2 Representation of electrical resistivity of rocks, Minerals and Soils. (After Palacky, 1988)

4.4 ERT Data Acquisition Process

ERT employs the principles of resistivity in determining the nature of the subsurface. The earth's subsurface layer resistivity is related to various geological parameters of subsurface formation such as minerals, fluid content, and porosity, degree of water saturation as well as salinity of water in rocks (Grant and West 1965).

The ERT is a geo-electrical method of obtaining high resolution 2-D or 3-D image of a subsurface (Griffith and Baker, 1993), the technique employs continuous vertical sounding (CVES) which is a data acquisition process that combines lateral coverage with vertical sounding using a multi electrode resistivity meter system.

In 2-D ERT resistivity method, the 1-D resistivity measurement is repeated several times at different depths to make a complete image of the earth's subsurface. This is done by shifting the measurements with distance forward along the profile and also by increasing the separation between the electrodes to increases depth.

Transformation of the apparent resistivity pseudo-section into 2-D Models of the subsurface resistivity distribution is achieved using Res 2-D Inversion Software. The optimization technique tries to minimize the difference between the calculated and the measured apparent resistivity values by adjusting the resistivity of the model earth block. A measure of the difference is given after 3 -5 iterations by root Mean Square (RMS) error.

4.4.1 Instruments used in the Field

Lund imaging system was used for data collection, it consist of SAS 1000 ABEM Terrameter, transmitter unit, external battery and battery adapter, crocodile clips, stainless electrodes, and cable reels (Figures 4.3 a, b,c). The instrument are effective for resistivity measurement in many geological formations and has ability to reduce errors by calculating standard deviation (ABEM terameter,2006)

Figure 4.3 a, b, c: Components of ERT measuring instruments used in the field SAS 1000 Terrameter, Geo-reels and Lund imaging system Dr Kuria demonstrating use of ERT equipment .

4.4.2 Field Procedure and data Collection

Schlumberger electrode arrangement array with 41 electrodes was employed for the five sites; Maragua, Gikigie, Irate, Kaanja and Makomboki a total of 27 profiles were carried out.

A conceptual model of geological setting was derived from a combination of existing boreholes and coring data, previous geological work and findings from field investigation (Table 4.1) .This is correlated with general models to be able to interpret the ERT profiles.

Four main Lithological units with significant resistivity contrast for the study area were derived and the results are summarized in table 4.1

Table 4 .1 Lithological units along the Tunnel Section

No	Geologic Layer	Resistivity(Ωm)	Remarks
1	Loose pyroclasts and dry regorith	Over 10,000	
1	Massive and compact basalts	1500-10000	Fresh
1	Boulders and pyroclastic rock	1000-1500	Fractured
2	Weathered Basaltic agglomerates	500-1000	
3	Highly weathered Basaltic Agglomerate	100-500	
4	Very Highly weathered Basaltic agglomerates with pockets of clay	Less than 5-100	aquiferous

4.4.2 Data analysis

The data acquired in the study were processed using RES2DINV software. The software models for 2-D resistivity inversion program, comprise of rectangular blocks (Fig 4.4), the bottom of the block correspond to a data point which is approximately equal to its effective depth (Loke, 2000). A computer program is used to determine the resistivity of the blocks so that the calculated apparent resistivity values agree with the measured values from the field survey. The computer program automatically subdivides the subsurface into a number of blocks, and it then uses a least-squares inversion scheme to determine the appropriate resistivity value for each block. The location of the electrodes and apparent resistivity values must be entered into a text file which can be read by the RES2DINV program.

The software computes by inversion, the true resistivity that agrees with the measured apparent resistivity values from the survey.

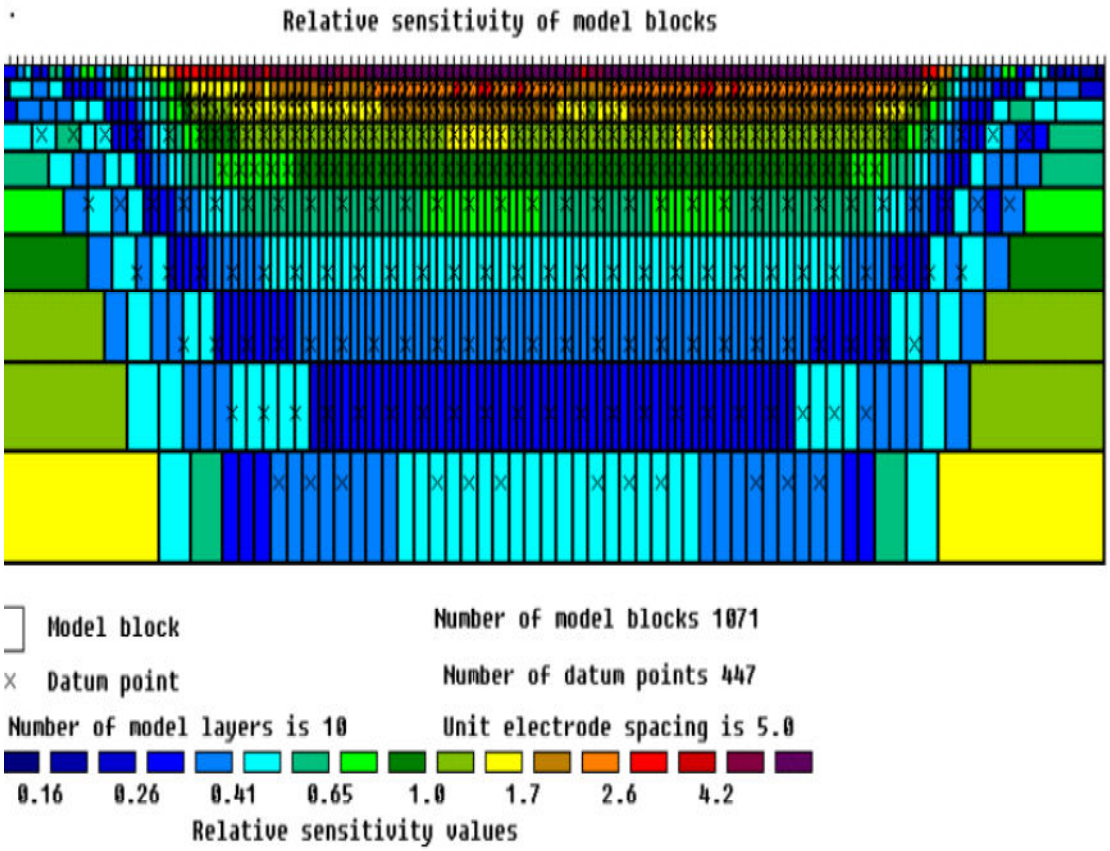

Figure 4.4: Arrangement of blocks used in inversion process by RES2DINV program together with data points in pseudo-section (adapted from Griffiths and Baker1993).

In order to understand the sub-surface geology through the tunnel section ERT profiles were carried out along the five rivers sections where the major engineering structures, such are the Adit portals, intake structures, treatment works may be constructed. Along each section, one ERT traverse was carried along drill holes and the results of the inversion of apparent resistivity compared with the available logging data as indicated in Appendix 5, 6 and 7 and supported by field observations from road cuts, open quarry and sections of landslides.

Apparent resistivity measurements recorded during the survey were entered into a text file in a format compatible with the RES2-D Inversion software and read into the computer.

The software produces a pseudo section of the subsurface by contouring the apparent resistivity values from the ERT survey, the following stages are involved;

- Removal of noisy data from each profile (negative values).
- Bad datum points for joined profiles are checked and removed.
- A trial for the inversion data is made and an initial model is performed.
- Root mean square between the observed and calculated apparent resistivity is calculated.
- Bad data points with large RMS errors are cut from original data.
- Final inversion model with least RMS errors accepted geologically are produced.

CHAPTER 5: RESULTS AND INTERPRETATION

5.1 Maragua Site

A total of six ERT profiles were carried along this section with the main profile of 800m carried out in a SW-NE direction from Ichichi market to the Maragua river as indicated in figure 5.1.

Figure 5.1 Google earth map of Maragua site, showing the six ERT profiles lay out.

5.1.1 ERT profile carried out at Maragua 800m line

The geo-electrical model (Fig 5.2) indicates an average modeled depth of 160m, and displaying three horizontal layers with variable resistivity values ranging from 8.21 to over 51651Ωm.

The ERT image reveals a zone of very low resistivity (less than 10 Ωm) at deep depths (130 to 150m below the ground), this is under the ridge section and close to the earth surface at the river crossing. The low resistivity of less than 5 Ωm indicates occurrence of clay zones, these results also correspond to the results from core data analysis from borehole 1A (appendix6) drilled near the main line.

The southwestern zone (0 to 320 m) is characterized by resistivities with sharp contrast; pockets of low resistivity (less than 60 Ωm) are enclosed within layers of moderate resistivity (100 to 350 Ωm) at a depth of 70m. These are inferred to be pockets of weathered agglomerates. The agglomerates grades from highly weathered to very highly weathered , the degree of weathering increasing from the ground surface to a depth of 70m where it completely weathers to clay.

Pockets of high resistivity layers (10,000 Ωm) are exposed at the surface within weathered agglomerates; these are remnants of pyroclastic rocks left after erosion and basaltic boulders observed at the earth surface. Pockets of the very high resistivity were interpreted as dry regolith under the tea bushes.

The portion between 320 to 420 m slopes gently, with the rock layers inclined in NE - SW direction at an average angle of 40^{o} from the horizontal. Notably the degree of weathering increases with depth. A section of sharp resistivity contrast runs from the earth surface inclined vertically to a depth of 50m. These zone marked by sharp resistivity contrast at 350m along the profile corresponds to a spring observed at the point.

The section between 420 to 800m is comprised mainly of very highly weathered agglomerates with a thin layer of pyroclastic material at the surface; the pyroclastic layer thins out towards the river.

The section between 350 and 600m is comprised of two geo-electric layers; the upper most layer which is highly resistive is composed of weathered agglomerates and the underlying layer is composed of very highly weathered agglomerates. Noteworthy, the very highly weathered agglomerates (8-60 Ωm) are water bearing with flow running towards northern side.

The basal layer is geologically composed of highly weathered basalts that from a pseudo-dome shaped structure located between 360-600m. Towards the terminal of the profile on the northern side the basalts were found to be outcropping.
Figure 5.2 reveals that the tunnel is expected to cut through layers of very highly weathered agglomerates on the southern end through highly weathered basalt at the valley section at the middle and finally highly weathered at the northern end.

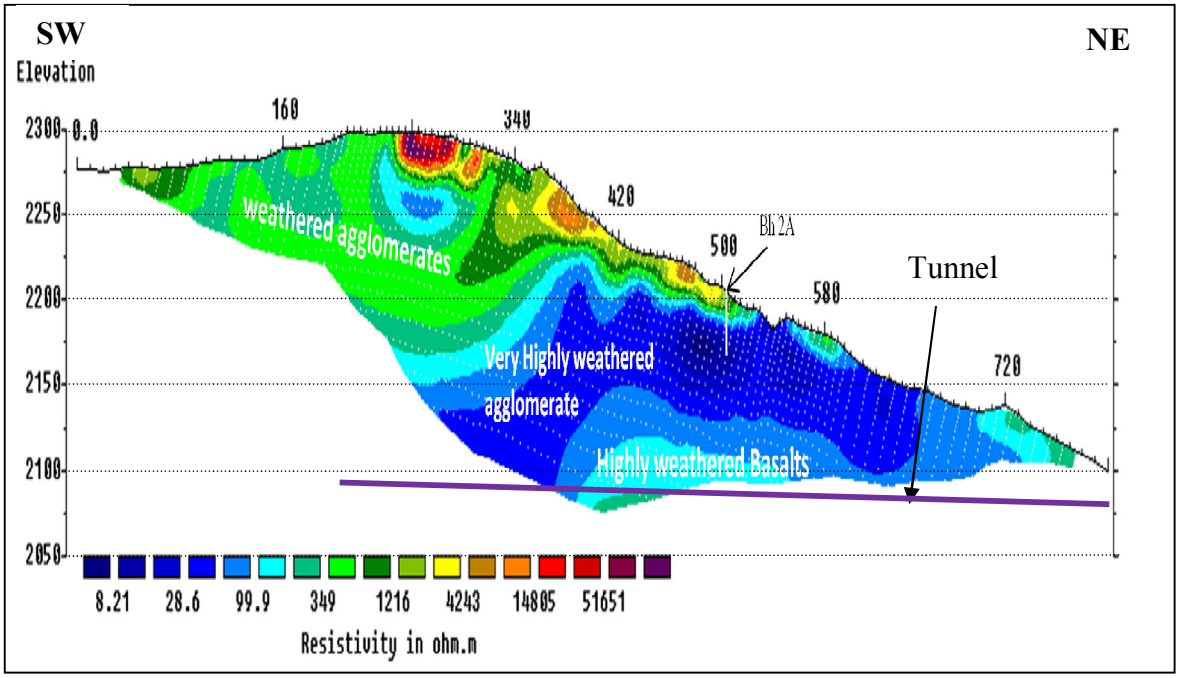

Figure 5.2 ERT 800m traverse at Maragua site

Resistivity/structural relationship

The South western portion shows an easterly sloping ground within horizontally deposited agglomerates. Sharp resistivity difference can be inferred to indicate change of lithology or change in the degree of weathering. The zone between 420 and 800m shows a very highly weathered layer of agglomerate with pocket of clay together with water table occurring at shallow depth. Borehole 2A drilled at point (Easting 260079.690, Northing 9922988.663) and shown in appendix 5, shows no core recovery from 0 to 30 m depth, and water rest level at 2m, this relationship is also observed from the geo-electric model (figure 5.2) where the resistivity (10-100 Ωm) indicates aquiferous and weathered conditions.

5.1.2 ERT profile carried out at Maragua site line1 (L1)

The ERT profile (L1) was carried out in S-N direction and cuts the 800m profile. From the southern end, the ground has an extended steep slope that terminates at a valley and then rises sharply before grading into a very gentle slope.

The geo-electrical model figure 5.4 shows the geological characteristic of the probed depth along L1.

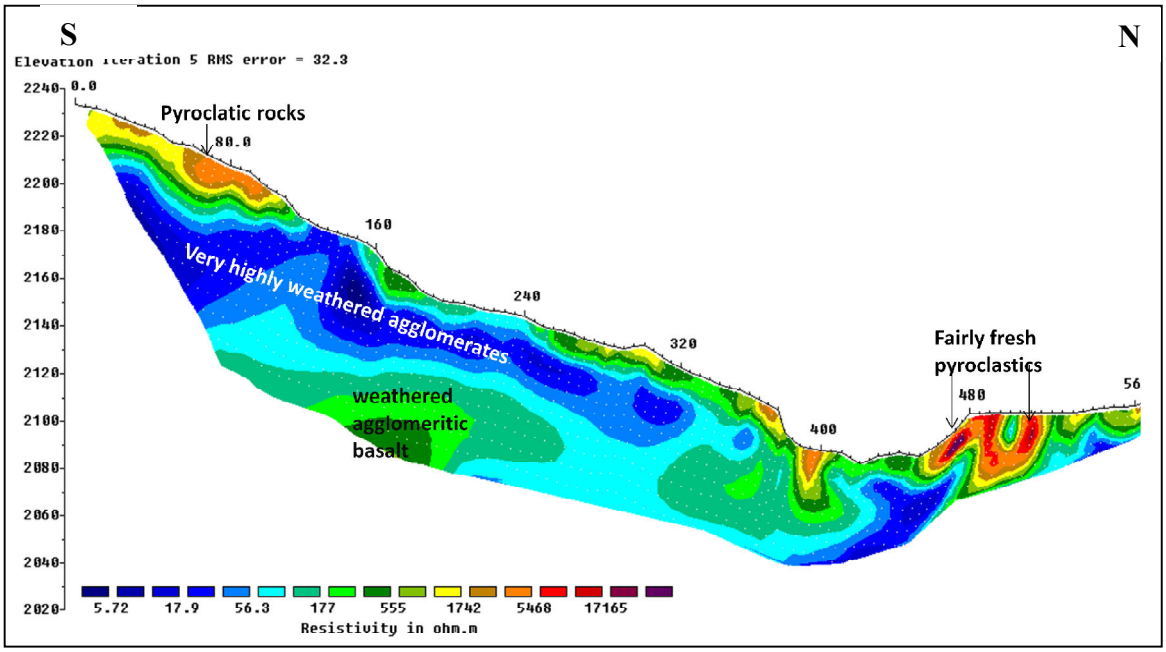

Figure 5.3 ERT profile carried out at Maragua site line 1(L1)

The geo-electrical model show layers of high resistivity (4,000 to over 10,000Ωm) at the surface along the profile with pockets more pronounced at steep slopes, which mark sections where infiltration of water is minimum and rate of erosion is high. The northern side shows a near horizontal surface with pockets of low resistivity within high resistivity zones; an indicator of erosion followed by deposition within the cavities. The high resistivity is characteristic of pyroclastic material. Thomsons (1964) classified the pyroclastic materials as tuffs and noted that they are light colored and soft.

In the southern zone (200-300 m), an average depth of 100m was probed. The upper portion of 5m consists of weathered material (resistivity 100-600Ωm), the layer overlies a zone of very highly weathered agglomerates (10-100 Ωm) which encloses sections of clay indicated by the blue polygons.

5.1.3 ERT profile carried out at Maragua site, line 2 (L2)

This profile was carried out in a NW-SE direction with electrode spacing of 5m. Three major lithologies can be identified as indicated in figure 5.4.

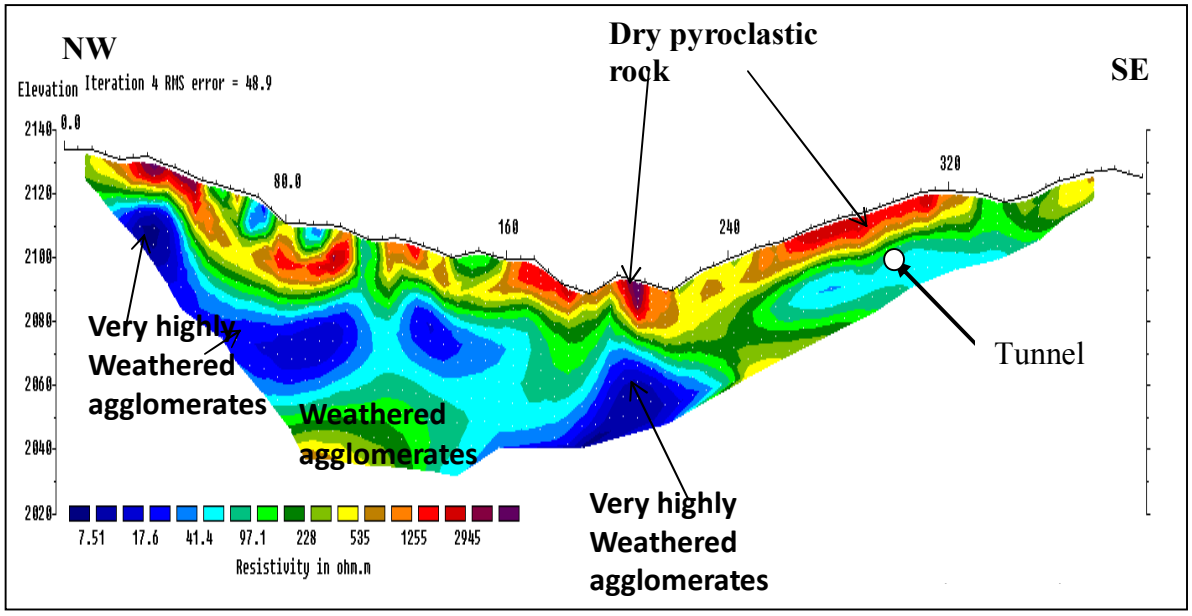

Figure 5.4 ERT profile carried out at Maragua site (L 2)

The geo-electric model indicates three lithological units from the surface to the bottom of the probe. A high resistivity zone (1,200-3,000 Ωm) covers the top 10m from the surface; this is interpreted to be the pyroclastic materials running along the entire profile.

Underlying the pyroclastic material is a thin horizontal layer of weathered agglomerates (10-100 Ωm), the degree of weathering increases towards the bottom of the probe. The agglomerates are exposed at the surface between 105 and 110 m.

At the bottom of the probe lies a less weathered zone of agglomerates, this layer can be projected to join a layer of similar resistivity towards southern end, and therefore confining the highly weathered aquiferous layer.

5.1.4 ERT profile carried out at Maragua site line 3 (L3)

The profile was carried out in NW-SE direction (Figure 5.5) and covers a large portion along the river valley and targeting the damming area; the volume of water is expected to exert pressure on the ground below. The geo-electrical model indicates three main lithological units.

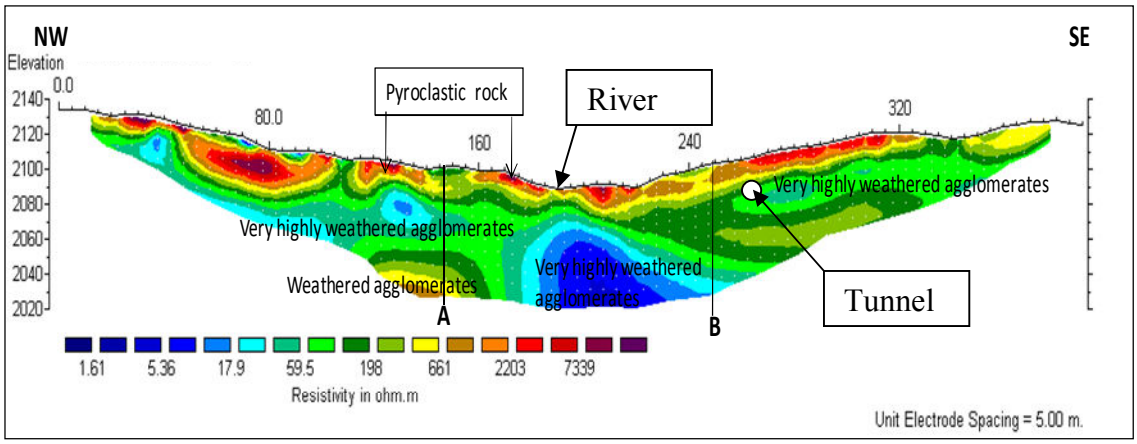

Figure 5.5 ERT profile carried out at Maragua site (L 3)

The geo-electric model indicates the near surface layer of about 5m of pyroclastic material (1,000-2,500 Ωm) running along the whole profile, the continuity being broken by erosion at the river section .

The entire profile is marked by a layer of pyroclastics with variable thickness between 5-10m. the layer is thickened on the northwestern end but maintains almost a uniform thickness for the rest of the profile. The pyroclastics are underlain by a layer of very highly weathered agglomerates that form a wedge shaped structure terminating at the central part of the profile. Some pockets of clay are distributed within the very highly weathered agglomerates.

At the central part, the profile has two vertically inclined geo-electric layers namely weathered agglomerates and very highly weathered agglomerates. The highly weathered agglomerates indicate presence of groundwater which corresponds to location of the river at 190 m mark. Notably, this aquiferous layer extends to below maximum probed depth.

Exposed at an erosion gulley, is a highly fracture basaltic boulder (figure 5.6), the rock is fine grained and shows some joints. Other boulders with diameters ranging from 900mm and above are seen at the background. These conditions are reflected on the geo-electrical model (fig 5.5) at around 210m predisposed within pyroclastics.

Figure 5.6 Basaltic boulder at an erosion gulley in Maragua

5.1.5. ERT profile carried out at Maragua site line 4 (L4)

The 400m ERT traverse was carried along the river in a NW-SE direction, the western part being relatively higher than the eastern part**.**

The geo-electric model (figure 5.7) indicates a thin layer of pyroclastic rocks of almost uniform thickness (8 -10 m) though interspaced at a distance of 10m at the crossing of the river channel. It therefore follows that the continuity of these pyroclastics between left and right bank was result of erosion. In addition, the absence of the pyroclastics on the eastern part indicates erosional effects.

Underlying the pyroclastics are very highly weathered agglomeratic basalts with resistivities below 100 Ωm. These basaltic agglomerates occur as a narrow stretch with a thickness of about 8 m and stretching over a distance of about 30 metres. Towards the central part of the profile the very highly weathered basaltic agglomerates thickens into a roughly oval shaped structure about 25 m wide and 20 m thick. The central part of the very highly weathered agglomerates is marked by presence of very heavy clays i.e. resistivity of about 5 Ωm.

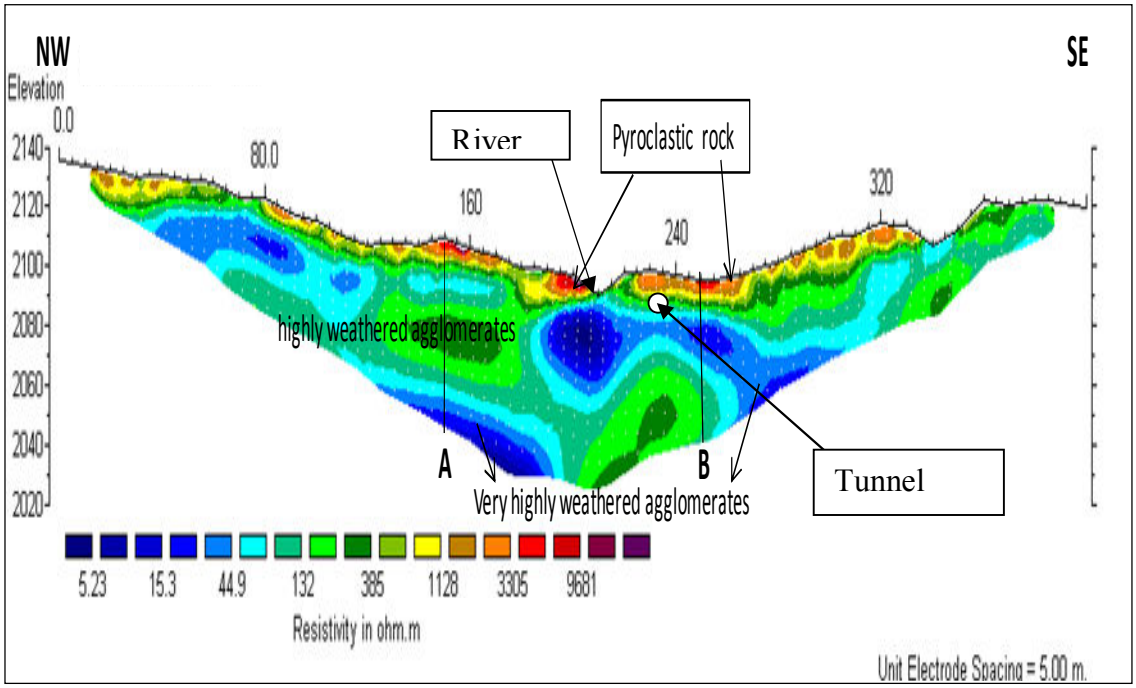

Figure 5.7 ERT profile carried out at Maragua site (L 4)

5.1.6 ERT profile carried out at Maragua site line 5 (L 5)

The ERT profile was carried out in a SW-NE direction traversing along the ridge in the south and cutting the river valley and ending at the opposite ridge in the east. Three major lithological units as presented in (figure 5.8) are interpreted from geo-electrical model

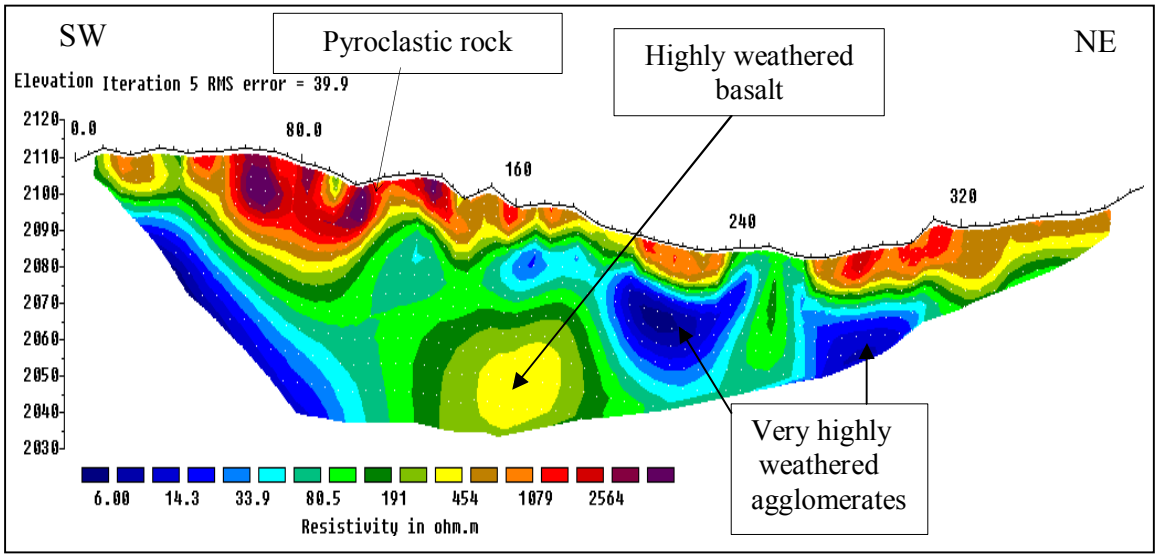

Figure 5.8 ERT profile carried out at Maragua site (L 5)

The model shows a surface layer of pyroclastic material (resistivity ranging between 1,000-3,000 Ωm) at either side of the river (260m). The pyroclastic layer thickens from the southern side attaining a 20m depth at 60m and thins out at the north eastern side towards the end of the profile, between 180m and 230 m along the profile, a portion of very highly weathered agglomerates separated by highly weathered agglomerates occurs at a depth between 10m to 60m below the surface.

On the north eastern side of the profile, an average depth of 110 m was probed, the top surface consist of pyroclastic material which thicken from 5m at the centre to 20m deep in the west, highly weathered agglomeratic basalts taking a dome shape underlies the Pyroclastic material. A section of very highly weathered agglomerates which were not fully probed lies at the bottom of highly weathered agglomerates.

5.2 Gikigie Site

This site is located within a wide valley with steep slopes at both edges, a total of six ERT profiles were carried out within the valley where most of the engineering structures will be constructed. The main profile of 800m was carried across the broad valley cutting through the river at two sections as indicated on figure 5.9; the other profiles have lengths ranging from 400-600m.

Figure 5.9 Google earth map of Gikigie site, showing the six ERT profile layout.

5.2.1 ERT profile carried out at Gikigie site 800M

The 800m profile was carried from S to N direction as indicated Figure 5.9. The geo-electric model as presented in figure 5.10 is characterized by two major lithostratigraphic units defined by varying resistivity ranging from 9.17 to over 4178 Ωm.

The model presents three sections, section 1 from 0 to 240m at the south western side has a maximum probed depth of 40m, the surface is covered by pyroclastic materials to a depth of about 20m except at the river crossing where they have been eroded completely. The pyroclastics are underlain by highly weathered basaltic agglomerates which forms a syncline at a depth of 15 to 30 m.

The middle section running from 240 to 425m mark forms an elevated ground dividing the two streams. A five metre thick weathered basaltic rock of resistivity (500-800 Ωm) is enclosed by weathered agglomerates. The eastern side (425-800) consists of horizontal layers of pyroclastic rocks covering the top 10m and eroded at the river section.

Resistivity structure/ relationship

Resistivity contrasts indicates a horizontal layer of pyroclastic rocks, overlying vertical layers of weathered basalts.

The ERT model reveals folded sub-vertical discontinuities; the surface consists of high resistivity layer of 600 to 4,000 Ωm and an average depth of 5 to 10m overlying a fractured basaltic layer of varying degree of weathering.

Between 260m and 420m, deep fractures extending from the ground surface and supported by SSW trending fractures forms the recharge path to the underground, these may have contributed to weathering of the agglomerates. The resistivity between 30 and 100Ωm suggests an aquiferous formation beneath.

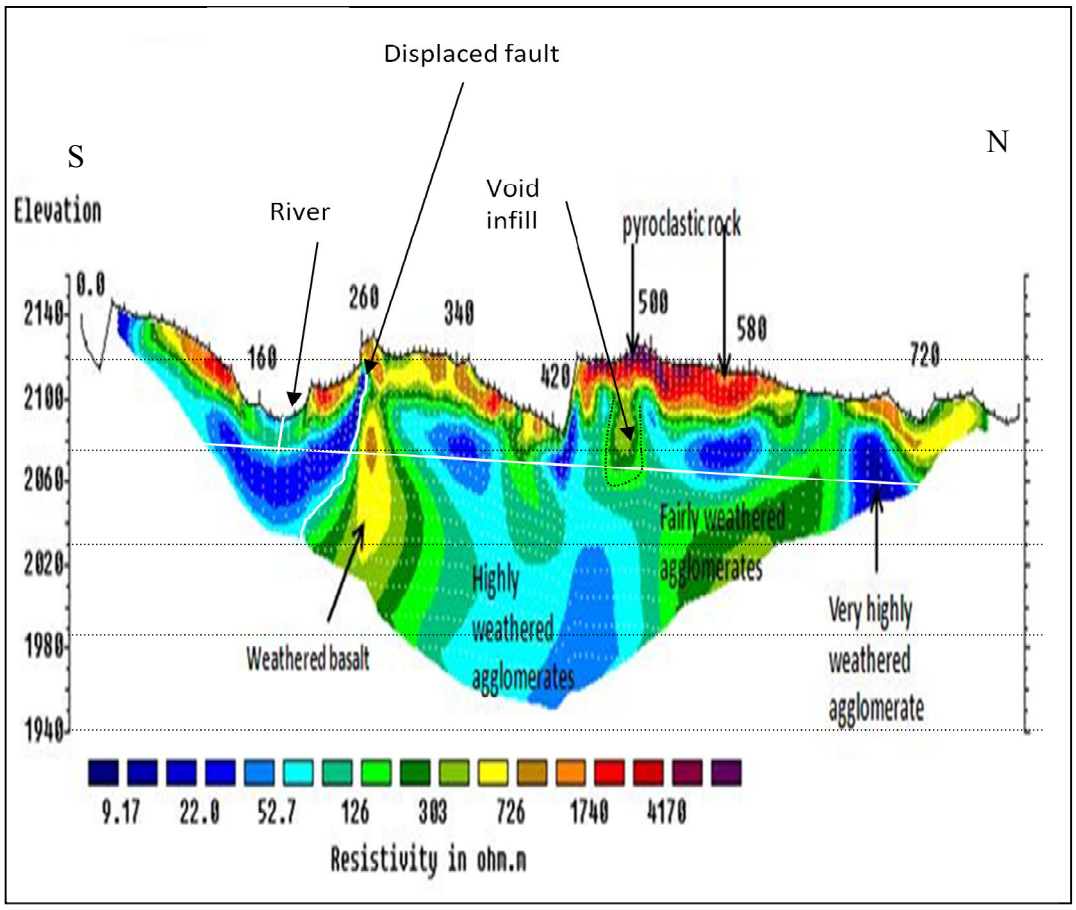

Figure 5.10: ERT profile carried out at Gikigie site 800M.

5.2.2 ERT profile carried out at Gikigie site line 1 (L 1)

The ERT profile was carried out in the SSW-NNE direction and cutting the 800m profile obliquely. The interpreted geo-electric model is presented in Figure 5.11.

The geo-electric model can be divided in three distinct sections from South to North with the highest point of the traverse at 2138m asl on southern side; here the pyroclastic material with resistivity ranging from 500 to 2,000 Ωm covers the upper 10m and runs from 0-220m mark. From a depth of 30 to 100m, a layer of highly weathered agglomeratic basalt (resistivity 50-200 Ωm) encloses portions of clay material. Below this layer, a ridge like structure with a resistivity range between 200 and 1,300 Ωm forms the base of the probe; this can be interpreted as weathered basalts.

The middle section consists of highly weathered agglomeratic basalt with resistivities of 50-200 Ωm, whose degree of weathering increases with depth. A concave layer of pyroclastic rock cover the upper section and thins out towards the northern end, the pyroclasts overlies a layer of highly weathered basaltic agglomerates.

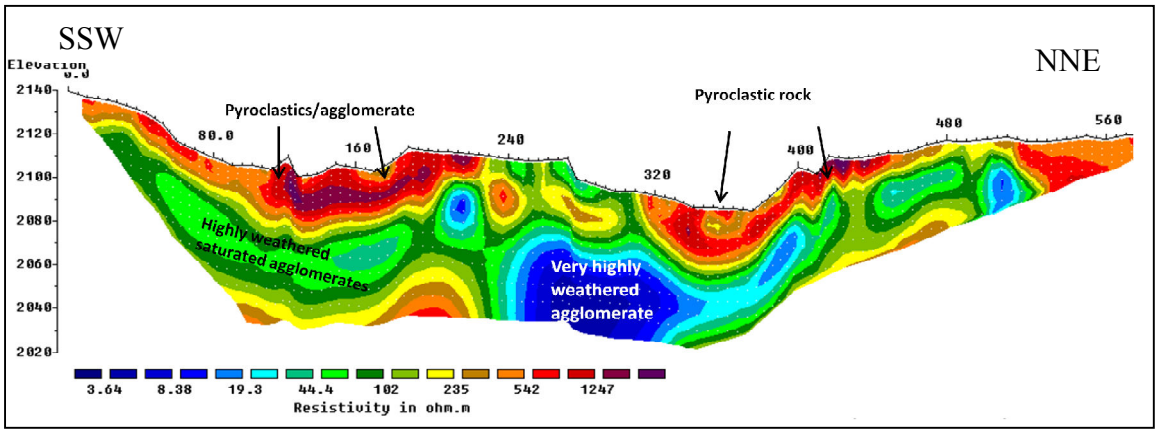

Figure 5.11: ERT profile carried out at Gikigie site (L1)

5.2.3 ERT profile carried out at Gikigie site line 2 (L2)

The ERT profile was carried out in the W-E direction along the valley bottom. The interpreted geo-electric model is presented in Figure 5.12.

The geo-electric model indicates three lithological units which include pyroclastic materials, highly weathered agglomeratic basalts and very highly weathered agglomeratic basalts. The profile runs along slightly sloping ground up to 80 m from the west from where it drops sharply. This zone consists of basaltic boulders and pyroclastics materials which have resisted erosion. The upper most 10m is covered by moist weathered pyroclastic rocks with resistivity between 600-2000 Ωm.

At the valley bottom highly weathered agglomeratic basalts with resistivity (20-100 Ωm) covers the zone between 20 and 40 m below the ground, this rock layer is aquiferous. The probed depth on the eastern side of the valley consists of dry pyroclastic rocks which have been exposed at the surface through erosion, the layer become moist and weathered towards the end.

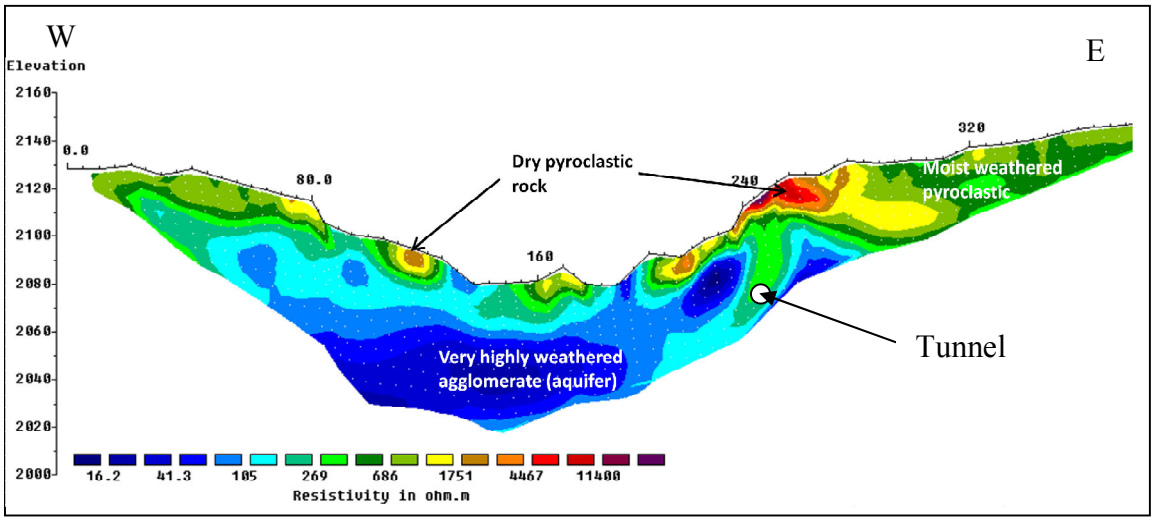

Figure 5.12: ERT profile carried out at Gikigie site (L2)

5.2.4 ERT profile carried out at Gikigie site line 3 (L3)

Similar to ERT profile L2, this ERT profile was carried out in the W-E direction. On the western part, the profile indicate very steep slope that terminate at the river valley before grading into a gentle slope on the eastern part. The interpreted geo-electric model is presented in Figure 5.13.

The geo-electric model indicates the top surface cover of pyroclastic rocks with varying thickness across the profile. At the western edge, a high resistivity layer (more than 2000 Ωm) at surface consists of dry soils and regolith under tea bushes. This layer overlies high weathered basaltic layer. The layer becomes more weathered and wet towards the river valley.

Along the river the pyroclastic rocks have been eroded and a layer of highly weathered agglomeratic rocks exposed, the layer overlies an aquiferous zone of very highly weathered agglomeratic basalts.

The depth of weathering reduces toward the eastern slopes. Across the river, dry pyroclastics rock covers the top 30m of the surface and extends to the forested section

of the profile. However, between 240 and 280m alng the profile, a tongue shape layer of 4,000 Ωm is enclosed by the pyroclastics rock and exposed at one end by erosion.

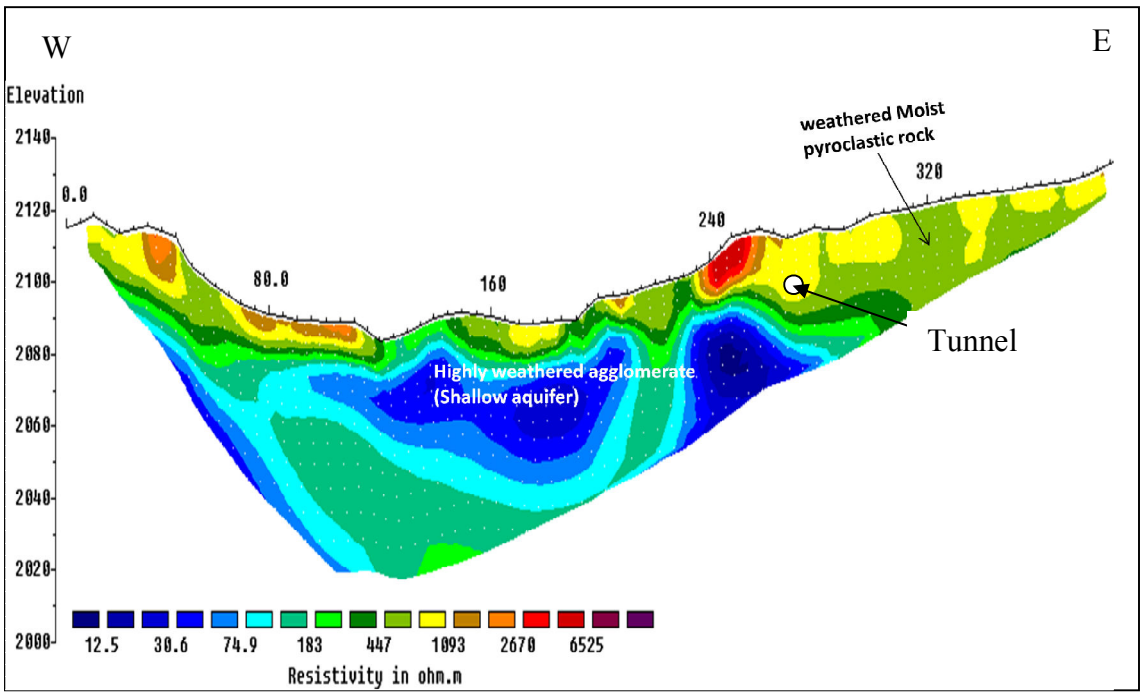

Figure 5.13: ERT profile carried out at Gikigie site (L3)

5.2.5: ERT profile carried out at Gikigie site line 4(L 4)

This ERT profile was carried out in the W-E direction; the area slopes gently from the western side to the valley bottom and rises sharply in the eastern edge. The interpreted geo-electric model is presented in Figure 5.14.

The model indicates a thin cover of pyroclastics rocks with a thickness of about 8m, which thins out towards the valley; this layer overlies a highly weathered material separating it from the very highly agglomeratic basalts.

Notably, the zone of very highly weathered agglomeratic basalts has resistivity ranging from 20-100 Ωm and is aquiferous. The aquifer extends from about 40m from the earth surface and can be projected to a depth of 100m.

The geo-electric section indicates a shallow water table along the traverse; the depth of water table is wider at the slopes and thins out towards the valley (approximately 2m). The highly weathered zone below 15m is aquiferous.

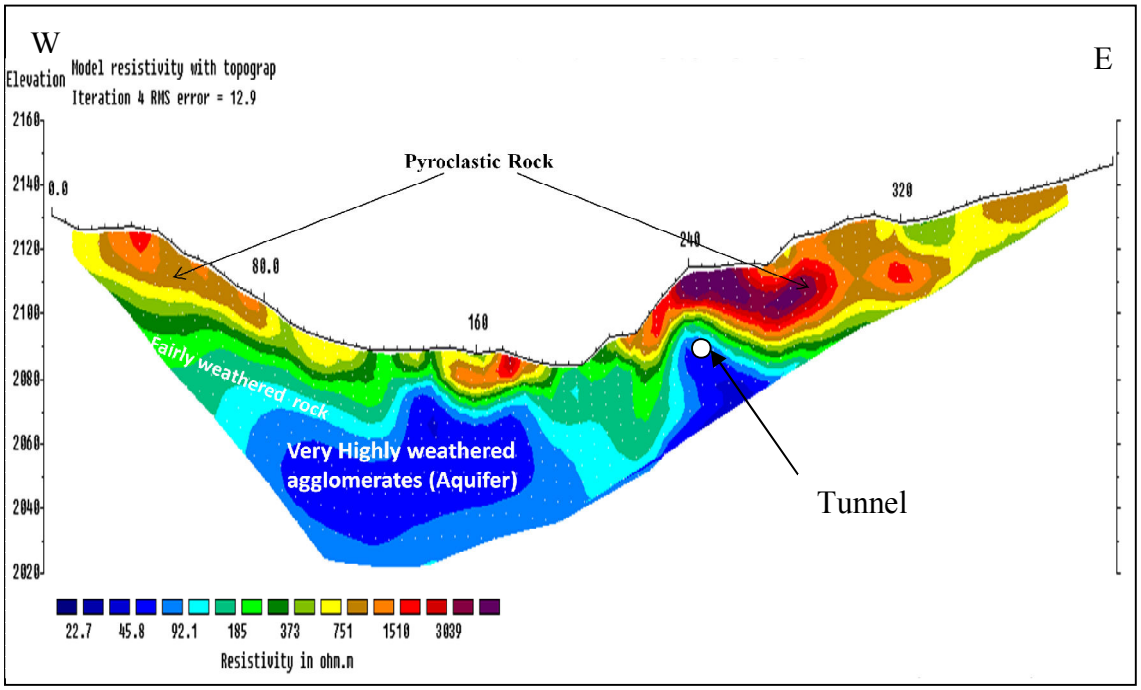

Figure 5.14 ERT profile carried out at Gikigie site (L 4).

5.2.6 ERT profile carried out at Gikigie site line 5 (L5)

The ERT profile was carried out in the W-E direction along the river channel. The interpreted geo-electric model is presented in Figure 5.15.

A depth of about 20m was probed in the southern end (0 to 60m), this area consist of portion of pyroclastics rock (3,000 Ωm) and fractured basalts with the parts of the fractures in filled by mud or residuals from weathering.

A thin layer of soil, grey in color overlies an aquiferous layer of agglomerates which forms at a depth of 5 to 35m within the valley; this layer deepens to about 100m at 200m mark and thins out towards the end. Between 100 and 200m,a layer of highly weathered basalts lies below the aquiferous zone between depths of 40 and 80 metres.

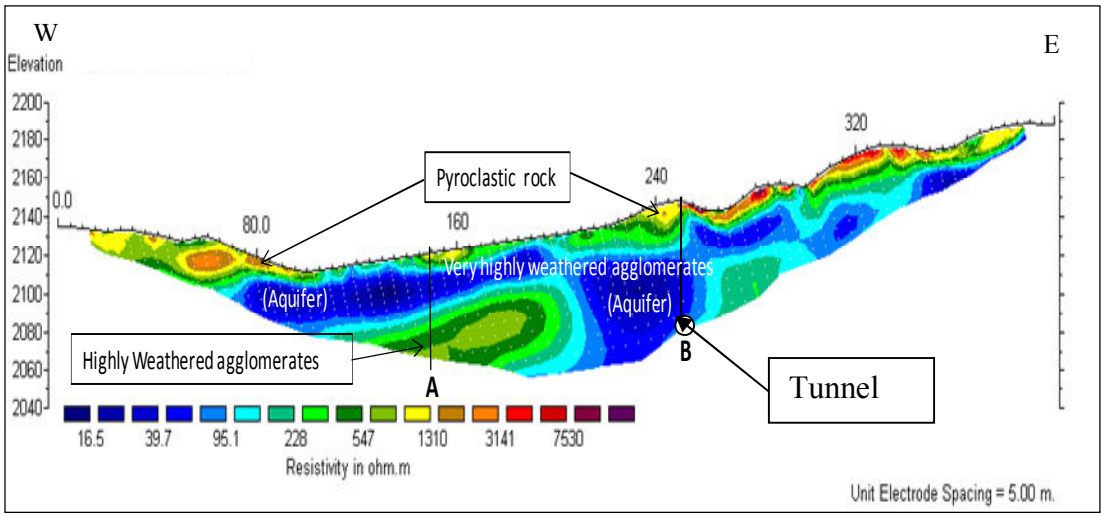

Figure 5.15 ERT profile carried out at Gikigie site (L5)

5.3 Irate Site

The site lies within a broad valley where two tributaries join the main river; large rock boulders are common along the river whose rounded nature suggest that they have been transported over long distances. Thick layers of red soils are common at the road cut. Figure 5.16 presents the five profiles layout at the site.

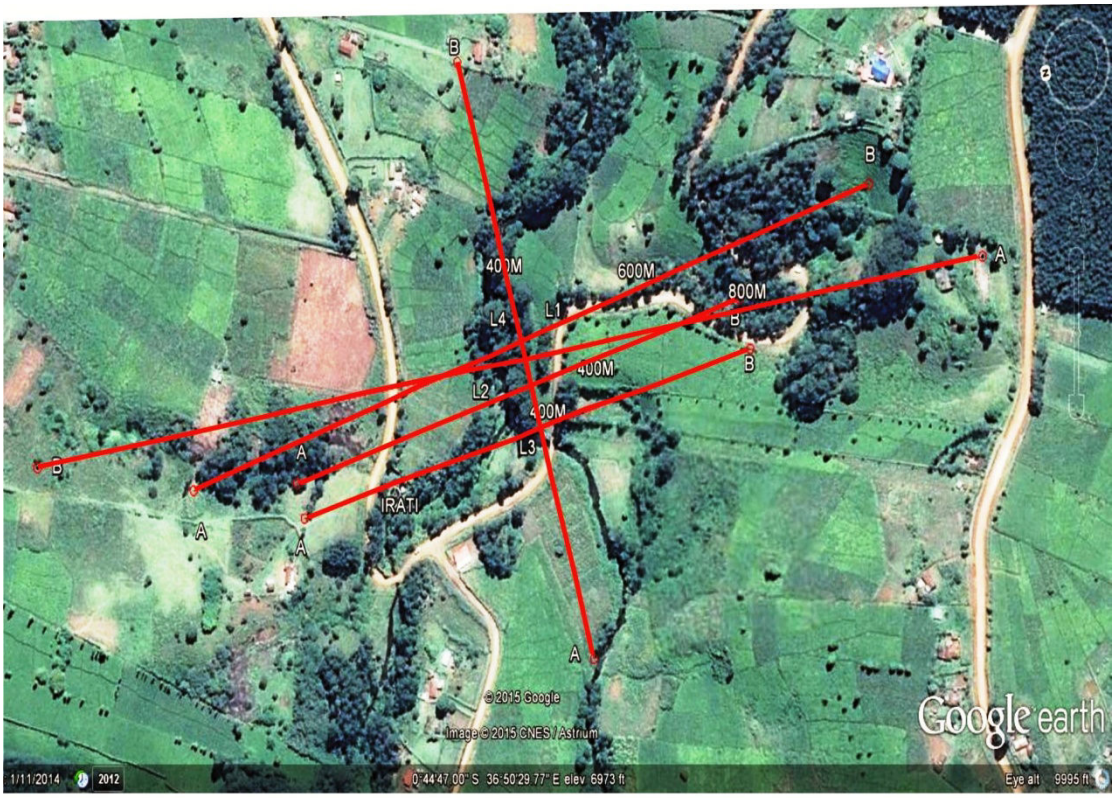

Figure 5.16 Google earth map of Irate site, showing the five ERT profiles layout

5.3.1 ERT 800 m profile

The 800m main profile was performed along the tunnel route in a SSW-NNE direction a shown in figure 5.17.

The geo-electric model indicates four distinct lithological zones namely: pyroclastic rocks, weathered basalts, highly weathered agglomeratic basalts and very highly weathered agglomerates within the probed section.

The top layer is comprised of pyroclastic rocks (2,000-10,000 Ω m) to a depth of about 5m on average and stretches across the whole section except for the river valley where it has been eroded.

The weathered basalt (1,000-1,400 Ω m) occurs as an oval shaped rock overlain by the pyroclastic rocks and underlain by very highly weathered agglomeratic basalts.

Very highly weathered agglomeratic basalts with resistivity range between 5-40 Ω m takes the shape of a broken basin below the pyroclastics, the layer encloses very low resistivity clays.

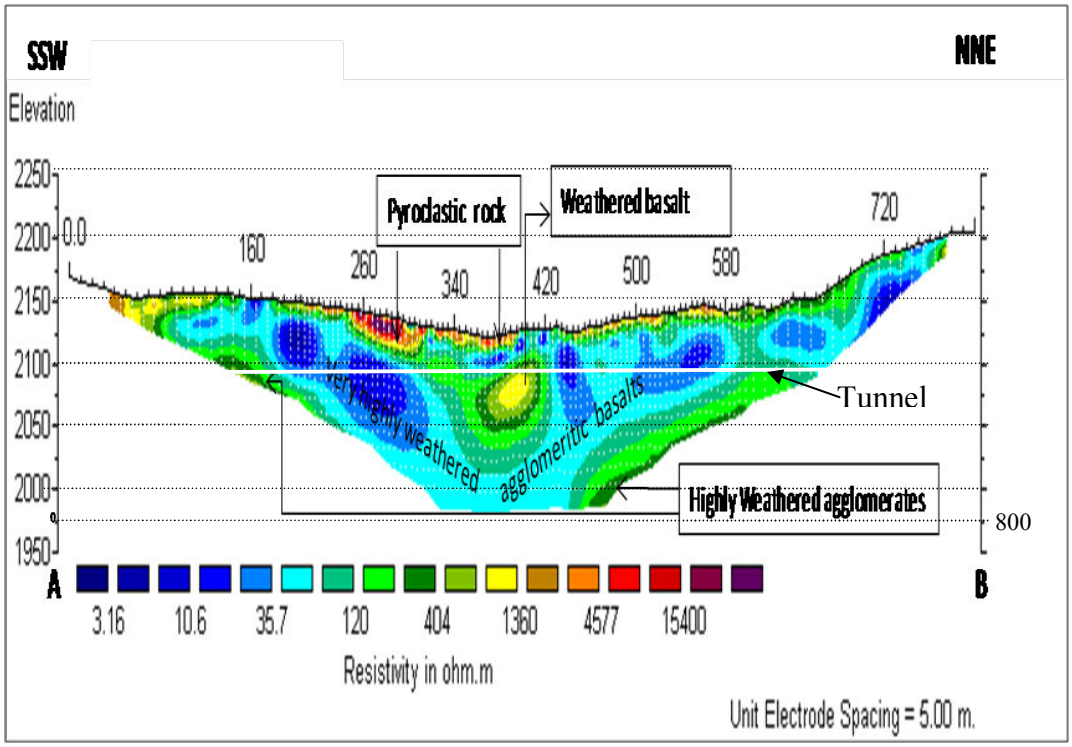

Figure 5.17 ERT 800m traverse at Irate site

5.3.2 Profile ERT –Irate line 1 (L1)

The ERT traverse L1 was carried out NNW-SSE direction; the area slopes gently towards the valley and then rises sharply to the southern end. The interpreted geo-electric model is presented in Figure 5.18.

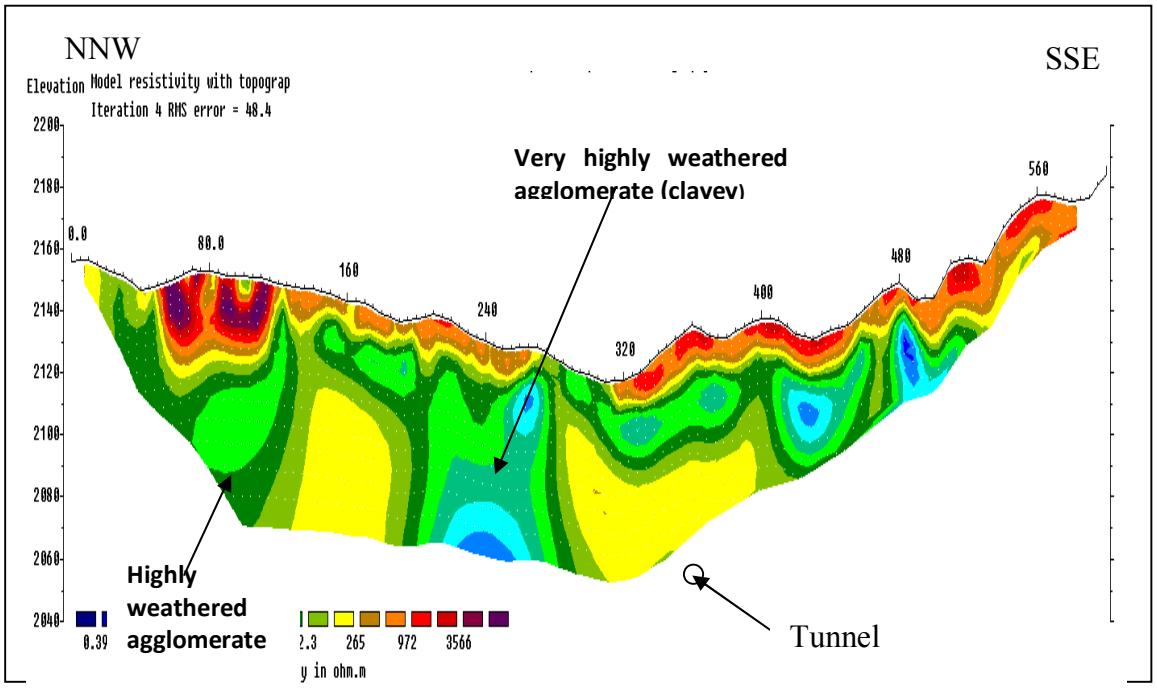

Figure 5.18 ERT 600 m traverse (L 1) at Irate site.

The interpreted geo-electric model indicates two major geological units consisting of pyroclastic rocks at the surface and the basaltic agglomerate which occurs as highly weathered to very highly weathered rock mass.

The pyroclastic rocks (1,000-6,000 Ω m) cover the top 5-10 m and stretches almost over the entire profile except at the valley bottom. Underlying the pyroclastics are the very highly weathered agglomeratic basalts that occurs between two segments; the eastern unit takes a laccoliths shaped structure and is separated from the pyroclasts by a layer of highly weathered agglomerate. This is a thin layer occurring between the pyroclastics and the highly weathered agglomerates. Further on, the layer attains a uniform thickness of about 20m and stretches over a distance of about 120 m (i.e. 280 – 400 m mark); the western portion of the profile consist of the pyroclastic rocks at the surface overlying the highly weathered agglomerates which extends to the bottom of the probe, the agglomerates encloses pockets of heavy clays.

At around 240 m mark on the horizontal distance, a second a plug shaped unit of very highly weathered agglomeratic basalt occurs under the pyroclastics and extends to a depth of about 60m below. Clay with resistivity below 5 Ωm is enclosed within this layer.

The feature identified as oval shaped weathered basalt along 800 m segment is also noted along L1. However, along L1, the basalts indicate increased weathering i.e. 500-1500 Ωm along 800 m segment compared to 300-500 Ωm along L1. It could therefore be inferred that weathering intensity increases westwards.

Resistivity/structure relationship

Two main structural units can be inferred from the model, the horizontal surface layer composed of pyroclastic rocks with a deep layer of soil at the surface.

Fractured agglomeratic basalts with south easterly dipping fractures are indicated by thin lines with sharp resistivity contrast. Borehole 4A (appendix 6) drilled at (259676.34) (9917893.8) reveals absolutely no material recovery for the first 20m and intermittent material recovery between 65 and 75m in fractured portions of the rock. Notably, clay materials and buff colored basalt are identified from the core logs, these information validates the ERT results. In addition, the poor recovery can be attributed

to the nature of pyroclastic material which have low compaction values and their deposition lacks continuity.

5.3.3 Profile ERT –Irate line 2 (L2)

The profile was carried out in the NNW-SSE direction along the river valley. The interpreted pseudo-section is presented in Figure 5.19

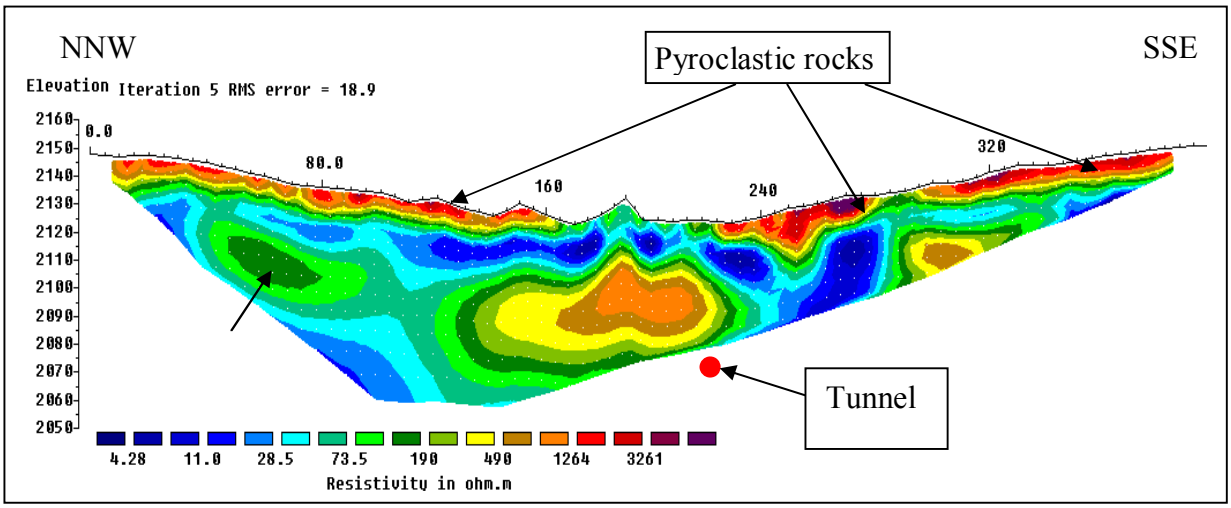

Figure 5.19: ERT 400m traverse (L 2) at Irate site

The interpreted geological model indicates a thin layer of pyroclastic rocks covering 10m depth from the surface along the profile. Along the river valley the rocks have been eroded and a thin layer of highly weathered basaltic rock is exposed.

The very highly weathered agglomeratic basalts (20-100 Ωm) occur at the middle of the profile forming a ridge which separates the two streams joining irate river. These agglomerates attains a thickness of about 20m stretching over the entire profile and encloses discontinuous len-shaped layers of very highly weathered basaltic agglomerates at a depth of 30m.

Below the agglomerates a less weathered basaltic layer forming an oval shape structure and with resistivity range (300-500 Ωm) occurs at a depth between 20 and 50m below the ground, the degree of weathering decreases towards the inner parts of the rock .The tunnel is expected to pass through these zone.

5.3.4 Profile ERT-Irate line (L 3)

The traverse was carried out in the NNW-SSE direction, with a broad valley and gentle slopes on either side. The interpreted geo-electric is presented in Figure 5.20.

The geo-electric model indicates a similar lithostratigraphy to that of L2. The pyroclastics form the top most geological unit averaging a thickness of 10m but at the valley bottom they have been completely eroded. Borehole 4A reveals 5m of red soil and no recovery of the core at shallow depth and in fractured zones; lack of recovery results from the highly weathered nature of rock encountered. The borehole results validate observation made from the geo-electrical model, which indicate that the borehole was drilled through highly weathered agglomeratic basalts with poor core recovery within agglomerates. Thomsons (1964) describes the red soil to result from weathered basaltic rocks.

The low resistivity (less than 100 Ωm) of the agglomerates is an indicator of the aquiferous nature of the rocks. Indeed groundwater was struck at a depth of 2m below the ground. Below the highly weathered agglomerate is the weathered basalt as noted also at Line 2 but the degree of weathering is slightly higher.

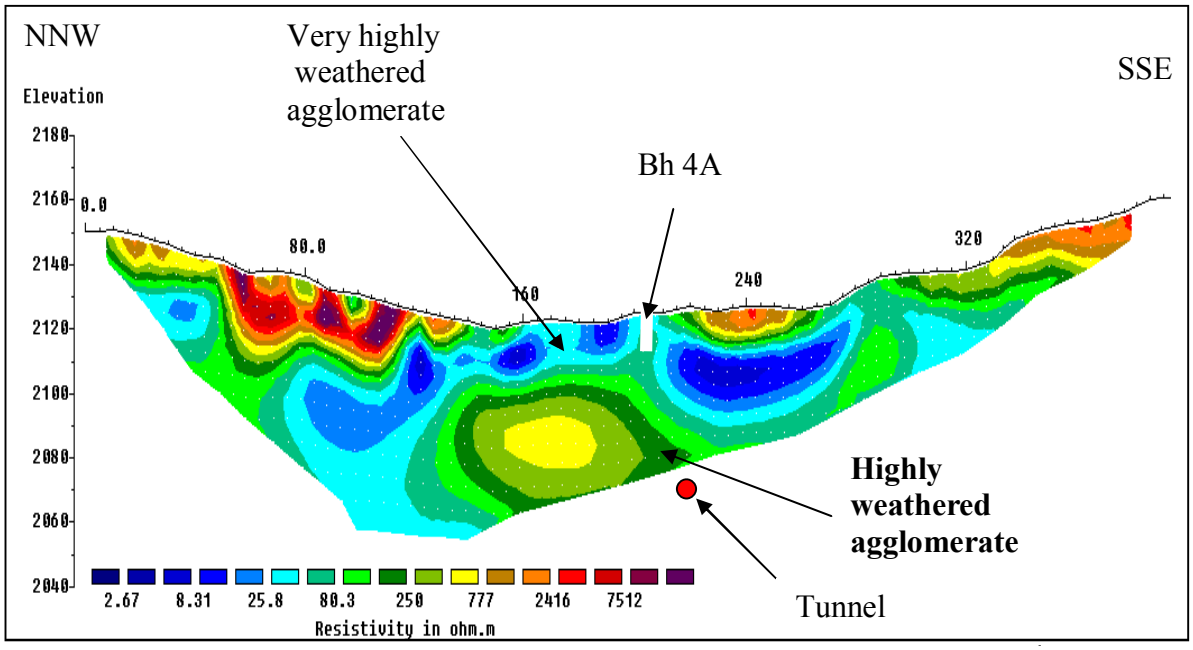

Figure 5.20: ERT 400m traverse (L3) at Irate site.

5.3.5 Profile ERT-Irate line 4 (L4)

The ERT Line 4 was carried out in W-E direction, on a generally flat ground to the west, while on the eastern part the ground forms small ridges. The interpreted geo-electric section is presented in Figure 5.21.

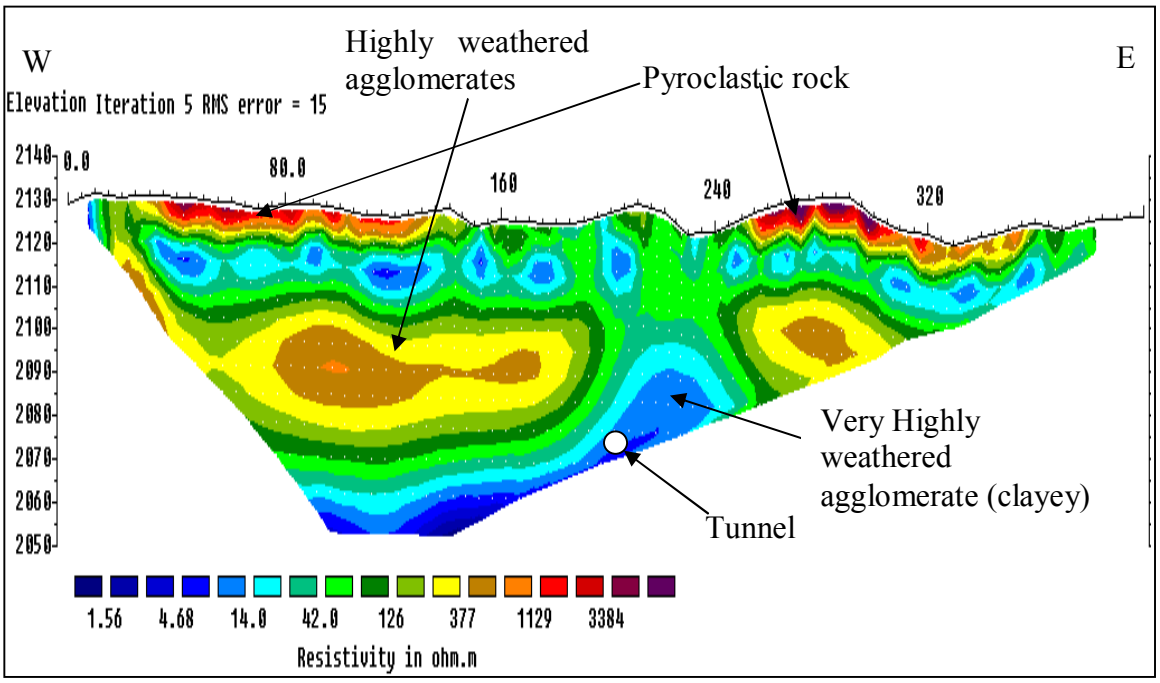

Figure 5.21: ERT 400m traverse (L4) at Irate site

The Profile 4 cuts across L1, 2 and 3 and presents the following geological units; Pyroclastic rocks with resistivity ranging from 1,000 to 4,000 Ωm occurs into segments i.e. 0-150m and 250-400m attaining a thickness of about 5-10 m.

A thin layer of about 10m of very highly weathered agglomeratic basalts occur as from 20m mark and stretches along the entire profile. However, between 200-240 m mark the layer of very highly weathered agglomeratic basalt open to earth surface. At a depth of 50m the agglomerates grades into clay of very low resistivity.

Between a depth of 15m and 60m a tongue shaped layer of highly weathered clay is enclosed between the very highly weathered agglomeratic basalts and the pyroclastic rocks at the surface.

5.4 Kaanja Site

Two traverses as indicated in Figure 5.23 were carried out at this site with the main 800m profile running in NW-SE direction and cut perpendicularly by a shorter profile covering a distance of 600m. The surface indicates deep layers of red volcanic soils with several minor landslides observed at the slopes.

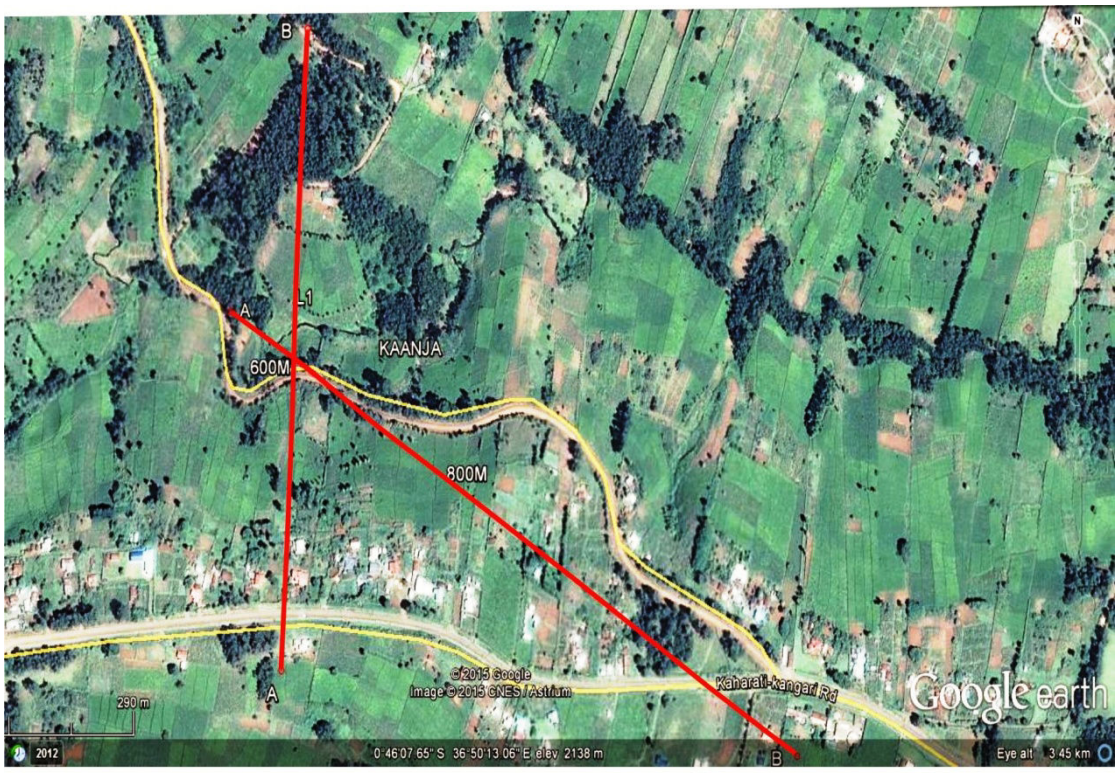

Figure 5.22. Google earth map of Kaanja site, showing the two ERT profile layout

5.4.1 Profile ERT-Kaanja 800m.

The Profile was performed along steep topography in a NW-SE direction from river valley to Miiri shopping centre. The geo-electrical model is as shown in figure 5.23.

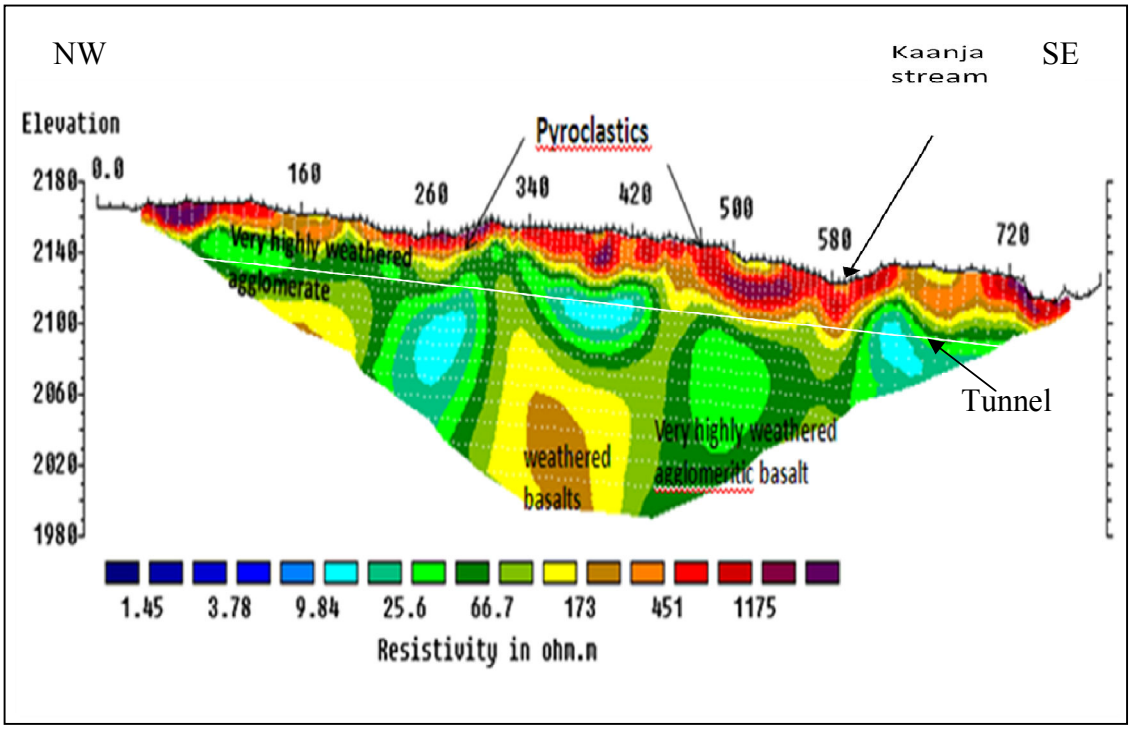

Figure 5.23: ERT 800m main traverse at Kaanja site.

The model reveals three lithological units i.e. pyroclastic rocks, very highly weathered agglomerates and weathered and fractured basalts.

The model presents a high resistivity layer (451- over 1,175 Ωm) at the earth surface; this is characteristic of top dry soil as observed at the road cut and the drill cores from borehole 7A drilled along the profile. The layer covers a uniform depth of 15m and runs along the surface of the whole the profile, a thin layer of about 5m lying horizontally separates the pyroclastics from the highly weathered agglomeratic basalt which extends from 15m to the bottom of the probed depth at 160m.

The depth below 15m is dominantly characterized by weathered agglomeratic basalts of varying degree. The very highly weathered agglomerates with resistivity ranging from 10-30 Ωm (i.e. dark and light blue polygons in Figure 5.24) occur as isolated features with almost a common depth. It could therefore be inferred that it represents a lithology that was mechanically weaker and therefore became completely decomposed.

The higher resistivity body at the base of the profile (150-450 Ωm) can be extrapolated to join a similar layer at 160m forming a confined aquifer in between. The basal layer is comprised of weathered and fractured basalt with a ridge like

structure (with resistivity above 500 Ωm) extending from 300 – 420 m mark and with the top most part occurring 70 m bgl (Fig. 5.23).

Resistivity/Structural relationship

All along the profile, significant lateral variation define sub vertical NNE dipping discontinuities with the sharp resistivity contrast occurring within homogeneous resistivity units. The thin layers may be inferred to be fractures or fault lines. Normally, the fault zones are characterized by lower resistivities due to high permeability.

5.4.2 ERT Profile Kaanja site line 1 (L1)

The ERT traverse was carried out in the S-N direction cutting the 800m line. The interpreted geo-electric model is presented in Figure 5.24.

The ground slopes steeply from the south towards the river valley at the central part of the profile. The valley is about 60m wide, the ground then rises to near vertical at 320m before rising gently towards the northern end.

The geo-electric model shows pyroclastic rocks at the surface running across the whole length of the profile; the rock thickens at the ridge section covering a depth of 40m at the top and thinning towards the valley bottom.

Notably, the pyroclastics on the southern side have higher resistivity (600-3,000 Ωm) compared to those of northern side (300-500 Ωm); this can be attributed to have resulted from difference in moisture content between the two sides.

Below the Pyroclastic surface is a 90m layer of very highly weathered agglomerates which runs through the entire profile; this is a high resistivity basaltic layer forming the base of the section.

The southern end is formed of fresh basalt at 60m below the surface forming concentric layers. On the northern side, the basalt has weathered and fractured with a buried relic tor-like structure. From the topographical and underground conditions the valley bottom between 230 and 410m mark seems to be a down-warped segment with the fault scarp localized at the two buried ridge like structures. Small spring cuts through the slopes exposing basaltic outcrops along the gulleys.

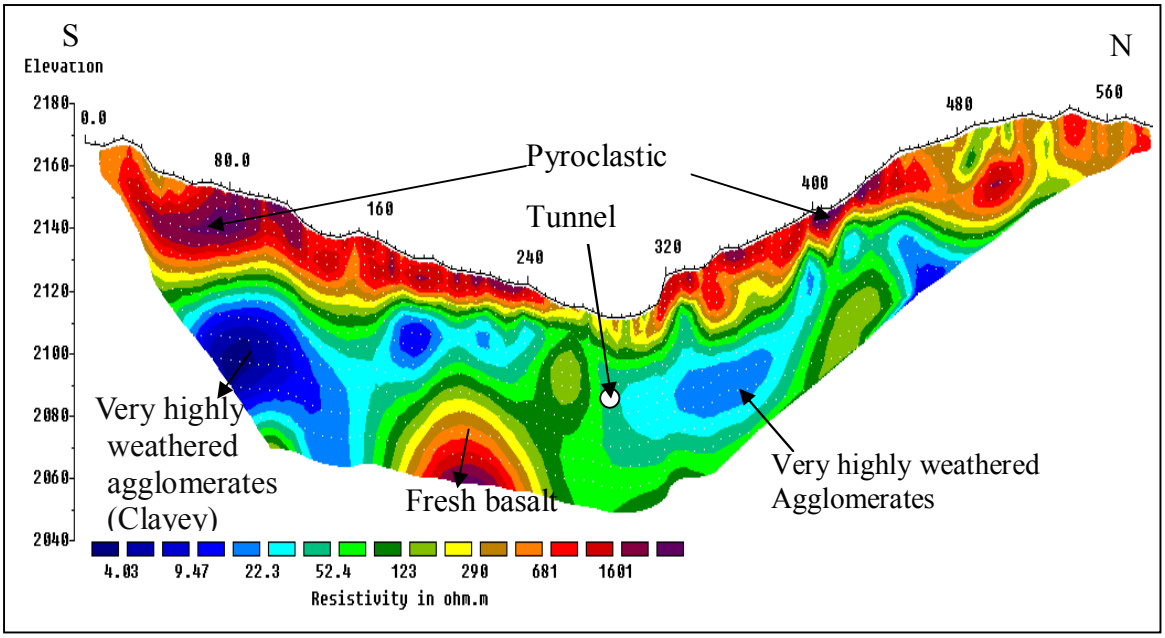

Figure 5.24 ERT profile at Kaanja site-L2

5.5 Makomboki Site

The site is within a deep valley, with the Gathika River at the valley bottom flowing towards Ndakaini dam. The edges consist of steep slopes covered by tea plantation and small bushes.

A total of seven ERT traverses were carried out in the area as indicated in figure 5.25. An exit Portal, erosion protection works and energy dissipation structures will be constructed at this site.

Figure. 5.25 Google earth map of Makomboki site, showing the Seven ERT profile layout.

5.5.1 Makomboki 800 m Profile

The 800m Profile was carried out along steep valleys slopping towards the Gathika River outfall; this is the zone where the exit portal will be positioned. The traverse was performed in the SSW – NNE direction. The topography rises steeply from the western side for about 260m to a flat surface towards the end of the traverse. The interpreted geo-electric is presented in Figure 5.26.

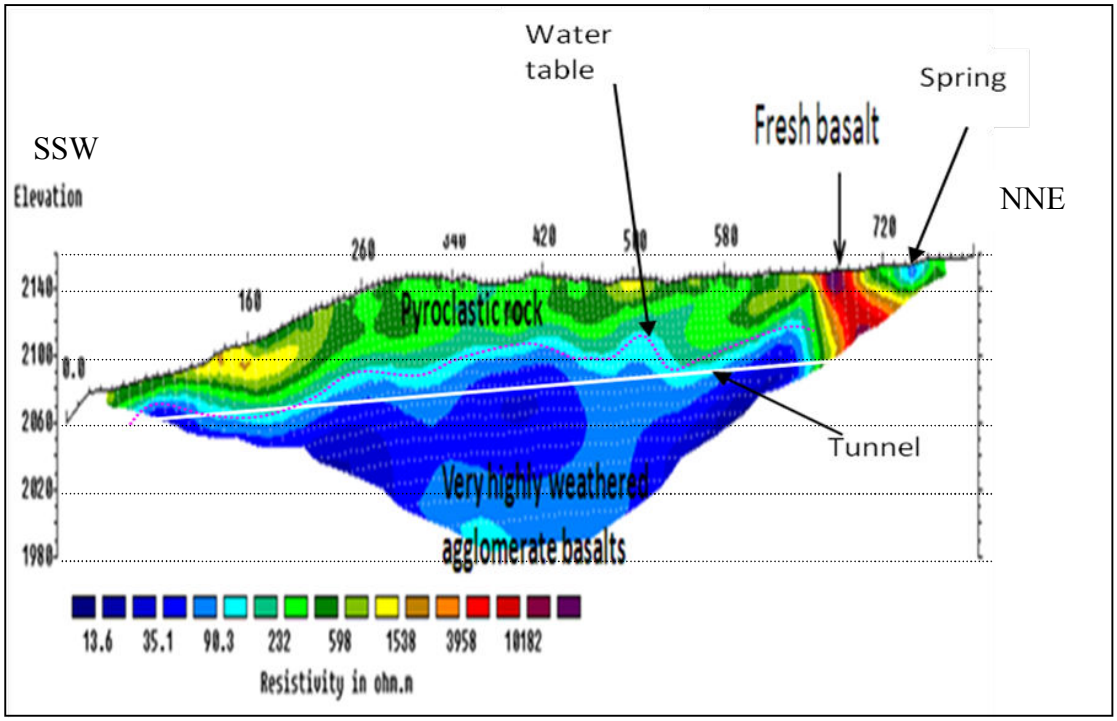

Figure. 5.26: ERT 800m profile at Makomboki site

From the geo-electric model, three geological units can be identified namely; pyroclastic rocks, very highly weathered agglomeratic basalts and fresh and massive basalts (Figure 5.26).

The model indicates small pockets of pyroclastic rocks within deep layer of red volcanic soil at the surface. This layer is underlain by very highly weathered agglomeratic basalts with resistivity ranging from 20 – 100 Ω at a depth of 30m below the ground. The zones with resistivity between 20-40 Ωm within the very highly weathered agglomeratic basalts denote aquiferous formation.

Between 10 to 15 m, a layer averaging 3m separates the highly weathered agglomerating basalts from the pyroclastic rocks at the surface. This layer dips at an angle of 75^{o} towards the end and marks the start of a mass of fresh basalt protruding at the surface, the basalt exhibits very high resistivity (3000 to 10,000 Ωm)

Although the probed depth towards the end was shallow (25m), extrapolating the formation deeper reveals weathered and the fresh basalt towards the bottom, the layer provides a strong base for construction of structures.

5.5.2 Profile ERT-Makomboki (L 1)

This ERT profile was carried out in the NE-SW direction as indicated in figure 5.27. The profile passes through a zone affected by a land slide near Gathika River.

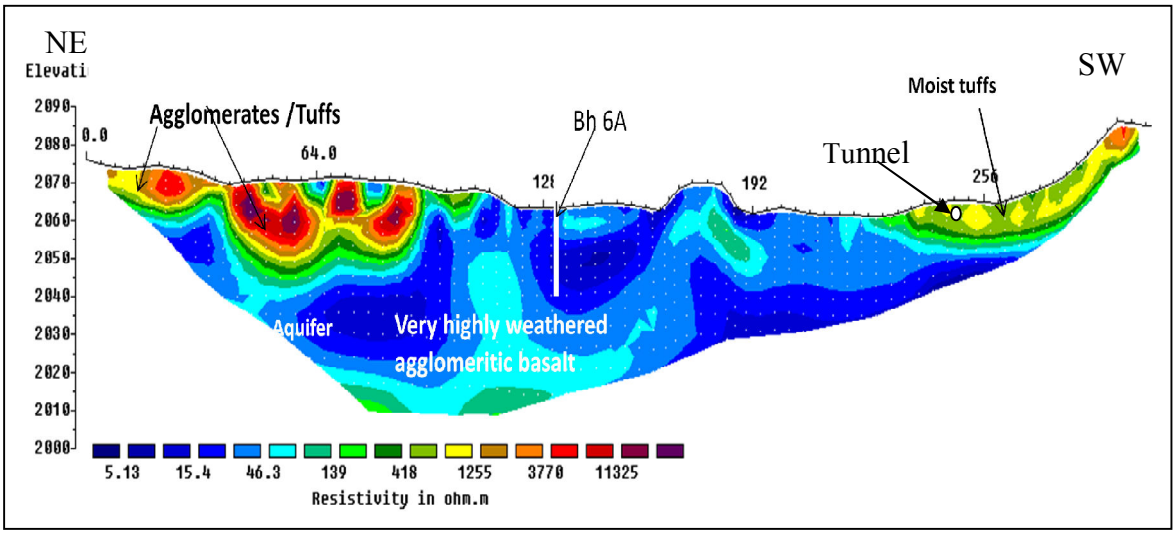

Figure 5.27: ERT profile (L 1) at Makomboki site

The interpreted geo-electric model reveals three zones of differing resistivity (Figure 5.27). Pyroclastic rocks consisting of welded tuffs cover the surface to the extreme ends. Between 0 to 95m, the pyroclastic rocks covers a depth of 25m, the zone has been affected by weathering, erosion and later deposition as shown by the wavy narrow layer separating the pyroclasts from the agglomeratic zone. Weathering is more pronounced along the river and extends to 60 m of the probed depth.

5.5.3 Profile ERT- Makomboki (L 2)

The ERT traverse runs in NNW-SSE direction (Figure 5.25). The interpreted geo-electric model is presented in Figure 5.28.

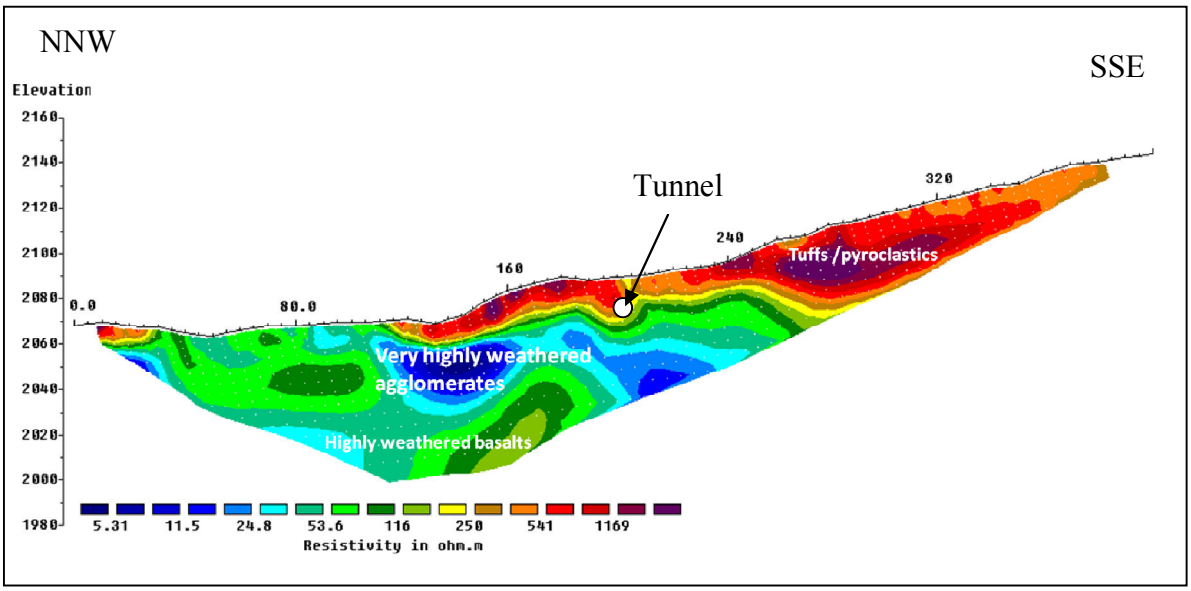

Figure. 5.28 ERT 400m traverse (L 2) at Makomboki site

The geo-electric model shows a gentle land surface near Gathika River which rises steadily to the South (Figure 5.25). The model indicates pyroclastic rocks with resistivity ranging from 500-1500 Ωm, very highly weathered agglomeratic basalts and highly weathered agglomerates (figure 5.28).

The pyroclastic rocks cover the top 5-10m of the earth surface from NW breaking at the valley bottom where weathered agglomerates are exposed. On the eastern slope the pyroclastic resurface. These pyroclastics are characterized by rounded very high resistivity (over 2,000 Ωm) rock mass that mark non-porphyritic fresh basalts; a common feature amongst Laikipian pyroclastics.

The pyroclastic rocks are underlain by flat – lying very highly weathered agglomeratic basalts that coincidently stretch within the targeted segment along L1 covering a distance of about 130 m. These agglomerates are characterized by resistivity values distributed within a narrow range i.e. 18 – 40 Ωm, which connotes presence of groundwater. It therefore follows that most of the springs emanating from the cliff (scarp) have their source from this geological unit. However, towards south western end (near point A) the resistivity drop sharply to below 8 Ωm, which represent a clayey formation that extend over a distance of about 30 m.

The basal layer along L2 is marked by highly weathered agglomerates that resemble a crest of some sort of a ridge whose western limbs are more weathered compared to the eastern side (i.e. resistivity of 8 compared 55 Ωm). This western limb could mark a fractured zone whose infilling geological material has become completely weathered to clays.

5.5.4 Profile ERT-Makomboki (L3)

This ERT traverse was carried out in the W-E direction cutting the 800m line, the profile is along a gently sloping ground in the west which falls along the river valley before rising to the east. The interpreted geo-electric model is presented in Figure 5.29.

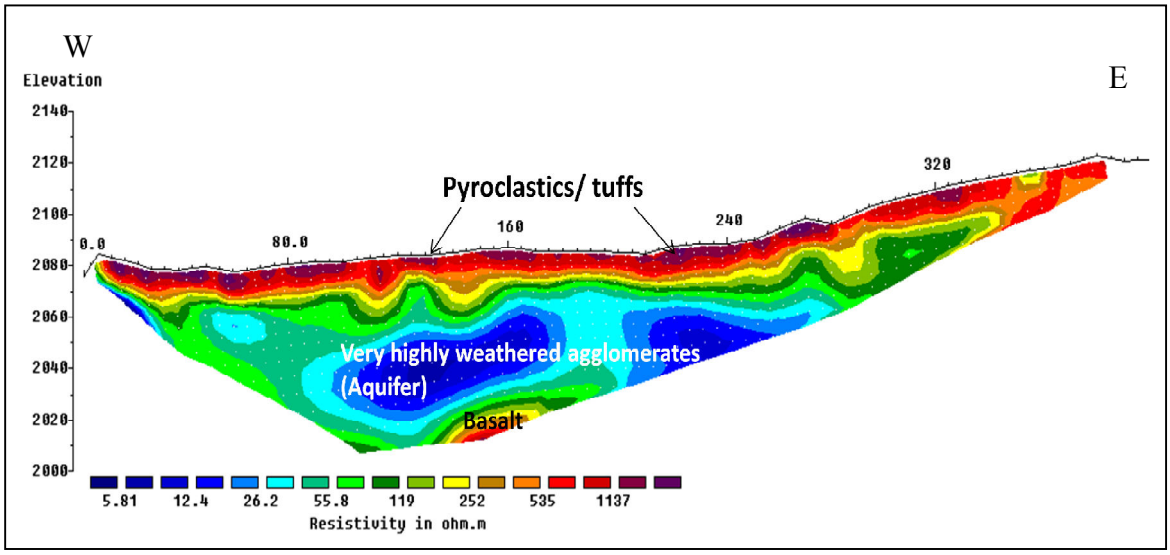

Figure 5.29 ERT 400m traverse (L 3) at Makomboki site

The geo-electric model shows characteristics similar to line 2, although in Line 3 the surface of pyroclastic rocks runs throughout the surface from western to eastern edge at a uniform depth of 5m. Notable are the difference in resistivity between the western side (1,000 and 3,000 Ωm) to (600 and 1,000 Ωm) in the eastern end. This can be attributed to difference in surface recharge between the flat and sloping grounds.

Below the pyroclasts, 15 m and 80 m depth, is an ellipsoidal layer of highly weathered agglomerates. The resistivity increase towards the middle where it completely decomposes to clay.The basal layer is formed of highly weathered agglomerates overlying a dome shaped high resistivity layer which is inferred to be fresh basalt.

5.5.5 Profile ERT-Makomboki (L 4)

This ERT traverse was carried out in a W-E direction and cutting through L1, the profile can be defined into three main zones.

Zone 1 running from 0 to 190m along the horizontal, zone 2 the valley section from 190 to 300m, and zone three from 300m to the end of the profile. The interpreted geo-electric model is presented in Fig 5.30.

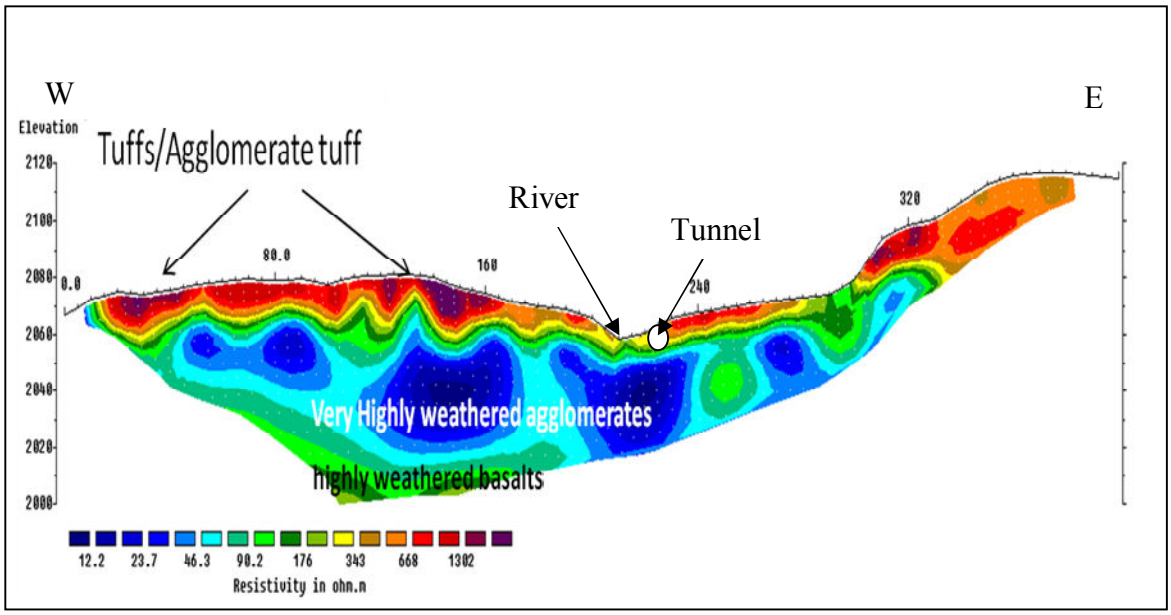

Figure 5.30 ERT 400 m traverse (L 4) at Makomboki site

Zone 1 can be described as the deepest section probed, 90m at the deepest, like L3 the pyroclastic rocks covers the top portion of this zone and runs across the entire profile maintaining a thickness of 5m and resistivity ranging between 500 and 2,000 Ωm.

Below the pyroclastic surface lies a 65m depth layer of highly weathered agglomerates (90 to 200 Ωm),the layer encloses a zone of low resistivity (less than 10 Ωm) whose degree decreases towards the middle. This formation may be interpreted to be weathered basaltic boulders. The pyroclastic layer is relatively thicker along zone 1 and 3 as compared to zone 2.

The tunnel is expected to cut through the rock layer with a resistivity of 50 Ωm, the rock is very highly weathered and is aquiferous.

5.5.6 Profile ERT-Makomboki (L 5)

This ERT traverse was carried out in the NW-SE direction along a gently sloping ground to the NW, falling sharply at the centre before rising gently towards the end. The interpreted geo-electric model is presented in Figure 5.31

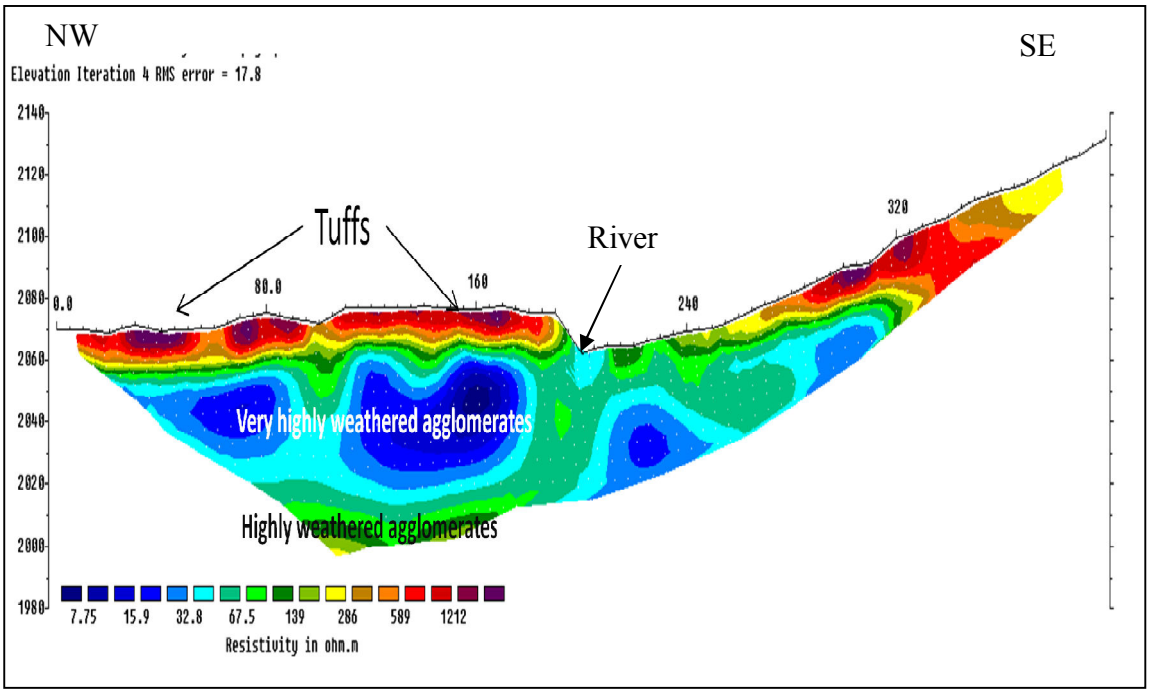

Figure 5.31 ERT 400m traverse (L 5) at Makomboki site

The model indicates a probe within welded tuffs at the western side (as exposed in an old quarry site along the river valley). The tuffs occurs as a thin layer of the pyroclastic material, which form a layer of uniform thickness stretching over a distance of about 185 m at the surface and is interpreted to a depth of 5-10 m. Within the valley, the pyroclastic materials have been eroded and the highly weathered agglomeratic materials are exposed at the surface. To the further east, the tuffs terminate against a steep high resistivity basaltic rock.

The very highly weathered agglomeratic basalts forms a basin shaped structure and stretches over a distance of about 50m. The thickness of this formation is about 45m. The central part of the profile shows a layer of very highly weathered agglomerates enclosing zones of very low resistivity that connote presence of clay. Like in L4, the

tunnel will through cut a very highly weathered rock but with a relatively higher resistivity.

5.5.7 Profile ERT-Makomboki (L 6)

This ERT traverse was carried out in the NW-SE direction as indicated in Figure 5.25and parallel to line 5. The interpreted geo-electric model is presented in Figure 5.32

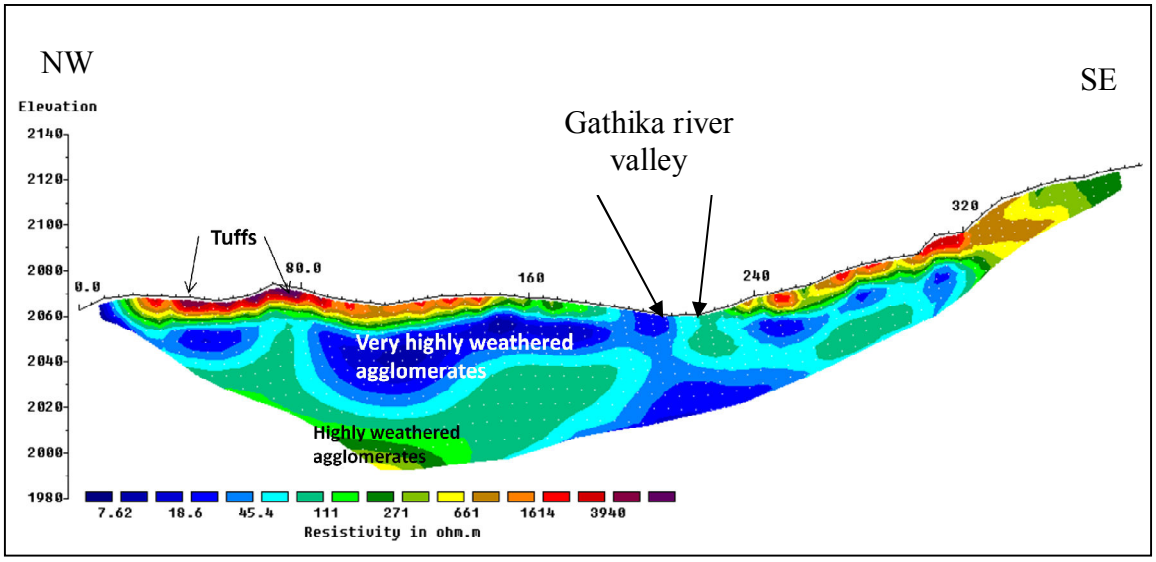

Figure 5.32 ERT 400m traverse (L 6) at Makomboki site

Three zones can be defined from the NW between 0 to 160m with a maximum probed depth of 160m towards the middle and a depth of 5 m at the start of the probe. The topography is generally flat with minor crests and troughs. The Pyroclastic rocks with resistivity 500 to 1,000 Ωm cover the top 3m, this surface overlies a very highly weathered basaltic layer to a depth of 60m. Pockets of clay material with very low resistivity (less than 7 Ωm) are enclosed within the basaltic layer.

Below 65 m, is a highly weathered layer of basaltic agglomerates (45 to 650 Ωm) which extends to the base of the probed depth.

The middle section of the profile shapes into a narrow valley, steepening towards the east, this area is highly weathered, with some springs coming out to the surface between the unconformities. Towards the end of the profile, resistivity increases at the surface and decreases towards the bottom; this can be attributed to reduced moisture content at the slopes.

CHAPTER 6: DISCUSSION

6.1 Discussion of the Results

The proposed tunnel construction sites are within volcanic ridges, basaltic boulders and phonolites from the Abadares Mountains are common along Maragua and Irate rivers. The valleys are wide and U-shaped with the rivers dissecting through the valleys and generally following the topography.

The difference in elevation between Maragua intake at 2088m asl and Makomboki portal at 2064m forms a good gradient for flow of water through gravity. This makes the selected sites good for intake structures and other engineering works. The occurrence of ridges between the target rivers makes abstraction of water through gravity difficult, pumping is also too expensive and uneconomical to manage and therefore the need for construction of an underground tunnel.

The ERT images and the site investigations reveal different lithological units at the pre-selected sites with the resistivity values defining the actual geological conditions at particular depths, from the topographical data a cross-section of the proposed tunnel is presented in figure 6.1

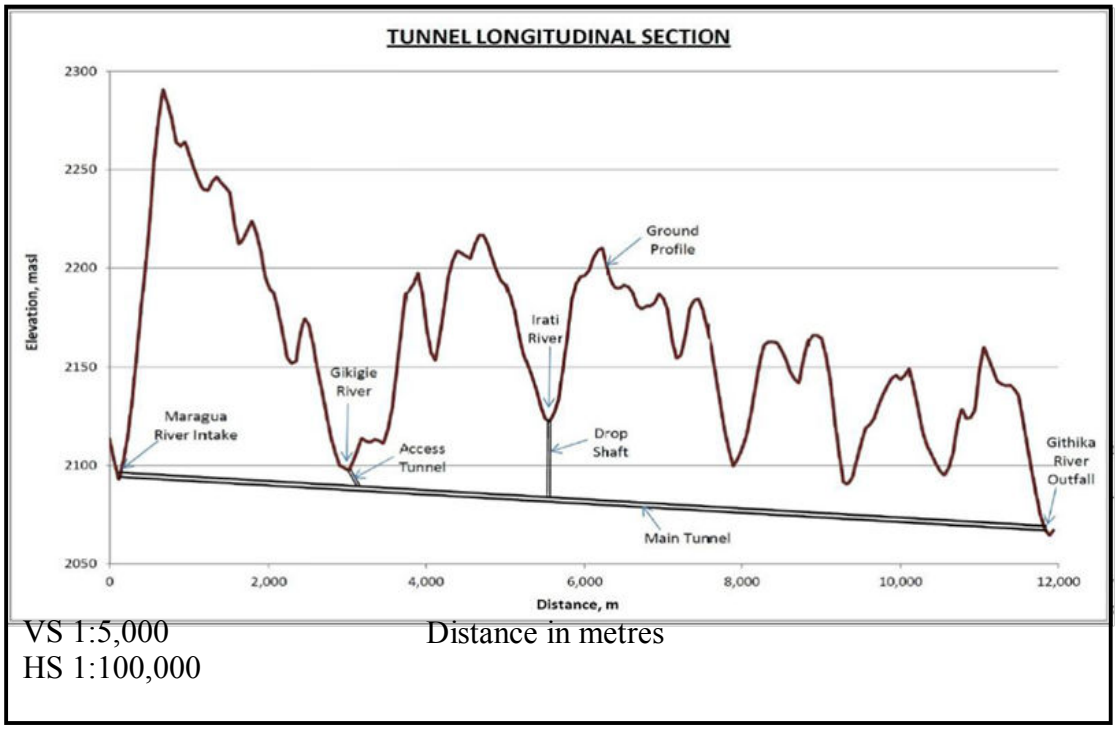

Figure 6.1 Cross-section along the proposed Tunnel from Maragua intake to

6.1.1 Maragua site

The site is within a broad valley at an elevation of 2088masl, the river cuts across the valley bottom where the topography starts rising gradually to 2270m at the top of the ridge. Large phonolites boulders from the abadares are common at the river bank, the meandering river indicates reduced river velocity. The low river velocity and the nearly flat valley form a good site for construction of the abstraction chambers and other surface engineering structures.

Although the basalts form the major geological unit, field observations combined with ERT data interpretation; reveals a surface layer of 3m average thickness of red soil underlain by a 5m layer of pyroclastic material which thickens along L2 and L4 making the area around L 2 and L4 the most ideal for engineering structures. L 2 and 3 which runs parallel to each other and perpendicular to 800m Line shows almost similar characteristic but with a relatively broader layer of pyroclastic surface.

Pyroclastic rocks are common at the surface along all the lines probed with the depth and continuity increasing at L 3. Very highly weathered agglomerates with pockets of clay dominates bottom layers .With the pyroclastic covering an average of 10m at the surface and overlying a less weathered layer of basaltic rocks at almost all the six profiles, the conditions are ideal for construction of cross weir and water abstraction chambers, the firm base can support masonry works and pressures exerted by water at the surface. The low gradient and rising topography at both sides of the valley makes it easy for damming of water.

The weathered nature of rocks makes it easy to excavate and will create no difficulties during the construction of the adit.

The inlet adit is expected to cover a depth of 10 m, excavation will be through the high resistivity layer (1000-5000 Ωm) consisting of weathered pyroclastic rocks intercalated with weathered basalts. The ground is expected to be unstable and therefore the need to construct supporting structures to prevent collapsing of the tunnel.

The tunnel penetrates the ridge from the valley and passes through highly weathered agglomerates (10-100 Ωm) at a depth of 170 m below the ridge. The invatigation reveal aquiferous nature of the formation at this depth and groundwater ingress into

the tunnel is expected to create challenges during the construction. However, use of impermeable roof membrane is expected to avert the situation

6.1.2 Irate site

Several relics of landslides have taken place at this site, a cross weir and a connecting shaft is expected to connect to the main tunnel at 40m below the ground.

A layer of pyroclastic material cover the top 10m depth of the probed depth, at the river valley,erosional activities have removed significant portion of the surface exposing a thick layer of very highly weathered basalts. This is the section where the cross weir will be constructed, and it will lie on 2m of pyroclatic rock, the rock is expected to bond firmly with the concrete. The vertical shaft will penetrate through the highly weathered basalts, the weathered and loose nature of the rock is predicted to be unstable and may collapse during boring. The aquiferous nature of the rocks creates a possible Influx of groundwater to tunnel, interfering with the tunneling process.

Basaltic rocks weathers to form kaolin soils, increased moisture in the soils causes change change in volume and when combined with steep slopes, movement down slope is easily triggered, indication Pockets of clay by the geo-electric section at the near surface at this site explains the reason why the area is prone to landslides. The pyroclastics at the top surface will form a good base for construction of surface structures. However, measures need to be put in place to prevent influx of ground water when tunneling through the very highly weathered agglomeratic material at the depth of 40 m.

6.1.3 Gikigie Site

The tunnel is expected to pass at 15 m below the ground at this section fig 6.1.0, although the pyroclastic rocks at the surface forms stable ground for surface structures, the mixed lithologies at the underground is expected to pose some challenges during construction. The connector tunnel will be constructed through fairly weathered agglomerates and join the main tunnel at 15 m below the surface.

Between 160 and 260m along the profile the tunnel is expected to cut through very highly weathered agglomerate with pockets of clayey material. Between 260 and 310, dipping stratas and a weathered basaltic boulders will be encountered, a mechanically

weaker zone; the tunnel is also expected to cut through aquiferous layer as it passes this section.

6.1.4 Kaanja Site

The geo-electric model indicates a formation of pyroclastic material over highly weathered agglomerates.

The intake shaft will be constructed through a layer of high resistivity pyroclastic rocks from the surface, the pyroclast extends to a depth of 15m below the ground, the ground is expected to be stable for the structure support.

The shaft will connect the main tunnel at a depth of 20m. The main tunnel will cut through a layer of very highly weathered agglomeratic basalt, these layers will be easy to bore through and minimum challenges will be expected upto to the exit portal at Makomboki.

6.2 Challenges

Field data collection was undertaken during the Months of August to October 2013, this time corresponds with the short rains in the area, in most cases our programs were interrupted by rains and we had to extend our schedule. The Terrameter which make use of the principles of electricity was affected by lightening in a few occasions, causing interruption of data collection and a repeat of the activity to correct the values affected.

ERT data collection requires experienced and trained staff, and a supported staff who are quick to learn and carry out the field procedures. It was very difficult to maintain the same group of support staff at each site, at every site we had to train a new team, because of the distance between one site to the other and also because the period of data collection coincided with the peak season for tea picking in the area.

All the sites were hilly and covered with tea bushes making the work tedious and risky, making straight traverses was time consuming and chances of making errors were high. This problem was minimized by making use of GPS and at times employing a large number of support staff. On several occasions we lost electrodes in the tea bushes and we had to replace them.

CHAPTER 7: CONCLUSION AND RECOMMENDATION

7.1 Conclusion

The interpretation of the 27 geo-electrical models carried out in the five sites shows a general horizontal deposition of rocks in the five sites investigated. A depth ranging from the ground survey to about 200m was probed in the five areas and compared with coring data for depths ranging from boreholes drilled in the area.

Where the core drilling method did not yield any core results.The ERT image was able to compensate and the information obtained. Considering both the ERT results and the borehole coring data the actual ground conditions were established. The research concludes that;

The pyroclastic rocks covers an average depth of 5m in almost all the sites, it thickens at the ridge tops and thins out at the river valleys where it has been eroded. At Maragua site the thick layer of unweathered pyroclasts between profile 2 and 4 forms good grounds for construction of engineering structures. Agglomeratic basalt of varying degrees of weathering lies below the pyroclasts, the tunnel is expected to cut through the highly weathered agglomerate in most of the sections and minimum resistance will be expected during excavation.

All the five geo-electric models reveal pockets of clay within highly weathered basaltic agglomerates.

ERT geo-electric models at Kaanja reveal deep a layer of soil cover at the surface; the results are also comparable to `the thick layer of red soil at the road cut and validating the ERT results. The soils have weathered from the basaltic rocks, and are characterized by low density, high water content, this explains the frequency of landslides at the site during rains.

Vibrations during tunneling are likely to cause disturbance to the grounds at the areas close to the tunnel . At Irate and Kaanja sites where landslides have previously occurred more landslides are likely to be triggered during tunneling; this will be specifically in areas within steep slopes.

Although no obvious cavities and structures were observed from the ERT images the sharp vertical resistivity contrasts at Gikigie and Kaanja sites infers zones of varying mechanical behavior, probably joints, fracture or fault lines, the sharp edge at Gikigie 800m profile is projected from the earth surface to extend deep into the ground. Inclinations of fractures relative to the tunnel direction is expected to play important roles on the stress and strength of the tunnel

The rugged terrain provides a good site for tunnel construction, the Maragua River valley standing a 2088 masl and Makomboki outfall at 2064,a difference of 24m head and an estimated gradient of 0.002 percent makes the gravity flow of water possible.

The ERT investigation reveal highly weathered and aquiferous rocks within the five sites and at the proposed tunnel route,both Gikige and Kaanja site shows rocks which are highly fracturedand groundwater influx into the tunnel is expected to create challenges during the tunnel phase.

7.2 Recommendation

The research finds the site to be good for tunnel construction and recommends that before implementation of the project the following factors to be considered.

The pyroclastic rocks and thick layers of volcanic soils covers the valley surface where major engineering structures will be constructed, the loose pyroclasts have highly erodability, low compaction strength and are subject to shear and deformation when loaded. Stabilization of the pyroclasts and excavation of loose soils will ensure that the structures are constructed on a stable grounds. Where the water energy is high, energy dissipation structures should be constructed to minimize the effects of erosion to the surrounding environment.

The vertical shafts at Irate and Gikigie sites will cut through the pyroclastic material from the earth surface to basaltic agglomerates of varying weathering degrees, these agglomerates are also aquiferous .The weathered nature of the rocks make them easy to cut through, however the loose nature of agglomerates may create falling conditions into the shaft and therefore endangering life of personnel and equipment. Proper wall supports by concrete linings and culverts is recommended where fast falls

of boulders are encountered, also the method employed during excavation should have minimum disturbance to the surrounding.

Clay behaves differently under different conditions, the clays, especially the kaolinites and montimorillonites creates swelling conditions when exposed to water. The swelling conditions may fill the tunnel and reduces the excavation speed. Wet clays are also subject to deformation and flows when triggered. Further analysis of the types of clays is recommended to determine the types of the clay and where excavation difficulties are encountered, use of rapid setting cements and polymers are recommended to stabilize the formation.

The project is expected to greatly have an impact on environment, in terms of movement of equipment, clearing of vegetation and deposition of material. Economical use of soil and rock excavated will reduce dumping on the ground, the rocks can be crushed and be used in construction of the engineering structures and upgrading the roads, replanting of trees where vegetation has been cleared is also recommended.

Minor tremors due to vibration during tunneling are likely to be felt, these may cause landslides and even cause cracking of the building walls and water tanks. Where possible vibrations should be minimized and if not avoidable, people should be informed at the earliest time possible.

Construction of the under drain tunnel is expected to create a short term drawdown in areas adjacent to the tunnel, this is likely to reduce with distance from the tunnel, this could be mitigated by pre-grouting and adopting shorter construction to lining time frames. In long term driven tunnels should be sealed.

Groundwater table is expected to be above the adit crown levels and pore pressures are expected to be high, pre-installation of horizontal drainage pipes below the adits will invert pore water pressures reducing seepage ingress and maintenance of relatively low hydraulic gradient compared with critical gradient for piping failure.

REFERENCES

A.B, Terrameter (2006): ABEM instruments SAS4000/SAS1000, Lund imaging system instruction manual.

Beall, J.V. (1973): Mining's place and contribution. In: Cummins and Given (Editors), SME Mining Engineering Handbook. AIME, New York

Bickel, J.O., Kuesel, T.R., and King, E.H. (1996): Tunnel Engineering Handbook (Second Edition), Chapman & Hall.

Bell, F.G.(1972): Geology and construction. Blyte Nottinghamshire, United Kingdom.

Bullard, E.C, (1936): Gravity measurements in East Africa. Phil. Trans. Roy. Soc London.

Dobecki, T.L. and Romig .(1985): Geotechnical and Groundwater Geophysics, Geophysical Society of London.

Driscoll, F.G, (1986): Ground water and wells (2nd Edition). Johnson Filtration systems, St Pauls Minnesota.

Fairburn, W.A. (1963): Geology of North Machakos- Thika area Report No.59.Geological Society of Kenya.

Gevaerts, E.A.L. (1964): Hydrogeology of Nairobi area (2nd Edition) Water development division, Ministry of Agriculture.

Geological Survey of Kenya, (Degree sheet 52): Coloured geological map 134/2 Kijabe

Geological Survey of Kenya, (Degree sheet 52): Coloured geological map 134/4 Mangu.

Grant, F.S. and West, G.F. (1965): Interpretation Theory in Applied Geophysics, McGraw-Hill, New York.

Gregory, J.W. (1921): The Great Rift Valley and Geology of East Africa. Seeley Service. London.

Griffiths, D.H. & Baker, R.D (1993): Two-dimensional resistivity imaging and modeling in areas of complex geology. Journal of Applied Geophysics.

Hemeda, S. (2013): Australian Journal of Basic and Applied Sciences.

Kenya Meteorological Department. (2001): The Climate of Nairobi and the Surrounding areas.

Kenya National Bureau of Statistics. (2010): 2009 Population and Housing Census results.

La Breezu, D.J. and Yang, X. (2001): Different inversion of ERT data; a first inversion method for 3-D Institution monitoring. Journal of environmental and engineering geophysics .Vol. 6, No. 2

Loke, M.H. (2002): Tutorials, 2-D and 3-D electrical imaging survey, Geotomo software.

Loke, M.H. (2000):Electrical imaging surveys for environmental and engineering studies; a practical guide to 2-D and 3-d surveys.

Maclin, S.R. and Field, G. R(1999): The response of London clay to full face TBM tunneling at West Ham, London Int. conf. on urban ground engineering, Hong Kong. 11-12 November 1998. London; Thomas Telford.

Mahtab, M.A .and Grasso, P.(1992): Geomechanics Principles in the Design of Tunnels and Caverns in Rocks, Elsevier Press.

Matsumoto, Y. and Takashi, N.(1991): Rock mechanics; University of Tokyo.

Ministry of Nairobi Metropolitan Development.(2008): Nairobi Metro 2030. "A world class African Metropolis. Building a safe, secure and prosperous Metropolitan."

Ministry of Water and Irrigation. (2004): Draft National Water Resources Management Strategy.

Ministry of Water and Irrigation. (2005): A Preliminary Report on the Groundwater Assessment of Nairobi and Its Environs (Unpublished Report).

Ministry of Water and Irrigation (2007): National Water Resources Management Strategy (NWRMS) 2007-2009. (Unpublished).

Ministry of Water Development.(1992): National Water Master Plan. Action Plan Towards 2000 part 2 vol. III. (Unpublished).

Mitchell, J, Baxter C.D.P. and Soga, K (1997): Time effect on stress deformation behavior of soil. In; Proc. Sakuro Marayama Memorial symposium, Kyoto,

Moukadaki, M.A., Karatzas, G .P., Pipadopoulou, M.P .andVafidis, A (2007): Identification of saline zones in coastal aquifer using electrical resistivity tomography data simulation. Water Resource Management.

Muff. (Maufe), H.B.(1908):"Report relating to the Geology of East African Protectorate". Col. Rep. Misc, No 45.

MWI/WSP (2005): Focus on Water Sector Reforms. Premier Issue February 2005. Ministry of Water and Irrigation (MWI) and Water and Sanitation Program-Africa (WSP) Nairobi. MWI/WSP (2005): Focus on Water Sector Reforms. Premier Issue February 2005. Ministry of Water and Irrigation (MWI) and Water and Sanitation Program-Africa (WSP), Nairobi.

NEMA. (2006): Environmental Management and Coordination Act.

Ngecu, W.M, Ichang'i ,D.W. (1999): The Environmental Impacts of Landslides on the Eastern Slopes of Mount Kenya. A case study of Maringa Village Land Slide. Journal of Environmental Geology, 38, No 3.

Oldenburg, D.W, Li. Y. and Ellis, R .G. (1997): Inversion of Geophysical data over copper gold porphyry deposit: "a case study for Mt.Milliga geophysics", Vol. 62. No 5.

Palacky, G.J. (1988):Resistivity Targets in Nabighian, Society of Exploratory Geophysics.

Parasins, D.S. (1962): Principles of applied geophysics. London; Methuen and Company Ltd.

Parker, H.W, (1996): Geotechnical Investigations, in Tunnel Engineering Handbook.

Shackleton, R.M. (1945): "Geology of Nyeri Area". Report No.12.Geological Survey of Kenya.

Shevinin,V., Delgado,O., Mousatov,A., Hernandez, D .F,Martinez ,H .Z,andRyjov,A.(2006):Estimation of soil Petro physical parameters from resistivity data; application to oil contaminated site characterization. Geofisica International.

Sikes, H.L. (1934): "The underground Water Resources of Kenya Colony", Geological Survey report of Kenya.

Telford, W.M, Geldrat, L.P.and Sherriff, R.E,(1990): Applied Geophysics 2nd Edition, Cambridge.

Terzaghi, K. (1946): Rock defects and loads on tunnel supports, Commercial Shearing and Stamping Co., Youngstown, Ohio.

Terzaghi, K.(1958): Design and performance of Sasmua Dam, Institute of civil Engineers.

Thomsons, A .O. (1964): Geology of Kijabe area, Mines and Geology report No. 67

Versteeg, B., Birkens, Sandberg, S .K and, Slate, L.(2000): Control imaging of fluid flow and saline tracer using time lapse GPR and electrical resistivity Tomography. Proceeding of symposium on the application of Geophysics in engineering and environmental problems.

Walhlstrom, E.E.(1973): Tunneling in Rock, Elsevier.

White, F. (1983): The Vegetation of Africa. UNESCO.

World Bank (2004): The Republic of Kenya. Towards Water Secure, Water resources sector memorandum, Water and Urban Africa region.

APPENDIX 1

Discharge Data Gikigie River (source WRMA Office Muranga)

Jan	Feb	March	April	May	June	July	Aug	Sept	Oct	Nov	Dec
-	-	-	-	-	-	-	-	-	4.904	78.755	24.431
13.645	8.533	-	111.725	56.382	8.892	9.64	8.082	5.271	12.732	21.094	16.098
13.998	16.214	6.688	72.158	81.12	46.754	12.231	8.129	5.667	9.723	12.468	10.288
5.758	5.544	4.689	9.878	53.777	28.156	9.231	1.573	6.865	7.01	57.235	26.619
9.339	5.214	8.263	63.148	78.995	14.021	7.024	5.999	4.864	4.787	-	-
-	5.498	3.511	28.457	140.938	-	8.615	9.096	10.259	20.143	75.365	28.11
9.914	5.19	3.505	9.141	166.502	80.306	15.161	13.149	11.038	26.341	27.845	13.039
7.735	2.406	1.898	-	1.736	1.801	-	-	-	-	-	-
-	-	-	-	-	-	-	-	-	-	-	-
-	-	-	-	-	-	-	-		-	-	-
-	-	-	-	-	-	-	-		-	-	-
-	-	-	-	-	-	-	-	-	-	-	-
-	-	-	-	-	-	-	-	-	-	-	-
-	-	19.316	53.795	67.856	17.773	7.921	7.188	6.107	10.258	39.693	20.186
9.818	4.068	3.929	9.269	72.765	23.905	9.977	7.259	5.564	7.581	8.394	10.932
7.129	4.782	2.648	14.649	51.957	19.943	15.693	7.792	5.986	11.043	35.765	45.894
25.18	23.524	10.078	11.461	42.364	27.573	13.276	8.745	3.178	4.263	8.922	37.311
9.252	4.04	4.097	18.649	-	14.601	-	13.722	10.332	-	-	46.575
12.352	-	8.296	-	77.646	-	14.123	6.935	18.921	53.926	88.176	-
-	-	7.628	27.531	62.05	61.145	20.763	12.3	8.821	7.337	19.338	36.035
13.824	4.86	6.16	88.202	70.051	16.749	20.287	14.061	-	-	-	-

APPENDIX 2

Borehole Data in Muranga County (Source Ministry Of Water And Irrigation)

ID	LOCALITY	MAPNO	GRIDX	GRIDY	ALT	TDEPTH	M_WSL	WRL	YIELD
9288	GIATHA-INI					200	173	57	5.16
9834	MAKUTANO	135/3			1500	228.8	218	89.3	6
9555	KAHARO	135/3			1480	118	71	74.6	4.95
9055	SALV.ARMY FARM	149/1	292278	883889	1468	180	146	44.9	2.16
9390	KANDANI					200	40		
10921	KANGEMA TOWN	134/2			1760	161	44		
4788	KAMBIRWA	135/1			1180	150	108	28	2.64
11127	MURANGA					125	100	30.5	
387	MITUBIRI	135/3	305264	9893107	1433	137	107	2	3.12
403	MITUBIRI	135/3	294124	9909688	1463	159	77	30	
724	MITUBIRI	149/1	295995	9885738	1463	110	102	40	9.84
1120	MITUBIRI	135/3	297839	9893103	1463	40	34	16	2.82
1338	MITUBIRI	135/3	290424	9894946	1493	188	79	18	3.3
1339	CHUI WEST	149/1	301560	9887576	1463	113	107	54	3.18
1375	TANA RANCH	135/4	316391	9900488	1158	46	27	23	2.7
1479	TANA RANCH	135/4	314532	9900487	1158	73	24	20	0.3
1894	MITUBIRI	135/3	294133	9891266	1463	69	58		0.9
1901	MITUBIRI	135/3	297835	9900479	1378	46	37	2	8.1
1976	KANDARA	135/3	277429	9900468	1615	218	31	36	0.24
1985	KANGEMA	134/2	275558	9926268	1692	153	151	9	3.24
2171	THIKA	135/3	294131	9894948	1494	64	32	30	5.4
2204	THIKA	135/4	307125	9889426	1439	183		46	
2392	KANGEMA	134/2	275558	9926268	1679	183			0.42
2683	MURANGA	135/1	294120	9918911	1341	76	50	44	24.12
2835	MITUBIRI	149/2	316397	9887584	1325	105	101	6	4.02
3034	MURANGA	135/1	294120	9918911	1341	134	122	18	8.4
3049	MITUBIRI	135/3	290424	9894946	1494	87	79	12	9.06
3285	NEAR THIKA/L.R175	135/3	284857	9896790	1554	76	67	27	13.5
3293	NEAR MURANGA/LR1722	134/2	275558	9926268	1830	76	37		6.78
3300	NEAR SAGANA	135/1	301542	9926278	1220	15	11	2	5.4
3359	A.C.GITHUNGURI	135/3	286704	9898626	1524	153	148	46	2.28
3640	MURANGA	135/3	281138	9898623	1585	124	110	26	1.8
3662	KAMUNE	135/1	279273	9935493	1676	153	40	37	0.9
3716	HORTICALTURAL/ KARI	135/3	286707	9893097	1524	70	64	16	9.06
3876	MURANGA	135/1	292261	9917063	1280	122	63	8	0.84
3888	KIAMA	135/3	281141	9893094	1555	110	88	115	13.62
3921	MURANGA	93/1			1311	165	160	21	3.6
4054	MURANGA	93/2			1500	182	46	2	1.8

4175	MITUBIRI	135/3	294132	9893101	1490	122	87	28	10.92
4479	MITUBIRI RANCH	135/2			1470	122	103	27	13.62
4571	MURANGA					140	64	14	4.5
4744	KIRUARA	134/4	270005	9898617	1680	130	66	28	2.94
5158	ITHANGA	135/4	307118	9902330	1370	46	3	1	1.2
5326						151	148	28	10.5
5344	KIRUARA					120	92	16	5.1
6295	GITUMBUINI	135/3	281141	9893094	1540	150	98	16	4.98
8093	GAICHANJIRU	135			1620	165	136	85	4.02
8475	GITURA	135/3	288563	9898627	1540	120	88	32	5.82
8476	MARIANI	135/3	277428	9902315	1520	70	43	21	56.7
11168	SAMMER MBOI-KAMITI				1200	83	74	32	8.8
7738	GATITU								
10635	NJUMBI								
5536	KARIGUINI					58	40	16	6.8
106	MITUBIRI	134/4				85	32	32	0.38
115	MITUMBIRI	134/4				26	20	11	2.6
93	MITUMBIRI	134/4				28			0
1210	MITUBIRI	149/1	292278	9883889	1463	131	129	36	2.28
3663	KAMUNE	135/1	279273	9935493	1676	46	43	4	13.5
6264	GAICHANJIRU				1500	180	76	16	2.28
1228	MITUBIRI	149/1	297843	9885739	1463	61	55	24	5.88
1326	ISINDIRI/THIKA	135/3	283002	9889412	1524	153	122	51	1.92
2472	THIKA	149/1	301560	9887576	1554	122	50	24	0.06
2868	MURANGA	135/1	294120	9918911	1341	122	98	16	2.04
4076	ITHANGA	135/3	299694	9900480	1390	103	94	12	3.36
3172	MURANGA	134/4	271866	9894935	1646	110	104	46	6.54
7402	KAGWATHI	135/3	284852	9906002	1505		50	37	3.54
11628	NGINDA	135/3			1340	210	68	45	7.2

APPENDIX 3

Electrode Coordinates of the Entire Profile (source field data collected)

lat	lon	ns1:time2	ns1:name	ns1:ele
-0.70448	36.84514	2013-08-28T09:24:17Z	173	2277.694
-0.70433	36.84513	2013-08-28T09:25:39Z	174	2276.203
-0.70415	36.84511	2013-08-28T09:26:04Z	175	2278.362
-0.70397	36.84507	2013-08-28T09:26:21Z	176	2278.028
-0.70379	36.84503	2013-08-28T09:26:41Z	177	2278.886
-0.70362	36.84502	2013-08-28T09:27:11Z	178	2282.137
-0.70346	36.84504	2013-08-28T09:32:36Z	179	2283.201
-0.70328	36.84499	2013-08-28T09:33:37Z	180	2283.03
-0.70311	36.84504	2013-08-28T09:34:30Z	181	2289.21
-0.70295	36.84507	2013-08-28T09:35:00Z	182	2291.146
-0.70278	36.8451	2013-08-28T09:35:28Z	183	2294.776
-0.7027	36.84511	2013-08-28T09:48:57Z	184	2299.339
-0.70262	36.84514	2013-08-28T09:49:30Z	185	2298.837
-0.70253	36.84517	2013-08-28T09:49:46Z	186	2298.65
-0.70245	36.84519	2013-08-28T09:50:05Z	187	2299.489
-0.70236	36.8452	2013-08-28T09:50:15Z	188	2299.323
-0.70227	36.84521	2013-08-28T09:50:26Z	189	2299.266
-0.70217	36.84521	2013-08-28T09:50:38Z	190	2298.712
-0.70208	36.84521	2013-08-28T09:50:50Z	191	2297.179
-0.702	36.84522	2013-08-28T09:51:03Z	192	2296.32
-0.70189	36.84521	2013-08-28T09:51:30Z	193	2293.111
-0.70181	36.84524	2013-08-28T09:53:28Z	194	2290.699
-0.70173	36.84524	2013-08-28T09:53:53Z	195	2289.013
-0.70165	36.84525	2013-08-28T09:54:17Z	196	2285.565
-0.70157	36.84531	2013-08-28T09:55:44Z	197	2282.904
-0.70151	36.84533	2013-08-28T09:57:16Z	198	2275.647
-0.70148	36.84532	2013-08-28T09:57:49Z	199	2279.009
-0.70141	36.84532	2013-08-28T09:59:22Z	200	2271.343
-0.70137	36.84535	2013-08-28T10:00:58Z	201	2264.716
-0.70127	36.84533	2013-08-28T10:02:13Z	202	2253.552
-0.70121	36.84533	2013-08-28T10:03:14Z	203	2249.018
-0.70116	36.84533	2013-08-28T10:06:04Z	204	2241.946

-0.70106	36.84535	2013-08-28T10:08:43Z	205	2234.676
-0.701	36.84538	2013-08-28T10:22:38Z	206	2230.296
-0.70091	36.84537	2013-08-28T10:24:14Z	207	2227.918
-0.70082	36.84538	2013-08-28T10:24:44Z	208	2226.541
-0.70074	36.84539	2013-08-28T10:24:58Z	209	2224.505
-0.70065	36.8454	2013-08-28T10:25:10Z	210	2222.863
-0.70057	36.84542	2013-08-28T10:26:27Z	211	2218.561
-0.70042	36.84544	2013-08-28T10:34:00Z	212	2209.904
-0.70031	36.84544	2013-08-28T10:34:50Z	213	2208.737
-0.70025	36.84546	2013-08-28T10:36:31Z	214	2200.319
-0.70017	36.84547	2013-08-28T10:37:37Z	215	2195.906
-0.7001	36.84544	2013-08-28T10:38:39Z	216	2194.769
-0.70003	36.84549	2013-08-28T10:40:36Z	217	2183.825
-0.69994	36.84552	2013-08-28T10:42:06Z	218	2190.699
-0.69986	36.84551	2013-08-28T10:42:50Z	219	2186.013
-0.69978	36.84552	2013-08-28T10:44:23Z	220	2182.79
-0.69967	36.84554	2013-08-28T10:45:53Z	221	2180.677
-0.69961	36.84552	2013-08-28T10:47:49Z	222	2176.157
-0.69955	36.84554	2013-08-28T10:49:12Z	223	2168.636
-0.69947	36.84554	2013-08-28T10:51:19Z	224	2156.898
-0.69932	36.84554	2013-08-28T10:52:30Z	225	2150.454
-0.69915	36.84556	2013-08-28T10:53:18Z	226	2148.573
-0.69897	36.84557	2013-08-28T10:54:44Z	227	2147.745
-0.69879	36.84559	2013-08-28T10:55:09Z	228	2139.255
-0.69862	36.84562	2013-08-28T10:55:38Z	229	2135.144
-0.69846	36.84566	2013-08-28T11:01:21Z	230	2138.488
-0.69828	36.84567	2013-08-28T11:04:51Z	231	2126.953
-0.69812	36.84568	2013-08-28T11:06:44Z	232	2117.962
-0.69794	36.84572	2013-08-28T11:08:32Z	233	2109.695
-0.6978	36.84575	2013-08-28T11:09:58Z	234	2100.607

MARAGUA LINE 1: Electrode Coordinates of the entire profile

lat	lon	ns1:time2	ns1:name	ns1:ele
-0.701096	36.845348	2013-08-28T13:28:55Z	236	2233.366
-0.701018	36.845342	2013-08-28T13:29:36Z	237	2231.901
-0.700924	36.845347	2013-08-28T13:29:54Z	238	2228.878
-0.700849	36.845371	2013-08-28T13:30:11Z	239	2225.48
-0.70076	36.845383	2013-08-28T13:30:26Z	240	2222.596
-0.700678	**36.8454**	**2013-08-28T13:33:18Z**	**241**	**2217.325**
-0.700572	36.845394	2013-08-28T13:34:32Z	242	2215.678
-0.700489	36.845405	2013-08-28T13:36:24Z	243	2216.304
-0.700406	36.845421	2013-08-28T13:38:42Z	244	2211.26
-0.700317	36.845426	2013-08-28T13:39:31Z	245	2207.398
-0.700239	36.845442	2013-08-28T13:40:06Z	246	2204.432
-0.700157	36.845459	2013-08-28T13:42:09Z	247	2198.797
-0.700115	**36.845436**	**2013-08-28T13:42:39Z**	**248**	**2194.086**
-0.700041	36.845488	2013-08-28T13:43:47Z	249	2186.434
-0.699943	36.845495	2013-08-28T13:44:44Z	250	2182.106
-0.699849	36.845505	2013-08-28T13:45:12Z	251	2179.021
-0.699784	36.845527	2013-08-28T13:46:07Z	252	2176.98
-0.6997	36.845521	2013-08-28T13:47:02Z	253	2172.362
-0.699639	**36.845549**	**2013-08-28T13:48:22Z**	**254**	**2164.571**
-0.699628	36.845519	2013-08-28T13:49:07Z	255	2165.192
-0.699559	36.845528	2013-08-28T13:50:55Z	256	2160.694
-0.699498	36.845525	2013-08-28T13:52:44Z	257	2154.1
-0.699507	36.845524	2013-08-28T13:55:21Z	258	2155.218
-0.69941	36.84554	2013-08-28T13:57:46Z	259	2150.511
-0.699417	36.84552	2013-08-28T13:58:54Z	260	2149.578
-0.699327	36.845549	2013-08-28T13:59:37Z	261	2146.964
-0.699243	36.845547	2013-08-28T14:00:17Z	262	2145.797
-0.699163	36.845555	2013-08-28T14:00:34Z	263	2143.837
-0.699055	36.845569	2013-08-28T14:00:46Z	264	2142.883
-0.69897	36.845581	2013-08-28T14:01:02Z	265	2139.753
-0.698892	36.84559	2013-08-28T14:01:14Z	266	2138.009
-0.698808	36.845604	2013-08-28T14:01:25Z	267	2134.885
-0.698717	36.845609	2013-08-28T14:01:38Z	268	2132.322

-0.698625	36.845624	2013-08-28T14:01:52Z	269	2130.5
-0.698528	36.845622	2013-08-28T14:02:38Z	270	2132.331
-0.698442	36.845646	2013-08-28T14:03:04Z	271	2132.025
-0.698356	36.845649	2013-08-28T14:04:31Z	272	2126.753
-0.698275	36.845672	2013-08-28T14:05:53Z	273	2122.302
-0.698199	36.845666	2013-08-28T14:06:39Z	274	2118.803
-0.698107	36.845673	2013-08-28T14:07:36Z	275	2115.18
-0.698032	36.845682	2013-08-28T14:08:32Z	276	2112.709
-0.697944	36.845715	2013-08-28T14:10:14Z	277	2109.284
-0.697875	36.845727	2013-08-28T14:11:31Z	278	2104.309
-0.697795	36.845781	2013-08-28T14:12:35Z	279	2104.916
-0.697702	36.845783	2013-08-28T14:31:18Z	280	2095.435
-0.697557	36.845806	2013-08-28T14:32:04Z	281	2089.158
-0.697469	36.845816	2013-08-28T14:32:16Z	282	2087.634
-0.697384	36.845839	2013-08-28T14:32:33Z	283	2086.709
-0.69731	36.845885	2013-08-28T14:33:39Z	284	2081.729
-0.697224	36.845866	2013-08-28T14:39:07Z	285	2085.185
-0.697144	36.845896	2013-08-28T14:39:45Z	286	2086.388
-0.697064	36.845923	2013-08-28T14:40:02Z	287	2085.183
-0.69698	36.845962	2013-08-28T14:40:56Z	288	2089.953
-0.696913	36.845982	2013-08-28T14:42:52Z	289	2095.636
-0.69683	36.846005	2013-08-28T14:44:09Z	290	2095.095
-0.696759	36.846018	2013-08-28T14:45:48Z	291	2103
-0.696696	36.846102	2013-08-28T14:46:34Z	292	2103.873
-0.696694	36.846102	2013-08-28T14:46:36Z	293	2103.658
-0.696699	36.846097	2013-08-28T14:46:37Z	294	2103.592
-0.6967	36.846099	2013-08-28T14:46:38Z	295	2103.771
-0.6967	36.8461	2013-08-28T14:46:39Z	296	2103.792
-0.696687	36.846092	2013-08-28T14:46:42Z	297	2103.847
-0.696681	36.846091	2013-08-28T14:46:45Z	298	2104.852
-0.696672	36.846095	2013-08-28T14:46:48Z	299	2105.856
-0.696667	**36.846094**	**2013-08-28T14:46:50Z**	**300**	**2106.217**
-0.696669	36.846091	2013-08-28T14:46:52Z	301	2106.46
-0.69671	36.846059	2013-08-28T14:47:11Z	302	2109.712
-0.696613	36.846064	2013-08-28T14:48:10Z	303	2111.07
-0.696532	36.846092	2013-08-28T14:48:51Z	304	2120.568

-0.696449	36.846117	2013-08-28T14:50:22Z	305	2123.219
-0.696361	36.84613	2013-08-28T14:50:46Z	306	2124.838
-0.696192	36.846155	2013-08-28T14:51:24Z	307	2125.128

MARAGUA LINE 2: Electrode Coordinates of the entire profile

lat	lon	ns1:ele	ns1:Time2	ns1:name
-0.69658	36.84407	2124.931641	2013-08-29T09:04:24Z	393
-0.696713	36.844186	2121.577881	2013-08-29T09:05:19Z	394
-0.69684	36.844293	2113.039062	2013-08-29T09:05:51Z	395
-0.696877	36.84436	2109.087158	2013-08-29T09:06:35Z	396
-0.696934	36.844426	2105.833252	2013-08-29T09:09:08Z	397
-0.697019	36.844471	2103.526123	2013-08-29T09:11:42Z	398
-0.697074	36.844525	2098.400635	2013-08-29T09:13:20Z	399
-0.697115	36.844569	2092.801025	2013-08-29T09:15:02Z	400
-0.697146	36.844622	2093.135742	2013-08-29T09:15:52Z	401
-0.697205	36.844676	2090.36377	2013-08-29T09:16:22Z	402
-0.697296	36.844751	2090.616943	2013-08-29T09:16:33Z	403
-0.697341	36.844834	2094.263428	2013-08-29T09:17:22Z	404
-0.697425	36.844806	2105.902832	2013-08-29T09:21:52Z	405
-0.697554	36.845033	2098.584717	2013-08-29T09:25:02Z	406
-0.697637	36.84505	2097.782715	2013-08-29T09:25:44Z	407
-0.697721	36.845112	2096.152832	2013-08-29T09:26:34Z	408
-0.697745	36.845165	2092.829346	2013-08-29T09:27:55Z	409
-0.697731	36.845232	2099.933838	2013-08-29T10:13:22Z	410
-0.697869	36.845248	2097.066895	2013-08-29T10:15:43Z	411
-0.697917	36.845312	2099.911377	2013-08-29T11:02:00Z	412
-0.697958	36.845346	2108.6521	2013-08-29T11:04:53Z	413
-0.698009	36.845432	2110.062988	2013-08-29T11:06:20Z	414
-0.698077	36.845489	2113.493408	2013-08-29T11:08:01Z	415
-0.698162	36.845554	2115.497314	2013-08-29T11:08:43Z	416
-0.698226	36.845596	2117.996338	2013-08-29T11:09:17Z	417
-0.698279	36.845647	2119.893311	2013-08-29T11:10:07Z	418
-0.698361	36.845696	2125.179199	2013-08-29T11:12:13Z	419
-0.698434	36.845738	2125.849365	2013-08-29T11:13:34Z	420

-0.69852	36.845783	2125.886475	2013-08-29T11:14:10Z	421
-0.698602	36.845798	2123.04126	2013-08-29T11:14:31Z	422
-0.698689	36.845838	2123.714844	2013-08-29T11:15:16Z	423
-0.698774	36.845869	2123.257812	2013-08-29T11:17:09Z	424
-0.698834	36.845887	2128.686279	2013-08-29T11:18:54Z	425
-0.698909	36.845919	2135.445312	2013-08-29T11:20:55Z	426
-0.698983	36.84595	2138.010254	2013-08-29T11:22:18Z	427
-0.699063	36.846006	2141.16626	2013-08-29T11:24:58Z	428
-0.699145	36.84603	2145.708984	2013-08-29T11:26:04Z	429
-0.699223	36.846063	2147.480225	2013-08-29T11:26:25Z	430
-0.699215	36.846059	2148.453857	2013-08-29T11:26:43Z	431

MARAGUA LINE 3: Electrode Coordinates of the entire profile

lat	lon	ns1:ele	ns1:time	ns1:name
-0.69898	36.84623	2127.315	2013-08-29T07:07:14Z	352
-0.6989	36.84618	2125.531	2013-08-29T07:07:45Z	353
-0.69879	36.84617	2127.818	2013-08-29T07:08:08Z	354
-0.69872	36.84612	2126.74	2013-08-29T07:08:29Z	355
-0.69864	36.84609	2124.49	2013-08-29T07:09:02Z	356
-0.69856	36.84605	2119.699	2013-08-29T07:09:34Z	357
-0.69849	36.846	2117.968	2013-08-29T07:09:45Z	358
-0.69842	36.84596	2120.568	2013-08-29T07:10:08Z	359
-0.69834	36.84591	2121.124	2013-08-29T07:10:34Z	360
-0.69826	36.84586	2121.019	2013-08-29T07:11:15Z	361
-0.69819	36.84581	2117.944	2013-08-29T07:12:05Z	362
-0.69812	36.84577	2114.5	2013-08-29T07:12:45Z	363
-0.69805	36.84572	2112.709	2013-08-29T07:14:45Z	364
-0.69798	36.84568	2109.754	2013-08-29T07:15:49Z	365
-0.6979	36.84563	2105.437	2013-08-29T07:16:48Z	366
-0.69782	36.84559	2103.57	2013-08-29T07:17:16Z	367
-0.69776	36.84554	2099.583	2013-08-29T07:17:46Z	368
-0.69771	36.84549	2096.449	2013-08-29T07:18:57Z	369
-0.69765	36.84544	2089.942	2013-08-29T07:21:07Z	370
-0.69752	36.84537	2112.842	2013-08-29T07:24:27Z	371
-0.69754	36.84534	2094.523	2013-08-29T07:45:46Z	372

-0.69746	36.84529	2089.041	2013-08-29T07:47:00Z	373
-0.69741	36.84521	2092.077	2013-08-29T07:47:37Z	374
-0.69735	36.84514	2099.795	2013-08-29T07:48:18Z	375
-0.6973	36.84513	2099.679	2013-08-29T07:49:13Z	376
-0.69721	36.84506	2102.44	2013-08-29T07:49:38Z	377
-0.69716	36.84498	2100.252	2013-08-29T07:52:23Z	378
-0.69708	36.84489	2104.056	2013-08-29T07:52:55Z	379
-0.69699	36.84488	2106.358	2013-08-29T07:53:44Z	380
-0.69693	36.84485	2105.899	2013-08-29T07:54:27Z	381
-0.69688	36.84479	2110.23	2013-08-29T07:54:49Z	382
-0.69681	36.84474	2110.606	2013-08-29T07:55:41Z	383
-0.6967	36.84471	2111.129	2013-08-29T07:57:27Z	384
-0.69671	36.84467	2119.319	2013-08-29T07:59:33Z	385
-0.69664	36.8446	2121.903	2013-08-29T08:00:43Z	386
-0.69656	36.84454	2124.349	2013-08-29T08:02:10Z	387
-0.69651	36.8445	2128.596	2013-08-29T08:03:58Z	388
-0.69646	36.84443	2131.882	2013-08-29T08:05:03Z	389
-0.69638	36.84439	2130.889	2013-08-29T08:05:58Z	390
-0.6963	36.84433	2134.104	2013-08-29T08:07:41Z	391
-0.69622	36.84428	2134.069	2013-08-29T08:08:15Z	392

MARAGUA LINE 4: Electrode Coordinates of the entire profile

lat	lon	ns1:ele	ns1:time2	ns1:name
-0.69595	36.84452	2136.145	2013-08-29T06:16:22Z	309
-0.69604	36.84458	2134.383	2013-08-29T06:17:00Z	310
-0.6961	36.84462	2132.907	2013-08-29T06:17:18Z	311
-0.69619	36.84466	2130.505	2013-08-29T06:17:54Z	312
-0.69625	36.84472	2131.095	2013-08-29T06:18:17Z	313
-0.69633	36.84477	2129.571	2013-08-29T06:18:35Z	314
-0.69641	36.84481	2128.739	2013-08-29T06:19:01Z	315
-0.69647	36.84487	2128.079	2013-08-29T06:20:04Z	316
-0.69655	36.84492	2123.306	2013-08-29T06:21:57Z	317
-0.69661	36.84497	2123.916	2013-08-29T06:24:51Z	318
-0.69671	36.84502	2118.282	2013-08-29T06:29:03Z	319
-0.69676	36.84507	2115.86	2013-08-29T06:30:50Z	320

-0.69683	36.84511	2111.125	2013-08-29T06:31:16Z	321
-0.69692	36.84516	2107.988	2013-08-29T06:31:44Z	322
-0.69699	36.84522	2108.548	2013-08-29T06:32:07Z	323
-0.69707	36.84526	2107.754	2013-08-29T06:32:45Z	324
-0.69714	36.8453	2110.109	2013-08-29T06:33:48Z	325
-0.69722	36.84536	2106.531	2013-08-29T06:34:13Z	326
-0.69731	36.84542	2104.435	2013-08-29T06:34:47Z	327
-0.69736	36.84547	2099.876	2013-08-29T06:35:41Z	328
-0.69735	36.84547	2099.518	2013-08-29T06:35:47Z	329
-0.69735	36.84548	2099.337	2013-08-29T06:35:53Z	330
-0.69741	36.84553	2097.834	2013-08-29T06:37:17Z	331
-0.69746	36.84558	2090.76	2013-08-29T06:43:08Z	332
-0.69749	36.84564	2098.137	2013-08-29T06:44:51Z	333
-0.69756	36.84571	2098.997	2013-08-29T06:45:20Z	334
-0.69762	36.84577	2097.759	2013-08-29T06:45:35Z	335
-0.69769	36.84583	2095.979	2013-08-29T06:45:47Z	336
-0.69775	36.84587	2096.379	2013-08-29T06:46:04Z	337
-0.69784	36.84591	2099.161	2013-08-29T06:47:00Z	338
-0.6979	36.84596	2102.043	2013-08-29T06:48:26Z	339
-0.69796	36.84601	2106.191	2013-08-29T06:49:02Z	340
-0.69805	36.84605	2109.833	2013-08-29T06:50:03Z	341
-0.69812	36.8461	2111.332	2013-08-29T06:50:52Z	342
-0.69817	36.84615	2115.104	2013-08-29T06:51:53Z	343
-0.69826	36.8462	2114.205	2013-08-29T06:53:11Z	344
-0.69834	36.84624	2108.028	2013-08-29T06:55:07Z	345
-0.69839	36.8463	2112.457	2013-08-29T06:56:09Z	346
-0.69843	36.84636	2122.927	2013-08-29T06:58:20Z	347
-0.69852	36.8464	2121.408	2013-08-29T06:58:44Z	348
-0.69859	36.84645	2122.759	2013-08-29T06:59:00Z	349
-0.6987	36.8465	2121.865	2013-08-29T07:00:42Z	350
-0.69876	36.84656	2120.445	2013-08-29T07:02:00Z	351
-0.69898	36.84623	2127.315	2013-08-29T07:07:14Z	352

MARAGUA LINE 5: Electrode Coordinates of the entire profile

lat	lon	ns1:ele	ns1:time	ns1:name
-0.69859	36.84417	2108.898	2013-08-29T11:55:12Z	432
-0.69855	36.84422	2112.323	2013-08-29T11:55:43Z	433
-0.69849	36.8443	2110.591	2013-08-29T11:55:58Z	434
-0.69845	36.84437	2112.363	2013-08-29T11:58:42Z	435
-0.69837	36.84445	2111.325	2013-08-29T11:59:05Z	436
-0.69834	36.8445	2111.42	2013-08-29T11:59:19Z	437
-0.69829	36.84459	2112.422	2013-08-29T11:59:55Z	438
-0.69823	36.84467	2111.62	2013-08-29T12:00:06Z	439
-0.69818	36.84475	2108.494	2013-08-29T12:00:36Z	440
-0.69814	36.84482	2106.436	2013-08-29T12:01:55Z	441
-0.69808	36.84489	2102.39	2013-08-29T12:04:36Z	442
-0.69803	36.84498	2104.482	2013-08-29T12:05:21Z	443
-0.698	36.84504	2105.504	2013-08-29T12:06:09Z	444
-0.69797	36.84512	2104.708	2013-08-29T12:06:41Z	445
-0.69788	36.84517	2098.616	2013-08-29T12:08:08Z	446
-0.6978	36.84524	2101.896	2013-08-29T12:09:58Z	447
-0.69776	36.84526	2096.382	2013-08-29T12:12:17Z	448
-0.69773	36.8453	2097.287	2013-08-29T12:12:41Z	449
-0.69766	36.8454	2096.588	2013-08-29T12:12:57Z	450
-0.69762	36.8455	2091.457	2013-08-29T12:13:15Z	451
-0.69758	36.8456	2089.628	2013-08-29T12:13:33Z	452
-0.69752	36.84566	2087.458	2013-08-29T12:16:51Z	453
-0.69746	36.84574	2085.64	2013-08-29T12:17:09Z	454
-0.69743	36.84583	2084.114	2013-08-29T12:17:37Z	455
-0.69736	36.84588	2084.987	2013-08-29T12:18:50Z	456
-0.69729	36.84593	2085.373	2013-08-29T12:19:28Z	457
-0.69726	36.84603	2082.923	2013-08-29T12:21:36Z	458
-0.69723	36.84609	2082.559	2013-08-29T12:25:08Z	459
-0.69716	36.84618	2084.605	2013-08-29T12:28:01Z	460
-0.69711	36.84626	2085.813	2013-08-29T12:28:43Z	461
-0.69707	36.84634	2086.306	2013-08-29T12:29:09Z	462
-0.69702	36.8464	2092.756	2013-08-29T12:33:49Z	463
-0.69697	36.84645	2090.939	2013-08-29T12:34:22Z	464

-0.69696	36.84655	2091.162	2013-08-29T12:34:45Z	465
-0.69692	36.84661	2092.764	2013-08-29T12:35:04Z	466
-0.69686	36.84669	2093.99	2013-08-29T12:35:22Z	467
-0.69682	36.84677	2094.083	2013-08-29T12:35:39Z	468
-0.69678	36.84685	2096.081	2013-08-29T12:36:11Z	469
-0.69675	36.84693	2100.179	2013-08-29T12:36:36Z	470
-0.6967	36.847	2103.567	2013-08-29T12:36:57Z	471
-0.69667	36.84708	2104.84	2013-08-29T12:37:16Z	472

GIKIGIE LINE 800M: Electrode Coordinates of the entire profile

lat	lon	ns1:ele	ns1:time2	ns1:name
-0.72155	36.84289	2134.288818	2013-08-25T07:18:00Z	1675
-0.72171	36.84289	2125.164062	2013-08-25T07:21:02Z	1676
-0.72188	36.84291	2113.702637	2013-08-25T07:22:15Z	1677
-0.72103	36.84291	2146.064209	2013-08-25T07:28:35Z	1678
-0.72112	36.84291	2143.483398	2013-08-25T07:29:09Z	1679
-0.7212	36.8429	2139.740479	2013-08-25T07:29:34Z	1680
-0.72131	36.8429	2140.012695	2013-08-25T07:30:09Z	1681
-0.72138	36.8429	2137.918457	2013-08-25T07:30:22Z	1682
-0.72147	36.84291	2135.677246	2013-08-25T07:30:33Z	1683
-0.72155	36.84291	2132.065918	2013-08-25T07:30:44Z	1684
-0.72164	36.84291	2127.859619	2013-08-25T07:30:58Z	1685
-0.72171	36.8429	2124.065674	2013-08-25T07:31:10Z	1686
-0.72178	36.8429	2118.65332	2013-08-25T07:31:29Z	1687
-0.72187	36.84289	2113.896484	2013-08-25T07:31:59Z	1688
-0.72194	36.84287	2105.879883	2013-08-25T07:32:30Z	1689
-0.72199	36.84286	2097.955322	2013-08-25T07:33:28Z	1690
-0.72209	36.84284	2098.36792	2013-08-25T07:35:04Z	1691
-0.72214	36.84286	2092.434326	2013-08-25T07:35:51Z	1692
-0.72218	36.84284	2090.785156	2013-08-25T07:37:31Z	1693
-0.7223	36.84283	2093.338623	2013-08-25T07:37:58Z	1694
-0.72237	36.84281	2097.99585	2013-08-25T07:38:15Z	1695
-0.7225	36.84276	2106.882812	2013-08-25T07:38:54Z	1696
-0.72258	36.84275	2105.802002	2013-08-25T07:39:27Z	1697

-0.72265	36.84276	2108.54248	2013-08-25T07:39:42Z	1698
-0.72273	36.84281	2110.97998	2013-08-25T07:41:15Z	1699
-0.72277	36.84283	2116.843506	2013-08-25T07:41:33Z	1700
-0.72285	36.84282	2126.76123	2013-08-25T07:42:09Z	1701
-0.72295	36.84282	2130.466797	2013-08-25T07:42:38Z	1702
-0.72304	36.84279	2123.366211	2013-08-25T07:43:07Z	1703
-0.72313	36.84281	2120.839355	2013-08-25T07:43:22Z	1704
-0.7232	36.84277	2121.683838	2013-08-25T07:43:40Z	1705
-0.72331	36.84277	2123.715576	2013-08-25T07:44:15Z	1706
-0.7234	36.84277	2121.639648	2013-08-25T07:44:32Z	1707
-0.7235	36.84274	2122.087402	2013-08-25T07:44:51Z	1708
-0.72372	36.8427	2117.244141	2013-08-25T07:45:44Z	1709
-0.72387	36.84269	2119.10498	2013-08-25T07:46:23Z	1710
-0.7239	36.8427	2108.023926	2013-08-25T07:47:10Z	1711
-0.72396	36.84271	2105.763916	2013-08-25T07:47:27Z	1712
-0.72403	36.84274	2100.63208	2013-08-25T07:48:14Z	1713
-0.72411	36.84273	2096.46167	2013-08-25T07:49:35Z	1714
-0.7242	36.84271	2094.919922	2013-08-25T07:50:30Z	1715
-0.72427	36.84269	2091.376221	2013-08-25T07:50:52Z	1716
-0.72434	36.84268	2087.167725	2013-08-25T07:51:13Z	1717
-0.72443	36.84266	2082.843018	2013-08-25T07:51:44Z	1718
-0.728	36.8425	2120.174561	2013-08-25T08:24:17Z	1719
-0.72784	36.84246	2118.416016	2013-08-25T08:25:00Z	1720
-0.72764	36.84245	2119.341553	2013-08-25T08:25:35Z	1721
-0.72747	36.8424	2117.917725	2013-08-25T08:26:05Z	1722
-0.72731	36.84239	2121.593262	2013-08-25T08:26:33Z	1723
-0.72713	36.84236	2125.802246	2013-08-25T08:27:05Z	1724
-0.72695	36.84239	2124.629395	2013-08-25T08:27:32Z	1725
-0.72678	36.84243	2118.573242	2013-08-25T08:28:03Z	1726
-0.72661	36.84248	2116.741943	2013-08-25T08:28:39Z	1727
-0.72644	36.84252	2116.94458	2013-08-25T08:29:05Z	1728
-0.72617	36.84253	2116.755615	2013-08-25T08:38:18Z	1729
-0.72609	36.84255	2115.375977	2013-08-25T08:42:49Z	1730
-0.726	36.84255	2113.529297	2013-08-25T08:44:05Z	1731
-0.72591	36.84256	2112.790039	2013-08-25T08:44:55Z	1732
-0.72581	36.84255	2112.839355	2013-08-25T08:45:31Z	1733

-0.72572	36.84256	2112.013428	2013-08-25T08:45:49Z	1734
-0.72563	36.84256	2109.434326	2013-08-25T08:46:10Z	1735
-0.72555	36.84258	2105.757324	2013-08-25T08:46:40Z	1736
-0.72546	36.84258	2104.644043	2013-08-25T08:47:04Z	1737
-0.72537	36.84259	2102.9104	2013-08-25T08:47:37Z	1738
-0.72528	36.84259	2102.440186	2013-08-25T08:48:08Z	1739
-0.72519	36.8426	2101.357422	2013-08-25T08:48:38Z	1740
-0.72502	36.84262	2100.260742	2013-08-25T08:49:37Z	1741
-0.72491	36.84263	2100.748535	2013-08-25T08:50:34Z	1742
-0.72484	36.84262	2101.127686	2013-08-25T08:50:55Z	1743
-0.72475	36.8426	2102.611328	2013-08-25T08:51:53Z	1744
-0.72464	36.84259	2096.691406	2013-08-25T08:52:58Z	1745
-0.72457	36.84261	2092.344971	2013-08-25T08:53:33Z	1746
-0.72452	36.84264	2088.446289	2013-08-25T08:54:10Z	1747

GIKIGIE LINE1: Electrode Coordinates of the entire profile

lat	lon	ns1:ele	ns1:time2	ns1:name
-0.72135	36.84282	2139.534	2013-08-26T13:38:54Z	006
-0.72142	36.84281	2136.627	2013-08-26T13:39:45Z	007
-0.72151	36.84281	2135.437	2013-08-26T13:40:01Z	008
-0.72158	36.84282	2132.914	2013-08-26T13:40:19Z	009
-0.72167	36.84282	2129.774	2013-08-26T13:40:41Z	010
-0.72174	36.84279	2124.836	2013-08-26T13:41:00Z	011
-0.72186	36.8428	2117.182	2013-08-26T13:42:05Z	012
-0.72191	36.84275	2112.99	2013-08-26T13:42:39Z	013
-0.72197	36.84273	2109.172	2013-08-26T13:43:22Z	014
-0.72204	36.84271	2106.052	2013-08-26T13:44:49Z	015
-0.72211	36.84272	2105.737	2013-08-26T13:45:27Z	016
-0.72219	36.84272	2103.807	2013-08-26T13:46:11Z	017
-0.72223	36.84276	2109.502	2013-08-26T13:46:35Z	018
-0.7222	36.84267	2100.549	2013-08-26T13:47:40Z	019
-0.72227	36.84268	2101.523	2013-08-26T13:48:09Z	020
-0.72247	36.8427	2106.132	2013-08-26T13:48:29Z	021
-0.72254	36.8427	2104.724	2013-08-26T13:48:51Z	022
-0.72261	36.84267	2102.956	2013-08-26T13:49:09Z	023

-0.7227	36.84268	2107.517	2013-08-26T13:49:32Z	024
-0.72282	36.84268	2113.849	2013-08-26T13:49:55Z	025
-0.72289	36.84261	2112.35	2013-08-26T13:50:42Z	026
-0.72299	36.84261	2111.994	2013-08-26T13:52:57Z	027
-0.72308	36.84261	2110.967	2013-08-26T13:53:20Z	028
-0.72319	36.84259	2109.924	2013-08-26T13:53:53Z	029
-0.72328	36.84256	2108.485	2013-08-26T13:54:37Z	030
-0.7233	36.84252	2107.714	2013-08-26T13:55:34Z	031
-0.72343	36.84252	2108.185	2013-08-26T13:56:04Z	032
-0.72351	36.8425	2108.588	2013-08-26T13:56:34Z	033
-0.72359	36.84252	2099.386	2013-08-26T13:57:45Z	034
-0.7237	36.84254	2096.794	2013-08-26T13:58:08Z	035
-0.72378	36.84255	2093.93	2013-08-26T13:58:34Z	036
-0.72386	36.84257	2094.15	2013-08-26T13:59:17Z	037
-0.72395	36.84255	2092.04	2013-08-26T13:59:44Z	038
-0.72405	36.84251	2090.131	2013-08-26T14:00:00Z	039
-0.72411	36.84248	2086.377	2013-08-26T14:00:20Z	040
-0.7242	36.8425	2086.145	2013-08-26T14:00:36Z	041
-0.7243	36.8425	2086.062	2013-08-26T14:01:08Z	042
-0.72438	36.84248	2085.113	2013-08-26T14:04:14Z	043
-0.72444	36.84244	2091.22	2013-08-26T14:05:20Z	044
-0.72451	36.84243	2097.688	2013-08-26T14:06:16Z	045
-0.72458	36.8424	2105.023	2013-08-26T14:07:37Z	046
-0.72468	36.84238	2101.691	2013-08-26T14:09:35Z	047
-0.72475	36.8424	2109.842	2013-08-26T14:10:45Z	048
-0.72483	36.84241	2108.51	2013-08-26T14:11:09Z	049
-0.72493	36.84241	2109.453	2013-08-26T14:11:30Z	050
-0.72502	36.84239	2111.753	2013-08-26T14:12:22Z	051
-0.7251	36.84239	2111.769	2013-08-26T14:12:58Z	052
-0.7252	36.84237	2115.402	2013-08-26T14:13:51Z	053
-0.72529	36.84235	2117.135	2013-08-26T14:14:19Z	054
-0.72538	36.84234	2116.519	2013-08-26T14:14:50Z	055
-0.72547	36.8423	2117.615	2013-08-26T14:15:29Z	056
-0.72556	36.84231	2118.421	2013-08-26T14:16:33Z	057
-0.72565	36.8423	2116.796	2013-08-26T14:17:20Z	058
-0.72572	36.84229	2116.678	2013-08-26T14:17:48Z	059

-0.72579	36.84227	2117.751	2013-08-26T14:18:21Z	060
-0.72588	36.84226	2118.916	2013-08-26T14:19:38Z	061
-0.72598	36.84225	2117.647	2013-08-26T14:20:54Z	062
-0.72606	36.84223	2119.551	2013-08-26T14:21:28Z	063
-0.72614	36.8422	2119.644	2013-08-26T14:22:29Z	064
-0.72623	36.8422	2120.294	2013-08-26T14:23:23Z	065
-0.72635	36.8422	2120.904	2013-08-26T14:24:18Z	066

GIKIGIE LINE2: Electrode Coordinates of the entire profile

lat	lon	ns1:ele	ns1:time2	ns1:name
-0.72268	36.84076	2135.986	2013-08-27T12:16:39Z	130
-0.72275	36.8409	2134.999	2013-08-27T12:31:55Z	131
-0.72278	36.84096	2133.569	2013-08-27T12:34:35Z	132
-0.72278	36.84104	2133.944	2013-08-27T12:35:52Z	133
-0.72281	36.84113	2131.466	2013-08-27T12:37:39Z	134
-0.7228	36.84121	2128.199	2013-08-27T12:38:49Z	135
-0.72281	36.84132	2130.92	2013-08-27T12:41:45Z	136
-0.72276	36.84138	2125.204	2013-08-27T12:42:36Z	137
-0.72279	36.84148	2119.608	2013-08-27T12:43:07Z	138
-0.72281	36.84154	2114.875	2013-08-27T12:43:47Z	139
-0.72286	36.84161	2112.062	2013-08-27T12:53:22Z	140
-0.72288	36.84177	2096.498	2013-08-27T12:58:08Z	141
-0.72295	36.84186	2096.644	2013-08-27T12:59:46Z	142
-0.72289	36.84189	2091.449	2013-08-27T13:01:00Z	143
-0.72289	36.84193	2090.995	2013-08-27T13:02:13Z	144
-0.7229	36.84196	2085.528	2013-08-27T13:02:43Z	145
-0.72296	36.84206	2081.069	2013-08-27T13:05:32Z	146
-0.72297	36.84215	2082.702	2013-08-27T13:05:48Z	147
-0.72298	36.84223	2084.511	2013-08-27T13:06:13Z	148
-0.72301	36.84232	2086.234	2013-08-27T13:08:29Z	149
-0.72302	36.84243	2080.642	2013-08-27T13:11:40Z	150
-0.72302	36.84243	2091.341	2013-08-27T13:20:29Z	151
-0.723	36.84249	2084.454	2013-08-27T13:32:15Z	152
-0.72299	36.84261	2092.407	2013-08-27T13:32:45Z	153
-0.72299	36.84269	2099.09	2013-08-27T13:33:10Z	154

-0.72302	36.84277	2103.357	2013-08-27T13:33:43Z	155
-0.723	36.84285	2106.984	2013-08-27T13:34:11Z	156
-0.72303	36.84294	2114.581	2013-08-27T13:34:40Z	157
-0.72302	36.84302	2119.128	2013-08-27T13:35:04Z	158
-0.72306	36.84309	2118.587	2013-08-27T13:35:31Z	159
-0.7231	36.84318	2120	2013-08-27T13:35:54Z	160
-0.72312	36.84325	2123.843	2013-08-27T13:36:18Z	161
-0.72315	36.84331	2124.554	2013-08-27T13:36:41Z	162
-0.7232	36.8434	2128.012	2013-08-27T13:37:02Z	163
-0.72319	36.84351	2138.48	2013-08-27T13:37:28Z	164
-0.72321	36.84359	2143.281	2013-08-27T13:37:49Z	165
-0.72325	36.84366	2147.08	2013-08-27T13:38:21Z	166
-0.72328	36.84375	2147.738	2013-08-27T13:38:51Z	167
-0.72329	36.84382	2151.26	2013-08-27T13:39:36Z	168
-0.72328	36.84391	2152.195	2013-08-27T13:40:00Z	169
-0.72334	36.844	2153.907	2013-08-27T13:40:35Z	170

GIKIGIE LINE3: Electrode Coordinates of the entire profile

lat	lon	ns1:ele	ns1:time2	ns1:name
-0.72363	36.84395	2152.829	2013-08-26T09:14:23Z	1966
-0.72361	36.84388	2153.776	2013-08-26T09:14:49Z	1967
-0.72361	36.84381	2149.661	2013-08-26T09:15:27Z	1968
-0.72357	36.84372	2146.934	2013-08-26T09:15:50Z	1969
-0.72356	36.84364	2146.041	2013-08-26T09:16:08Z	1970
-0.72355	36.84355	2143.847	2013-08-26T09:16:33Z	1971
-0.72352	36.84348	2140.423	2013-08-26T09:16:58Z	1972
-0.72351	36.84337	2138.737	2013-08-26T09:17:17Z	1973
-0.72349	36.84329	2137.62	2013-08-26T09:17:40Z	1974
-0.72345	36.84321	2132.455	2013-08-26T09:18:07Z	1975
-0.72342	36.84313	2131.946	2013-08-26T09:18:30Z	1976
-0.7234	36.84308	2130.539	2013-08-26T09:18:52Z	1977
-0.72334	36.843	2131.731	2013-08-26T09:19:41Z	1978
-0.72334	36.8429	2126.177	2013-08-26T09:20:03Z	1979
-0.7233	36.8428	2126.054	2013-08-26T09:20:29Z	1980
-0.72326	36.84271	2119.552	2013-08-26T09:21:24Z	1981

-0.72324	36.84265	2112.333	2013-08-26T09:22:29Z	1982
-0.72328	36.84259	2102.838	2013-08-26T09:23:12Z	1983
-0.72325	36.84252	2098.633	2013-08-26T09:24:00Z	1984
-0.72326	36.84245	2091.737	2013-08-26T09:26:04Z	1985
-0.72325	36.84235	2092.891	2013-08-26T09:27:02Z	1986
-0.7264	36.84221	2095.872	2013-08-26T09:32:12Z	GL1
-0.72595	36.84227	2100.859	2013-08-26T09:33:31Z	GL2
-0.7255	36.84234	2105.375	2013-08-26T09:35:06Z	GL3
-0.72504	36.84239	2113.053	2013-08-26T09:36:06Z	GL4
-0.72459	36.84245	2106.434	2013-08-26T09:37:11Z	GL5
-0.72423	36.8425	2106.577	2013-08-26T09:38:19Z	GL6
-0.72387	36.84255	2106.766	2013-08-26T09:39:25Z	GL7
-0.72351	36.8426	2109.159	2013-08-26T09:40:45Z	GL8
-0.72314	36.84264	2103.584	2013-08-26T09:42:05Z	GL9
-0.72278	36.8427	2097.376	2013-08-26T09:43:11Z	GL10
-0.72262	36.84271	2097.592	2013-08-26T09:44:28Z	GL11
-0.72217	36.84278	2092.115	2013-08-26T09:45:42Z	GL12
-0.72172	36.84283	2097.09	2013-08-26T09:46:52Z	GL13
-0.72126	36.84289	2102.547	2013-08-26T09:47:52Z	GL14
-0.72081	36.84296	2106.305	2013-08-26T09:49:07Z	GL15
-0.72324	36.84228	2079.568	2013-08-26T11:22:52Z	1987
-0.72321	36.84221	2079.895	2013-08-26T11:25:02Z	1988
-0.72319	36.84213	2087.14	2013-08-26T11:26:14Z	1989
-0.7232	36.84194	2081.323	2013-08-26T11:28:18Z	1990
-0.72321	36.84185	2080.641	2013-08-26T11:28:37Z	1991
-0.72322	36.84179	2080.088	2013-08-26T11:29:31Z	1992
-0.72322	36.84169	2090.932	2013-08-26T11:32:45Z	1993
-0.7232	36.84161	2095.087	2013-08-26T11:33:12Z	1994
-0.7232	36.84152	2099.021	2013-08-26T11:33:37Z	1995
-0.7232	36.84142	2100.563	2013-08-26T11:33:58Z	1996
-0.72319	36.84136	2105.666	2013-08-26T11:34:24Z	1997
-0.72318	36.84128	2114.868	2013-08-26T11:35:30Z	1998
-0.7232	36.84121	2117.731	2013-08-26T11:36:03Z	1999
-0.72319	36.84113	2121.133	2013-08-26T11:36:29Z	2000
-0.72319	36.84104	2124.587	2013-08-26T11:36:46Z	001
-0.72318	36.84096	2128.181	2013-08-26T11:37:58Z	002

-0.72315	36.84087	2126.103	2013-08-26T11:39:13Z	003
-0.72305	36.84075	2129.654	2013-08-26T11:40:45Z	004
-0.72307	36.84074	2128.266	2013-08-26T11:41:02Z	005

GIKIGIE LINE4: Electrode Coordinates of the entire profile

lat	lon	ns1:ele	ns1:time2	ns1:name
-0.72325	36.84074	2130.629	2013-08-26T08:19:21Z	1924
-0.72331	36.84078	2126.36	2013-08-26T08:20:05Z	1925
-0.72335	36.84086	2126.792	2013-08-26T08:34:52Z	1926
-0.72339	36.84096	2127.33	2013-08-26T08:35:09Z	1927
-0.7234	36.84103	2126	2013-08-26T08:35:23Z	1928
-0.72341	36.84112	2118.632	2013-08-26T08:36:08Z	1929
-0.72339	36.84121	2115.401	2013-08-26T08:37:00Z	1930
-0.7234	36.84127	2108.373	2013-08-26T08:37:55Z	1931
-0.72341	36.84134	2104.058	2013-08-26T08:39:59Z	1932
-0.72341	36.84141	2097.335	2013-08-26T08:40:30Z	1933
-0.72341	36.8415	2093.547	2013-08-26T08:40:54Z	1934
-0.72342	36.84159	2090.9	2013-08-26T08:41:15Z	1935
-0.72342	36.84168	2088.988	2013-08-26T08:41:31Z	1936
-0.72339	36.84178	2088.838	2013-08-26T08:44:35Z	1937
-0.72343	36.84186	2089.315	2013-08-26T08:46:10Z	1938
-0.72343	36.84195	2089.841	2013-08-26T08:46:48Z	1939
-0.72342	36.84204	2088.294	2013-08-26T08:47:25Z	1940
-0.72343	36.84211	2089.115	2013-08-26T08:47:52Z	1941
-0.72345	36.84222	2085.885	2013-08-26T08:48:23Z	1942
-0.72347	36.84229	2084.318	2013-08-26T08:48:39Z	1943
-0.7235	36.84238	2084.349	2013-08-26T08:52:14Z	1944
-0.72351	36.84245	2092.924	2013-08-26T08:53:08Z	1945
-0.72353	36.84255	2094.394	2013-08-26T08:54:00Z	1946
-0.72353	36.84254	2115.577	2013-08-26T08:56:41Z	1947
-0.72353	36.84269	2114.507	2013-08-26T08:57:36Z	1948
-0.72354	36.8427	2114.533	2013-08-26T08:57:43Z	1949
-0.72356	36.84275	2115.647	2013-08-26T08:58:03Z	1950
-0.72358	36.84282	2115.346	2013-08-26T08:58:42Z	1951
-0.72361	36.84291	2123.885	2013-08-26T09:03:07Z	1952
-0.72363	36.84302	2125.529	2013-08-26T09:03:33Z	1953

-0.72366	36.8431	2129.238	2013-08-26T09:03:58Z	1954
-0.72369	36.84318	2130.835	2013-08-26T09:04:20Z	1955
-0.7237	36.84325	2128.641	2013-08-26T09:04:54Z	1956
-0.72371	36.84334	2129.414	2013-08-26T09:05:21Z	1957
-0.72372	36.84342	2132.298	2013-08-26T09:05:43Z	1958
-0.72374	36.84351	2135.561	2013-08-26T09:06:08Z	1959
-0.72374	36.84359	2137.366	2013-08-26T09:06:32Z	1960
-0.72375	36.84366	2138.948	2013-08-26T09:06:55Z	1961
-0.72376	36.84375	2141.085	2013-08-26T09:07:21Z	1962
-0.72377	36.84385	2143.897	2013-08-26T09:07:42Z	1963
-0.72376	36.84393	2146.362	2013-08-26T09:08:02Z	1964
-0.72377	36.84403	2150.293	2013-08-26T09:08:29Z	1965

GIKIGIE LINE5: ELECTRODE COORDINATES OF THE ENTIRE PROFILE

lat	lon	ns1:ele	ns1:time2	ns1:name
-0.72358	36.84068	2115.382324	2013-08-26T05:53:47Z	1880
-0.72357	36.84078	2118.50708	2013-08-26T05:57:55Z	1881
-0.72362	36.84083	2114.048584	2013-08-26T05:59:10Z	1882
-0.7236	36.84104	2115.730469	2013-08-26T06:05:23Z	1883
-0.7236	36.84111	2112.810303	2013-08-26T06:05:49Z	1884
-0.7236	36.84119	2104.49585	2013-08-26T06:07:01Z	1885
-0.7236	36.84126	2099.023682	2013-08-26T06:07:35Z	1886
-0.72357	36.84132	2094.270996	2013-08-26T06:07:57Z	1887
-0.72356	36.84141	2091.402588	2013-08-26T06:08:11Z	1888
-0.72356	36.84149	2089.922363	2013-08-26T06:08:30Z	1889
-0.72368	36.84165	2089.230469	2013-08-26T06:09:59Z	1890
-0.72368	36.84172	2089.455322	2013-08-26T06:10:16Z	1891
-0.72368	36.84182	2084.073975	2013-08-26T06:13:39Z	1892
-0.72368	36.84192	2086.302734	2013-08-26T06:14:33Z	1893
-0.7237	36.84201	2090.429199	2013-08-26T06:14:50Z	1894
-0.72369	36.84211	2091.880615	2013-08-26T06:16:07Z	1895
-0.7237	36.84219	2090.954102	2013-08-26T06:16:22Z	1896
-0.72371	36.84226	2088.60376	2013-08-26T06:16:40Z	1897
-0.72374	36.8423	2089.26001	2013-08-26T06:22:13Z	1898
-0.72376	36.8424	2089.814941	2013-08-26T06:42:52Z	1899

-0.72376	36.8425	2096.139404	2013-08-26T06:43:58Z	1900
-0.7238	36.8426	2097.145996	2013-08-26T06:47:24Z	1901
-0.72381	36.84266	2099.6875	2013-08-26T06:48:26Z	1902
-0.7238	36.84275	2101.996582	2013-08-26T06:48:42Z	1903
-0.72383	36.84283	2105.896729	2013-08-26T06:49:01Z	1904
-0.72384	36.84291	2112.635254	2013-08-26T06:50:31Z	1905
-0.72385	36.84297	2114.875244	2013-08-26T06:51:11Z	1906
-0.72388	36.84302	2112.561035	2013-08-26T06:54:39Z	1907
-0.72386	36.84309	2115.336182	2013-08-26T06:55:10Z	1908
-0.72387	36.84318	2114.637939	2013-08-26T06:55:32Z	1909
-0.72389	36.84326	2118.619873	2013-08-26T06:55:58Z	1910
-0.7239	36.84328	2120.135254	2013-08-26T06:57:04Z	1911
-0.7239	36.84328	2121.767334	2013-08-26T06:58:56Z	1912
-0.72391	36.84335	2123.767822	2013-08-26T06:59:17Z	1913
-0.72393	36.84345	2125.113037	2013-08-26T06:59:38Z	1914
-0.72394	36.84343	2125.873535	2013-08-26T07:09:16Z	1915
-0.72394	36.84352	2127.283447	2013-08-26T07:09:40Z	1916
-0.72396	36.84351	2128.143311	2013-08-26T07:09:57Z	1917
-0.72399	36.8436	2130.970215	2013-08-26T07:12:21Z	1918
-0.72399	36.84368	2135.058838	2013-08-26T07:12:53Z	1919
-0.72401	36.84375	2138.837646	2013-08-26T07:13:16Z	1920
-0.72403	36.84385	2139.670654	2013-08-26T07:14:00Z	1921
-0.72403	36.84393	2141.316162	2013-08-26T07:14:22Z	1922
-0.72402	36.84402	2143.375488	2013-08-26T07:14:37Z	1923

GIKIGIE LINE6: Electrode Coordinates of the entire profile

lat	lon	ns1:ele	ns1:time2	ns1:name
-0.74873	36.84235	2184.413	2013-08-24T11:00:01Z	1649
-0.74867	36.84226	2176.991	2013-08-24T11:00:58Z	1650
-0.74859	36.84224	2175.532	2013-08-24T11:01:18Z	1651
-0.74849	36.84222	2177.293	2013-08-24T11:01:45Z	1652
-0.74841	36.84222	2178.004	2013-08-24T11:02:21Z	1653
-0.74832	36.84219	2173.866	2013-08-24T11:02:44Z	1654
-0.74822	36.84217	2167.036	2013-08-24T11:03:23Z	1655
-0.74818	36.84223	2155.663	2013-08-24T11:05:48Z	1656
-0.74809	36.84217	2157.476	2013-08-24T11:06:32Z	1657
-0.74802	36.84218	2155.619	2013-08-24T11:07:03Z	1658

-0.74794	36.84214	2144.687	2013-08-24T11:08:12Z	1659
-0.74788	36.84214	2144.089	2013-08-24T11:09:51Z	1660
-0.74779	36.84219	2149.442	2013-08-24T11:11:39Z	1661
-0.74764	36.8421	2146.643	2013-08-24T11:12:36Z	1662
-0.74754	36.84206	2141.072	2013-08-24T11:13:17Z	1663
-0.74747	36.84199	2135.854	2013-08-24T11:14:06Z	1664
-0.74739	36.84199	2134.091	2013-08-24T11:14:25Z	1665
-0.74734	36.84194	2131.366	2013-08-24T11:15:25Z	1666

IRATI LINE800 M: Electrode Coordinates of the entire profile

lat	lon	ns1:ele	ns1:time2	ns1:name
-0.74289	36.84199	2169.336	2013-08-27T07:14:59Z	67
-0.74308	36.84198	2163.5	2013-08-27T07:15:31Z	68
-0.74324	36.84198	2157.999	2013-08-27T07:15:54Z	69
-0.74341	36.84204	2153.723	2013-08-27T07:17:04Z	70
-0.74357	36.84206	2154.878	2013-08-27T07:17:57Z	71
-0.74373	36.84205	2158.155	2013-08-27T07:18:46Z	72
-0.7439	36.84198	2157.577	2013-08-27T07:19:49Z	73
-0.74408	36.84193	2157.497	2013-08-27T07:20:37Z	74
-0.74425	36.8419	2153.192	2013-08-27T07:21:18Z	75
-0.74443	36.84192	2153.265	2013-08-27T07:21:49Z	76
-0.74462	36.84194	2150.013	2013-08-27T07:22:53Z	77
-0.74471	36.84194	2149.345	2013-08-27T07:23:06Z	78
-0.74479	36.84193	2147.416	2013-08-27T07:23:19Z	79
-0.74489	36.84192	2145.317	2013-08-27T07:23:32Z	80
-0.74498	36.84191	2145.831	2013-08-27T07:23:46Z	81
-0.74507	36.84191	2144.267	2013-08-27T07:24:00Z	82
-0.74515	36.84189	2141.8	2013-08-27T07:24:14Z	83
-0.74524	36.84189	2140.477	2013-08-27T07:24:35Z	84
-0.74534	36.84189	2138.988	2013-08-27T07:24:50Z	85
-0.74542	36.84188	2136.521	2013-08-27T07:26:22Z	86
-0.74549	36.84187	2133.687	2013-08-27T07:26:44Z	87
-0.74557	36.84187	2131.549	2013-08-27T07:27:00Z	88
-0.74567	36.84186	2130.439	2013-08-27T07:27:27Z	89
-0.74575	36.84185	2128.521	2013-08-27T07:27:55Z	90

-0.74585	36.84183	2127.607	2013-08-27T07:28:30Z	91
-0.74594	36.84182	2125.736	2013-08-27T07:29:51Z	92
-0.74602	36.8418	2124.563	2013-08-27T07:31:16Z	93
-0.74611	36.8418	2121.573	2013-08-27T07:31:51Z	94
-0.74618	36.8418	2123.14	2013-08-27T07:32:20Z	95
-0.74626	36.8418	2125.617	2013-08-27T07:33:12Z	96
-0.7464	36.84178	2128.168	2013-08-27T07:34:04Z	97
-0.74645	36.84177	2129.501	2013-08-27T07:34:53Z	98
-0.74654	36.84181	2127.903	2013-08-27T07:35:54Z	99
-0.74663	36.84182	2130.562	2013-08-27T07:36:14Z	100
-0.74672	36.84183	2126.564	2013-08-27T07:37:31Z	101
-0.74679	36.84183	2127.007	2013-08-27T07:37:50Z	102
-0.74688	36.84182	2131.183	2013-08-27T07:38:53Z	103
-0.74696	36.84181	2131.854	2013-08-27T07:39:14Z	104
-0.74706	36.84181	2134.839	2013-08-27T07:39:39Z	105
-0.74714	36.84179	2136.739	2013-08-27T07:40:06Z	106
-0.74723	36.84179	2137.235	2013-08-27T07:40:46Z	107
-0.74731	36.84178	2140.665	2013-08-27T07:41:14Z	108
-0.74741	36.84178	2139.815	2013-08-27T07:41:41Z	109
-0.7475	36.84176	2141.632	2013-08-27T07:42:13Z	110
-0.74758	36.84175	2143.374	2013-08-27T07:42:40Z	111
-0.74767	36.84173	2145.885	2013-08-27T07:43:08Z	112
-0.74776	36.84171	2147.761	2013-08-27T07:43:50Z	113
-0.74785	36.8417	2145.724	2013-08-27T07:44:16Z	114
-0.74794	36.8417	2142.316	2013-08-27T07:44:52Z	115
-0.74802	36.84171	2144.218	2013-08-27T07:45:10Z	116
-0.74813	36.84172	2147.766	2013-08-27T07:46:18Z	117
-0.7483	36.84174	2145.015	2013-08-27T07:56:58Z	118
-0.74846	36.84173	2152.082	2013-08-27T07:58:49Z	119
-0.74862	36.8417	2153.586	2013-08-27T08:00:37Z	120
-0.74878	36.84168	2166.585	2013-08-27T08:12:14Z	121
-0.74889	36.84165	2179.824	2013-08-27T08:13:47Z	122
-0.74908	36.84161	2188.031	2013-08-27T08:14:51Z	123
-0.74923	36.84162	2193.052	2013-08-27T08:15:41Z	124

-0.74939	36.84161	2198.569	2013-08-27T08:16:34Z	125
-0.74954	36.84166	2204.865	2013-08-27T08:17:37Z	126
-0.74974	36.84168	2205.519	2013-08-27T08:20:21Z	127

IRATI LINE 1: Electrode Coordinates of the entire profile

lat	lon	ns1:ele	ns1:time2	ns1:name
-0.74378	36.84148	2156.402	2013-08-24T08:23:07Z	1601
-0.74384	36.84152	2157.034	2013-08-24T08:23:48Z	1602
-0.74392	36.84157	2153.919	2013-08-24T08:24:30Z	1603
-0.74398	36.84162	2151.617	2013-08-24T08:24:52Z	1604
-0.74404	36.84166	2147.171	2013-08-24T08:25:20Z	1605
-0.74414	36.84171	2148.376	2013-08-24T08:26:28Z	1606
-0.74424	36.8417	2150.444	2013-08-24T08:27:40Z	1607
-0.74431	36.84171	2153.464	2013-08-24T08:27:54Z	1608
-0.74442	36.84174	2153.361	2013-08-24T08:28:11Z	1609
-0.74449	36.84173	2151.867	2013-08-24T08:28:29Z	1610
-0.74457	36.84174	2151.581	2013-08-24T08:28:44Z	1611
-0.74464	36.84171	2151.053	2013-08-24T08:28:56Z	1612
-0.74473	36.84175	2149.098	2013-08-24T08:29:12Z	1613
-0.74483	36.8418	2148.139	2013-08-24T08:29:30Z	1614
-0.74493	36.84181	2147.455	2013-08-24T08:29:52Z	1615
-0.74503	36.8418	2145.945	2013-08-24T08:30:19Z	1616
-0.74511	36.8418	2143.486	2013-08-24T08:30:35Z	1617
-0.74519	36.84181	2143.008	2013-08-24T08:30:49Z	1618
-0.74528	36.84181	2139.49	2013-08-24T08:31:07Z	1619
-0.74536	36.84182	2136.864	2013-08-24T08:32:59Z	1620
-0.74545	36.84182	2137.944	2013-08-24T08:33:22Z	1621
-0.74555	36.84182	2139.161	2013-08-24T08:35:16Z	1622
-0.74564	36.84181	2137.365	2013-08-24T08:35:27Z	1623
-0.74571	36.84181	2133.116	2013-08-24T08:35:40Z	1624
-0.74579	36.84181	2130.731	2013-08-24T08:35:54Z	1625
-0.74588	36.84182	2128.428	2013-08-24T08:36:21Z	1626
-0.74589	36.84182	2128.032	2013-08-24T08:36:26Z	1627
-0.74591	36.8418	2128.239	2013-08-24T08:36:33Z	1628
-0.74592	36.8418	2128.033	2013-08-24T08:36:35Z	1629

-0.74595	36.84184	2128.814	2013-08-24T08:36:56Z	1630
-0.74595	36.84185	2128.574	2013-08-24T08:36:57Z	1631
-0.74595	36.84185	2128.515	2013-08-24T08:36:58Z	1632
-0.74596	36.84184	2128.467	2013-08-24T08:37:06Z	1633
-0.74605	36.84185	2125.322	2013-08-24T08:37:44Z	1634
-0.74612	36.84187	2121.573	2013-08-24T08:38:15Z	1635
-0.74617	36.84187	2119.718	2013-08-24T08:39:56Z	1636
-0.74628	36.84187	2117.381	2013-08-24T08:47:11Z	1637
-0.74639	36.84192	2118.049	2013-08-24T08:47:51Z	1638
-0.74652	36.84193	2118.132	2013-08-24T08:50:21Z	1639
-0.74659	36.84195	2120.712	2013-08-24T08:51:15Z	1640
-0.74665	36.84198	2126.753	2013-08-24T08:51:50Z	1641
-0.74675	36.84197	2131.062	2013-08-24T08:52:39Z	1642
-0.74684	36.84199	2135.84	2013-08-24T08:53:55Z	1643
-0.74715	36.84193	2131.803	2013-08-24T08:59:21Z	1644
-0.74715	36.84193	2132.273	2013-08-24T08:59:26Z	1645
-0.74689	36.84196	2131.633	2013-08-24T09:00:38Z	1646
-0.747	36.84197	2135.302	2013-08-24T09:01:10Z	1647
-0.74708	36.84196	2135.417	2013-08-24T09:01:26Z	1648
-0.74873	36.84235	2184.413	2013-08-24T11:00:01Z	1649
-0.74867	36.84226	2176.991	2013-08-24T11:00:58Z	1650
-0.74859	36.84224	2175.532	2013-08-24T11:01:18Z	1651
-0.74849	36.84222	2177.293	2013-08-24T11:01:45Z	1652
-0.74841	36.84222	2178.004	2013-08-24T11:02:21Z	1653
-0.74832	36.84219	2173.866	2013-08-24T11:02:44Z	1654
-0.74822	36.84217	2167.036	2013-08-24T11:03:23Z	1655
-0.74818	36.84223	2155.663	2013-08-24T11:05:48Z	1656
-0.74809	36.84217	2157.476	2013-08-24T11:06:32Z	1657
-0.74802	36.84218	2155.619	2013-08-24T11:07:03Z	1658
-0.74794	36.84214	2144.687	2013-08-24T11:08:12Z	1659
-0.74788	36.84214	2144.089	2013-08-24T11:09:51Z	1660
-0.74779	36.84219	2149.442	2013-08-24T11:11:39Z	1661
-0.74764	36.8421	2146.643	2013-08-24T11:12:36Z	1662
-0.74754	36.84206	2141.072	2013-08-24T11:13:17Z	1663
-0.74747	36.84199	2135.854	2013-08-24T11:14:06Z	1664
-0.74739	36.84199	2134.091	2013-08-24T11:14:25Z	1665

-0.74734	36.84194	2131.366	2013-08-24T11:15:25Z	1666
-0.74724	36.84192	2132.811	2013-08-24T11:16:53Z	1667
-0.74731	36.84195	2137.573	2013-08-24T11:17:44Z	1668
-0.74731	36.84195	2137.809	2013-08-24T11:17:47Z	1669

IRATI LINE 2: Electrode Coordinates of the entire profile

lat	lon	ns1:ele	ns1:time2	ns1:name
-0.74789	36.84172	2148.404	2013-08-24T06:57:30Z	1560
-0.74782	36.84171	2147.155	2013-08-24T06:59:00Z	1561
-0.74772	36.84174	2148.021	2013-08-24T07:00:14Z	1562
-0.74763	36.84175	2146.665	2013-08-24T07:00:58Z	1563
-0.74754	36.84173	2145.283	2013-08-24T07:01:41Z	1564
-0.74746	36.84171	2142.631	2013-08-24T07:02:49Z	1565
-0.74736	36.84171	2140.376	2013-08-24T07:03:43Z	1566
-0.74728	36.8417	2137.332	2013-08-24T07:04:20Z	1567
-0.7472	36.84171	2136.531	2013-08-24T07:04:59Z	1568
-0.7471	36.8417	2135.281	2013-08-24T07:05:46Z	1569
-0.74702	36.84167	2134.69	2013-08-24T07:07:14Z	1570
-0.74694	36.84166	2131.269	2013-08-24T07:08:00Z	1571
-0.74685	36.84167	2132.758	2013-08-24T07:08:55Z	1572
-0.74676	36.84164	2128.861	2013-08-24T07:09:33Z	1573
-0.7467	36.84165	2126.104	2013-08-24T07:10:00Z	1574
-0.74658	36.84165	2130.565	2013-08-24T07:11:32Z	1575
-0.74651	36.84169	2126.488	2013-08-24T07:12:39Z	1576
-0.74641	36.84166	2123.139	2013-08-24T07:13:28Z	1577
-0.74636	36.84163	2126.661	2013-08-24T07:15:53Z	1578
-0.74627	36.84164	2132.609	2013-08-24T07:24:30Z	1579
-0.74619	36.84162	2124.548	2013-08-24T07:27:46Z	1580
-0.74613	36.84162	2124.425	2013-08-24T07:27:57Z	1581
-0.7461	36.84162	2124.632	2013-08-24T07:28:04Z	1582
-0.74601	36.84162	2123.959	2013-08-24T07:28:19Z	1583
-0.74591	36.84163	2125.801	2013-08-24T07:28:34Z	1584
-0.74582	36.84164	2128.903	2013-08-24T07:28:50Z	1585
-0.74574	36.84163	2130.746	2013-08-24T07:29:04Z	1586
-0.74564	36.84164	2133.706	2013-08-24T07:29:21Z	1587
-0.74556	36.84164	2133.586	2013-08-24T07:29:42Z	1588

-0.74548	36.84165	2134.983	2013-08-24T07:30:03Z	1589
-0.74538	36.84168	2137.985	2013-08-24T07:31:52Z	1590
-0.74531	36.8417	2138.292	2013-08-24T07:32:16Z	1591
-0.74522	36.84174	2141.909	2013-08-24T07:35:02Z	1592
-0.74513	36.84177	2144.118	2013-08-24T07:35:30Z	1593
-0.74505	36.84178	2144.299	2013-08-24T07:35:44Z	1594
-0.74497	36.8418	2145.614	2013-08-24T07:35:58Z	1595
-0.74488	36.84182	2147.597	2013-08-24T07:36:19Z	1596
-0.7448	36.84186	2148.844	2013-08-24T07:36:32Z	1597
-0.74473	36.84189	2150.296	2013-08-24T07:36:45Z	1598
-0.74466	36.84193	2151.224	2013-08-24T07:36:58Z	1599
-0.74459	36.84201	2150.827	2013-08-24T07:43:36Z	1600

IRATI LINE 3: ELECTRODE COORDINATES OF THE ENTIRE PROFILE

lat	lon	ns1:ele	ns1:time2	ns1:name
-0.74471	36.84187	2150.588379	2013-08-24T06:04:36Z	1518
-0.74479	36.84184	2150.900879	2013-08-24T06:05:49Z	1519
-0.74487	36.8418	2148.942139	2013-08-24T06:06:01Z	1520
-0.74494	36.84175	2146.374268	2013-08-24T06:06:31Z	1521
-0.74501	36.8417	2143.38916	2013-08-24T06:06:51Z	1522
-0.74508	36.84166	2141.763916	2013-08-24T06:07:12Z	1523
-0.74516	36.84161	2137.511719	2013-08-24T06:07:52Z	1524
-0.74525	36.84154	2138.423584	2013-08-24T06:09:11Z	1525
-0.7453	36.84153	2136.921631	2013-08-24T06:09:44Z	1526
-0.74539	36.8415	2132.150879	2013-08-24T06:12:39Z	1527
-0.74547	36.84148	2131.235107	2013-08-24T06:12:59Z	1528
-0.74555	36.84147	2128.67627	2013-08-24T06:13:13Z	1529
-0.74564	36.84144	2126.119629	2013-08-24T06:13:23Z	1530
-0.74572	36.84143	2124.178467	2013-08-24T06:13:34Z	1531
-0.7458	36.84141	2122.79126	2013-08-24T06:13:46Z	1532
-0.7459	36.84139	2120.320068	2013-08-24T06:13:58Z	1533
-0.74608	36.84137	2122.246338	2013-08-24T06:16:38Z	1534
-0.74617	36.84139	2123.294678	2013-08-24T06:18:03Z	1535
-0.74626	36.84142	2122.562256	2013-08-24T06:18:38Z	1536
-0.74635	36.84141	2122.179688	2013-08-24T06:19:20Z	1537
-0.74644	36.8414	2123.069824	2013-08-24T06:25:40Z	1538

-0.74651	36.84141	2125.437256	2013-08-24T06:26:24Z	1539
-0.74659	36.84143	2125.134033	2013-08-24T06:26:45Z	1540
-0.74668	36.84143	2127.134277	2013-08-24T06:27:27Z	1541
-0.74678	36.84144	2125.873291	2013-08-24T06:28:01Z	1542
-0.74687	36.84144	2127.451172	2013-08-24T06:28:47Z	1543
-0.74695	36.84143	2127.107422	2013-08-24T06:28:59Z	1544
-0.74714	36.84141	2126.550781	2013-08-24T06:29:29Z	1545
-0.74722	36.8414	2127.671875	2013-08-24T06:29:44Z	1546
-0.74732	36.84139	2132.794922	2013-08-24T06:34:37Z	1547
-0.74737	36.84138	2136.654541	2013-08-24T06:36:05Z	1548
-0.74737	36.84142	2137.642578	2013-08-24T06:36:29Z	1549
-0.74739	36.84143	2138.083496	2013-08-24T06:36:33Z	1550
-0.74742	36.84141	2138.770264	2013-08-24T06:36:39Z	1551
-0.74745	36.8414	2141.804443	2013-08-24T06:37:00Z	1552
-0.74753	36.84139	2148.29126	2013-08-24T06:37:32Z	1553
-0.74762	36.84137	2151.188721	2013-08-24T06:37:49Z	1554
-0.7477	36.84135	2153.110107	2013-08-24T06:38:12Z	1555
-0.74779	36.84134	2153.883545	2013-08-24T06:38:27Z	1556
-0.74787	36.84132	2156.687988	2013-08-24T06:38:47Z	1557
-0.74795	36.8413	2160.540527	2013-08-24T06:39:16Z	1558
-0.74804	36.84131	2161.467529	2013-08-24T06:39:47Z	1559

IRATI LINE 4: Electrode Coordinates of the entire profile

lat	lon	ns1:ele	ns1:time2	ns1:name
-0.746891	36.8401	2129.358398	2013-08-23T12:53:17Z	1475
-0.746863	36.84026	2131.826904	2013-08-23T12:59:57Z	1476
-0.74686	36.84026	2131.070557	2013-08-23T13:00:04Z	1477
-0.746818	36.84036	2131.42041	2013-08-23T13:00:21Z	1478
-0.746781	36.84045	2130.77002	2013-08-23T13:00:36Z	1479
-0.746759	36.84054	2130.42749	2013-08-23T13:00:49Z	1480
-0.746732	36.84062	2129.612549	2013-08-23T13:01:02Z	1481
-0.746707	36.84071	2128.081055	2013-08-23T13:01:44Z	1482
-0.746679	36.84079	2129.341797	2013-08-23T13:01:59Z	1483
-0.746653	36.84088	2129.249023	2013-08-23T13:02:12Z	1484
-0.746621	36.84096	2128.174805	2013-08-23T13:02:26Z	1485

-0.746602	36.84104	2126.871094	2013-08-23T13:02:40Z	1486
-0.746569	36.84115	2126.415039	2013-08-23T13:02:55Z	1487
-0.746551	36.84122	2127.085449	2013-08-23T13:05:04Z	1488
-0.746517	36.84128	2128.183594	2013-08-23T13:07:25Z	1489
-0.746482	36.84139	2124.227783	2013-08-23T13:08:56Z	1490
-0.746445	36.84155	2125.599609	2013-08-23T13:10:11Z	1491
-0.746394	36.84161	2125.165039	2013-08-23T13:10:30Z	1492
-0.746385	36.84169	2124.703613	2013-08-23T13:10:51Z	1493
-0.746326	36.84188	2125.345703	2013-08-23T13:13:04Z	1494
-0.746336	36.84198	2127.553711	2013-08-23T13:13:31Z	1495
-0.746358	36.84206	2129.262451	2013-08-23T13:14:13Z	1496
-0.746336	36.84215	2127.182129	2013-08-23T13:14:40Z	1497
-0.746348	36.84227	2122.22583	2013-08-23T13:15:55Z	1498
-0.746397	36.84233	2122.951172	2013-08-23T13:17:13Z	1499
-0.746447	36.8424	2125.958008	2013-08-23T13:17:42Z	1500
-0.746465	36.84246	2128.486572	2013-08-23T13:18:04Z	1501
-0.746506	36.84249	2130.189941	2013-08-23T13:18:20Z	1502
-0.746567	36.84256	2130.947998	2013-08-23T13:18:38Z	1503
-0.746648	36.84264	2130.843994	2013-08-23T13:18:56Z	1504
-0.746751	36.8427	2126.494385	2013-08-23T13:19:20Z	1505
-0.746823	36.84277	2123.14624	2013-08-23T13:20:24Z	1506
-0.746905	36.8428	2122.171631	2013-08-23T13:21:24Z	1507
-0.746998	36.84285	2119.756104	2013-08-23T13:22:06Z	1508
-0.747038	36.84288	2121.551025	2013-08-23T13:22:34Z	1509
-0.747114	36.84291	2123.378662	2013-08-23T13:23:04Z	1510
-0.747184	36.84295	2124.958008	2013-08-23T13:23:33Z	1511
-0.747256	36.84302	2123.481445	2013-08-23T13:24:09Z	1512
-0.747323	36.8431	2125.155029	2013-08-23T13:24:41Z	1513

MAKOMBOKI LINE 800 M: Electrode Coordinates of the entire profile

lat	lon	ns1:ele	ns1:time2	ns1:name
-0.80268	36.83734	2059.996	2013-08-20T11:24:24Z	1004
-0.80252	36.83732	2078.359	2013-08-20T11:27:40Z	1005
-0.80234	36.83734	2079.783	2013-08-20T11:29:01Z	1006
-0.80217	36.83737	2083.53	2013-08-20T11:30:16Z	1007

-0.80199	36.83738	2087.986	2013-08-20T11:31:39Z	1008
-0.80181	36.83739	2090.557	2013-08-20T11:33:43Z	1009
-0.80164	36.83742	2094.317	2013-08-20T11:35:04Z	1010
-0.80148	36.83744	2104.742	2013-08-20T11:37:14Z	1011
-0.8013	36.83742	2107.383	2013-08-20T11:49:50Z	1012
-0.80115	36.83744	2112.138	2013-08-20T11:51:05Z	1013
-0.80097	36.83746	2121.006	2013-08-20T11:52:39Z	1014
-0.80088	36.83748	2123.621	2013-08-20T11:53:10Z	1015
-0.80079	36.83749	2127.703	2013-08-20T11:53:55Z	1016
-0.80072	36.8375	2129.432	2013-08-20T11:54:21Z	1017
-0.80063	36.83751	2133.504	2013-08-20T11:54:51Z	1018
-0.80054	36.8375	2134.959	2013-08-20T11:55:17Z	1019
-0.80046	36.83751	2138.361	2013-08-20T11:55:40Z	1020
-0.80036	36.83753	2141.004	2013-08-20T11:56:04Z	1021
-0.80028	36.83753	2144.182	2013-08-20T11:56:21Z	1022
-0.80019	36.83752	2145.571	2013-08-20T11:56:40Z	1023
-0.8001	36.83753	2146.513	2013-08-20T11:57:00Z	1024
-0.80001	36.83755	2147.484	2013-08-20T11:57:26Z	1025
-0.79992	36.83755	2147.229	2013-08-20T11:58:15Z	1026
-0.79984	36.83756	2146.833	2013-08-20T11:58:44Z	1027
-0.79975	36.83758	2144.777	2013-08-20T12:00:02Z	1028
-0.79966	36.83757	2146.837	2013-08-20T12:01:07Z	1029
-0.79957	36.83758	2143.738	2013-08-20T12:01:42Z	1030
-0.79948	36.83758	2143.134	2013-08-20T12:01:57Z	1031
-0.79939	36.83758	2142.635	2013-08-20T12:02:11Z	1032
-0.7993	36.83758	2143.578	2013-08-20T12:03:10Z	1033
-0.79923	36.83758	2144.773	2013-08-20T12:03:26Z	1034
-0.79912	36.83757	2148.253	2013-08-20T12:09:34Z	1035
-0.79904	36.83755	2148.483	2013-08-20T12:10:28Z	1036
-0.79894	36.83755	2146.709	2013-08-20T12:10:48Z	1037
-0.79886	36.83758	2146.383	2013-08-20T12:11:04Z	1038
-0.79878	36.8376	2144.556	2013-08-20T12:11:19Z	1039
-0.79868	36.83762	2145.417	2013-08-20T12:11:46Z	1040
-0.79859	36.83763	2143.92	2013-08-20T12:12:05Z	1041
-0.79849	36.83764	2142.67	2013-08-20T12:12:39Z	1042
-0.79838	36.83767	2146.051	2013-08-20T12:13:47Z	1043

-0.79832	36.83767	2145.173	2013-08-20T12:14:12Z	1044
-0.79822	36.83767	2145.738	2013-08-20T12:14:28Z	1045
-0.79814	36.83768	2144.965	2013-08-20T12:14:45Z	1046
-0.79805	36.83767	2143.466	2013-08-20T12:14:58Z	1047
-0.79796	36.83767	2144.141	2013-08-20T12:15:16Z	1048
-0.79788	36.83769	2147.478	2013-08-20T12:16:40Z	1049
-0.7978	36.83769	2147.241	2013-08-20T12:18:08Z	1050
-0.79769	36.8377	2147.267	2013-08-20T12:18:56Z	1051
-0.79762	36.83769	2148.394	2013-08-20T12:19:47Z	1052
-0.79753	36.83773	2147.566	2013-08-20T12:21:55Z	1053
-0.79743	36.83773	2147.354	2013-08-20T12:22:30Z	1054
-0.79726	36.83775	2149.227	2013-08-20T12:22:57Z	1055
-0.79707	36.83776	2149.62	2013-08-20T12:23:19Z	1056
-0.7969	36.83778	2149.517	2013-08-20T12:23:44Z	1057
-0.79671	36.83779	2151.365	2013-08-20T12:24:08Z	1058
-0.79653	36.83782	2151.642	2013-08-20T12:24:31Z	1059
-0.79636	36.83784	2153.889	2013-08-20T12:25:25Z	1060
-0.79618	36.83787	2154.149	2013-08-20T12:27:07Z	1061
-0.79599	36.83788	2157.718	2013-08-20T12:27:46Z	1062
-0.79582	36.83787	2157.642	2013-08-20T12:28:40Z	1063
-0.79565	36.8379	2159.478	2013-08-20T12:29:45Z	1064

MAKOMBOKI LINE 1: Electrode Coordinates of the entire profile

lat	lon	ns1:ele	ns1:time2	ns1:name
-0.80493	36.8362	2076.292	2013-08-21T06:05:13Z	1066
-0.80484	36.83625	2074.068	2013-08-21T06:05:48Z	1067
-0.80477	36.83631	2075.104	2013-08-21T06:06:12Z	1068
-0.80468	36.83635	2073.241	2013-08-21T06:06:50Z	1069
-0.80461	36.83639	2069.874	2013-08-21T06:07:19Z	1070
-0.80453	36.83641	2071.616	2013-08-21T06:07:59Z	1071
-0.80445	36.83645	2070.929	2013-08-21T06:08:39Z	1072
-0.80437	36.83649	2072.242	2013-08-21T06:09:25Z	1073
-0.80429	36.83652	2071.178	2013-08-21T06:10:21Z	1074
-0.80421	36.83656	2070.476	2013-08-21T06:11:05Z	1075
-0.80414	36.83661	2067.878	2013-08-21T06:11:32Z	1076

-0.80406	36.83665	2069.23	2013-08-21T06:11:53Z	1077
-0.80398	36.83669	2063.915	2013-08-21T06:12:59Z	1078
-0.80389	36.83671	2063.623	2013-08-21T06:13:42Z	1079
-0.8038	36.83675	2064.56	2013-08-21T06:14:53Z	1080
-0.80373	36.83682	2065.109	2013-08-21T06:15:50Z	1081
-0.80364	36.83682	2062.852	2013-08-21T06:16:46Z	1082
-0.80357	36.83688	2070.429	2013-08-21T06:17:21Z	1083
-0.8035	36.83695	2070.006	2013-08-21T06:18:29Z	1084
-0.8034	36.83695	2061.832	2013-08-21T06:19:15Z	1085
-0.80333	36.83697	2063.633	2013-08-21T06:20:36Z	1086
-0.80324	36.83702	2061.861	2013-08-21T06:22:44Z	1087
-0.80315	36.83707	2061.757	2013-08-21T06:24:07Z	1088
-0.80307	36.8371	2061.464	2013-08-21T06:24:31Z	1089
-0.80301	36.83717	2064.966	2013-08-21T06:25:21Z	1090
-0.80294	36.83722	2065.639	2013-08-21T06:25:36Z	1091
-0.80283	36.83726	2064.945	2013-08-21T06:25:54Z	1092
-0.80276	36.83729	2067.871	2013-08-21T06:26:16Z	1093
-0.80269	36.83733	2072.205	2013-08-21T06:26:38Z	1094
-0.80263	36.83735	2079.162	2013-08-21T06:27:05Z	1095
-0.80258	36.8374	2086.596	2013-08-21T06:28:53Z	1096
-0.8025	36.83745	2085.242	2013-08-21T06:30:19Z	1097
-0.80242	36.83749	2087.659	2013-08-21T06:30:36Z	1098
-0.80234	36.83754	2090.454	2013-08-21T06:31:07Z	1099
-0.80228	36.83759	2093.191	2013-08-21T06:31:56Z	1100
-0.80219	36.83763	2093.313	2013-08-21T06:32:35Z	1101
-0.80212	36.83767	2095.946	2013-08-21T06:33:14Z	1102
-0.80204	36.83771	2099.697	2013-08-21T06:34:03Z	1103
-0.80196	36.83775	2100.816	2013-08-21T06:34:41Z	1104
-0.80188	36.83778	2106.092	2013-08-21T06:35:26Z	1105
-0.80183	36.83781	2108.294	2013-08-21T06:36:07Z	1106

MAKOMBOKI LINE 2: Electrode Coordinates of the entire profile

lat	lon	ns1:ele	ns1:time2	ns1:name
-0.80029	36.83755	2143.617	2013-08-22T07:41:05Z	1279
-0.80036	36.83756	2141.917	2013-08-22T07:43:08Z	1280
-0.80044	36.83755	2140.196	2013-08-22T07:44:27Z	1281

-0.80053	36.83753	2139.135	2013-08-22T07:45:11Z	1282
-0.80062	36.83753	2135.55	2013-08-22T07:45:36Z	1283
-0.80072	36.83752	2131.031	2013-08-22T07:46:12Z	1284
-0.8008	36.83751	2129.665	2013-08-22T07:46:35Z	1285
-0.80087	36.8375	2126.502	2013-08-22T07:51:09Z	1286
-0.80096	36.83749	2123.876	2013-08-22T07:51:36Z	1287
-0.80105	36.83748	2120.575	2013-08-22T07:52:35Z	1288
-0.80114	36.83747	2117.595	2013-08-22T07:53:15Z	1289
-0.80122	36.83746	2114.846	2013-08-22T07:53:54Z	1290
-0.80131	36.83746	2112.874	2013-08-22T07:54:26Z	1291
-0.80138	36.83745	2107.871	2013-08-22T07:55:17Z	1292
-0.80146	36.83746	2106.059	2013-08-22T07:56:49Z	1293
-0.80154	36.83744	2101.592	2013-08-22T07:58:18Z	1294
-0.80164	36.83743	2096.65	2013-08-22T08:01:04Z	1295
-0.80172	36.83742	2093.818	2013-08-22T08:01:38Z	1296
-0.8018	36.83741	2092.958	2013-08-22T08:04:06Z	1297
-0.80189	36.8374	2090.468	2013-08-22T08:05:32Z	1298
-0.80198	36.8374	2089.681	2013-08-22T08:06:15Z	1299
-0.80207	36.83739	2089.338	2013-08-22T08:09:39Z	1300
-0.80215	36.83737	2088.327	2013-08-22T08:10:13Z	1301
-0.80224	36.83735	2089.449	2013-08-22T08:11:42Z	1302
-0.80233	36.83734	2086.581	2013-08-22T08:12:21Z	1303
-0.8024	36.83733	2083.712	2013-08-22T08:13:14Z	1304
-0.80245	36.83732	2080.833	2013-08-22T08:14:18Z	1305
-0.80249	36.83732	2078.604	2013-08-22T08:14:51Z	1306
-0.80258	36.83731	2072.569	2013-08-22T08:15:53Z	1307
-0.80265	36.83732	2068.814	2013-08-22T08:16:50Z	1308
-0.80276	36.83732	2070.718	2013-08-22T08:17:10Z	1309
-0.80282	36.8373	2069.716	2013-08-22T08:17:25Z	1310
-0.80293	36.83731	2069.505	2013-08-22T08:17:44Z	1311
-0.80301	36.83729	2068.907	2013-08-22T08:19:39Z	1312
-0.8031	36.83728	2068.191	2013-08-22T08:19:56Z	1313
-0.80318	36.83726	2067.819	2013-08-22T08:20:10Z	1314
-0.80327	36.83725	2066.183	2013-08-22T08:20:25Z	1315
-0.80336	36.83725	2063.422	2013-08-22T08:20:42Z	1316
-0.80346	36.83723	2064.844	2013-08-22T08:21:18Z	1317

-0.80353	36.83721	2067.317	2013-08-22T08:21:41Z	1318
-0.80358	36.83724	2067.872	2013-08-22T08:22:46Z	1319
-0.80362	36.83722	2069.688	2013-08-22T08:23:57Z	1320
-0.80361	36.83722	2068.099	2013-08-22T08:24:28Z	1321
-0.8037	36.83721	2069.707	2013-08-22T08:25:10Z	1322

MAKOMBOKI LINE 3: Electrode Coordinates of the entire profile

lat	lon	ns1:ele	ns1:time2	ns1:name
-0.80195	36.83558	2076.196	2013-08-22T05:38:29Z	1238
-0.802	36.83569	2084.85	2013-08-22T05:40:28Z	1239
-0.80203	36.83576	2082.462	2013-08-22T05:41:13Z	1240
-0.80207	36.83585	2079.353	2013-08-22T05:42:07Z	1241
-0.80209	36.83592	2078.828	2013-08-22T05:42:31Z	1242
-0.80213	36.83601	2080.007	2013-08-22T05:43:03Z	1243
-0.80217	36.83609	2077.983	2013-08-22T05:44:20Z	1244
-0.80221	36.83617	2079.635	2013-08-22T05:44:54Z	1245
-0.80225	36.83625	2081.239	2013-08-22T05:45:26Z	1246
-0.80228	36.83634	2082.072	2013-08-22T05:46:18Z	1247
-0.8023	36.83642	2082.286	2013-08-22T05:47:10Z	1248
-0.80231	36.8365	2083.465	2013-08-22T05:47:28Z	1249
-0.80233	36.8366	2084.55	2013-08-22T05:47:47Z	1250
-0.80235	36.83668	2084.698	2013-08-22T05:48:31Z	1251
-0.80238	36.83678	2085.446	2013-08-22T05:49:21Z	1252
-0.8024	36.83686	2087.016	2013-08-22T05:50:13Z	1253
-0.8024	36.83694	2087.35	2013-08-22T05:51:07Z	1254
-0.80243	36.83703	2086.199	2013-08-22T05:51:35Z	1255
-0.80245	36.83713	2086.226	2013-08-22T05:55:07Z	1256
-0.80247	36.83721	2086.043	2013-08-22T05:55:32Z	1257
-0.8025	36.8373	2085.572	2013-08-22T05:55:55Z	1258
-0.80249	36.83739	2085.033	2013-08-22T05:58:03Z	1259
-0.80251	36.83748	2087.939	2013-08-22T05:59:26Z	1260
-0.80253	36.83757	2088.998	2013-08-22T06:01:37Z	1261
-0.80254	36.83765	2089.094	2013-08-22T06:03:23Z	1262
-0.80255	36.83774	2090.692	2013-08-22T06:04:14Z	1263
-0.80257	36.83782	2094.691	2013-08-22T06:04:48Z	1264
-0.8026	36.83791	2098.973	2013-08-22T06:05:41Z	1265

-0.80261	36.838	2096.666	2013-08-22T06:06:40Z	1266
-0.80262	36.83808	2101.228	2013-08-22T06:07:19Z	1267
-0.80263	36.83817	2105.015	2013-08-22T06:08:16Z	1268
-0.80266	36.83825	2107.609	2013-08-22T06:09:25Z	1269
-0.80267	36.83834	2110.166	2013-08-22T06:10:05Z	1270
-0.80271	36.83841	2112.881	2013-08-22T06:10:40Z	1271
-0.80274	36.8385	2114.54	2013-08-22T06:11:09Z	1272
-0.80275	36.83858	2116.88	2013-08-22T06:11:35Z	1273
-0.80277	36.83866	2118.208	2013-08-22T06:12:33Z	1274
-0.80279	36.83875	2120.328	2013-08-22T06:12:54Z	1275
-0.80282	36.83885	2123.062	2013-08-22T06:13:32Z	1276
-0.80284	36.83892	2121.286	2013-08-22T06:16:18Z	1277
-0.80285	36.83899	2121.726	2013-08-22T06:16:51Z	1278

MAKOMBOKI LINE 4: Electrode Coordinates of the entire profile

lat	lon	ns1:ele	ns1:time2	ns1:name
-0.80217	36.8357	2066.681	2013-08-21T11:45:12Z	1196
-0.80217	36.83575	2072.271	2013-08-21T11:46:35Z	1197
-0.80221	36.83584	2074.885	2013-08-21T11:47:14Z	1198
-0.80225	36.83591	2074.247	2013-08-21T11:47:43Z	1199
-0.80228	36.836	2075.522	2013-08-21T11:48:16Z	1200
-0.80231	36.83609	2077.83	2013-08-21T11:48:45Z	1201
-0.80235	36.83618	2078.844	2013-08-21T11:49:22Z	1202
-0.80239	36.83625	2079.454	2013-08-21T11:49:51Z	1203
-0.80244	36.83633	2078.966	2013-08-21T11:50:18Z	1204
-0.80246	36.83641	2079.491	2013-08-21T11:50:48Z	1205
-0.80249	36.83649	2077.772	2013-08-21T11:51:09Z	1206
-0.80252	36.83659	2080.163	2013-08-21T11:51:47Z	1207
-0.80255	36.83668	2080.873	2013-08-21T11:52:14Z	1208
-0.80258	36.83677	2081.264	2013-08-21T11:52:54Z	1209
-0.80261	36.83683	2079.991	2013-08-21T11:53:57Z	1210
-0.80265	36.83694	2076.681	2013-08-21T11:55:06Z	1211
-0.80268	36.83701	2074.684	2013-08-21T11:55:44Z	1212
-0.80271	36.83708	2071.514	2013-08-21T11:56:38Z	1213
-0.80274	36.83717	2070.029	2013-08-21T11:57:33Z	1214

-0.80278	36.83727	2068.842	2013-08-21T11:58:13Z	1215
-0.8028	36.83735	2066.052	2013-08-21T11:58:52Z	1216
-0.80281	36.83739	2058.865	2013-08-21T12:01:16Z	1217
-0.80281	36.83738	2060.64	2013-08-21T12:01:26Z	1218
-0.80285	36.83746	2065.951	2013-08-21T12:01:57Z	1219
-0.80286	36.83756	2067.802	2013-08-21T12:02:22Z	1220
-0.80287	36.83766	2069.36	2013-08-21T12:02:48Z	1221
-0.80289	36.83775	2070.873	2013-08-21T12:03:08Z	1222
-0.80291	36.83784	2072.13	2013-08-21T12:03:31Z	1223
-0.80293	36.83793	2073.031	2013-08-21T12:03:56Z	1224
-0.80295	36.83801	2074.09	2013-08-21T12:04:32Z	1225
-0.80296	36.83808	2079.376	2013-08-21T12:05:18Z	1226
-0.80299	36.83816	2082.231	2013-08-21T12:06:08Z	1227
-0.80302	36.83824	2094.141	2013-08-21T12:09:51Z	1228
-0.80304	36.83829	2098.77	2013-08-21T12:11:41Z	1229
-0.80305	36.83835	2100.618	2013-08-21T12:12:41Z	1230
-0.80309	36.83843	2106.964	2013-08-21T12:13:45Z	1231
-0.80308	36.83851	2113.018	2013-08-21T12:14:11Z	1232
-0.80309	36.83859	2116.197	2013-08-21T12:14:32Z	1233
-0.80311	36.83868	2116.975	2013-08-21T12:14:57Z	1234
-0.80311	36.83878	2116.798	2013-08-21T12:15:18Z	1235
-0.80312	36.83885	2116.077	2013-08-21T12:15:57Z	1236
-0.80302	36.83886	2115.008	2013-08-21T12:16:26Z	1237
-0.80314	36.83893	2117.234	2013-08-21T12:17:43Z	1238

MAKOMBOKI LINE 5: Electrode Coordinates of the entire profile

lat	lon	ns1:ele	ns1:time2	ns1:name
-0.803863	36.838619	2131.716553	2013-08-21T09:09:38Z	1154
-0.803834	36.838542	2126.195068	2013-08-21T09:11:02Z	1155
-0.803778	36.838464	2122.666748	2013-08-21T09:11:26Z	1156
-0.80374	36.838382	2117.18457	2013-08-21T09:11:41Z	1157
-0.803712	36.838316	2114.772217	2013-08-21T09:12:03Z	1158
-0.803688	36.838228	2111.724854	2013-08-21T09:12:20Z	1159
-0.803653	36.83816	2106.20874	2013-08-21T09:13:09Z	1160
-0.803614	36.838078	2102.999512	2013-08-21T09:15:46Z	1161

-0.803573	36.838027	2099.383545	2013-08-21T09:16:57Z	1162
-0.803542	36.837949	2091.075684	2013-08-21T09:19:06Z	1163
-0.803499	36.83787	2090.425293	2013-08-21T09:19:40Z	1164
-0.803468	36.837791	2085.506104	2013-08-21T09:20:01Z	1165
-0.803424	36.837711	2081.384033	2013-08-21T09:20:33Z	1166
-0.803384	36.837649	2077.813965	2013-08-21T09:21:04Z	1167
-0.803348	36.83758	2073.680664	2013-08-21T09:21:41Z	1168
-0.803298	36.837502	2070.342773	2013-08-21T09:22:03Z	1169
-0.803251	36.837427	2069.332764	2013-08-21T09:22:19Z	1170
-0.803219	36.837357	2067.391113	2013-08-21T09:22:33Z	1171
-0.803175	36.837282	2064.798828	2013-08-21T09:22:44Z	1172
-0.803133	36.837196	2064.827637	2013-08-21T09:23:19Z	1173
-0.803278	36.837032	2062.370117	2013-08-21T09:30:01Z	1174
-0.803021	36.836969	2075.627197	2013-08-21T09:41:36Z	1175
-0.802978	36.836905	2075.251709	2013-08-21T09:41:55Z	1176
-0.802935	36.836832	2077.604248	2013-08-21T09:42:10Z	1177
-0.802901	36.836751	2076.252686	2013-08-21T09:42:24Z	1178
-0.802857	36.836672	2077.088135	2013-08-21T09:42:37Z	1179
-0.802809	36.836587	2077.274658	2013-08-21T09:42:55Z	1180
-0.802776	36.836502	2076.924316	2013-08-21T09:43:23Z	1181
-0.802734	36.83644	2076.787354	2013-08-21T09:43:52Z	1182
-0.802682	36.836378	2076.963623	2013-08-21T09:44:23Z	1183
-0.802638	36.836316	2071.996338	2013-08-21T09:44:56Z	1184
-0.802615	36.836243	2073.510986	2013-08-21T09:45:33Z	1185
-0.802556	36.836133	2075.419678	2013-08-21T09:45:50Z	1186
-0.802512	36.836047	2073.729492	2013-08-21T09:46:20Z	1187
-0.802454	36.835954	2070.204834	2013-08-21T09:47:38Z	1188
-0.802422	36.8359	2070.03125	2013-08-21T09:48:10Z	1189
-0.802386	36.835823	2069.476562	2013-08-21T09:48:55Z	1190
-0.802336	36.835731	2071.435059	2013-08-21T09:49:34Z	1191
-0.802291	36.835657	2068.907959	2013-08-21T09:50:59Z	1192
-0.802239	36.835582	2069.637695	2013-08-21T09:51:26Z	1193

MAKOMBOKI LINE 6: Electrode Coordinates of the entire profile

lat	lon	ns1:ele	ns1:time2	ns1:name
-0.80255	36.83546	2062.798096	2013-08-21T08:01:35Z	1107

-0.80261	36.83548	2067.892334	2013-08-21T08:05:32Z	1108
-0.80266	36.83555	2069.660645	2013-08-21T08:07:29Z	1109
-0.80265	36.83559	2069.421387	2013-08-21T08:07:38Z	1110
-0.80267	36.83559	2068.827148	2013-08-21T08:07:50Z	1111
-0.80264	36.83561	2068.424561	2013-08-21T08:08:01Z	1112
-0.80266	36.83563	2067.022949	2013-08-21T08:08:09Z	1113
-0.80266	36.83556	2068.963623	2013-08-21T08:09:27Z	1114
-0.8027	36.83565	2074.12207	2013-08-21T08:11:44Z	1115
-0.80274	36.83571	2072.409424	2013-08-21T08:12:02Z	1116
-0.8028	36.83579	2068.326172	2013-08-21T08:12:33Z	1117
-0.80282	36.83587	2067.340088	2013-08-21T08:12:59Z	1118
-0.80286	36.83595	2066.550781	2013-08-21T08:13:32Z	1119
-0.80289	36.83604	2065.309814	2013-08-21T08:13:49Z	1120
-0.80292	36.83613	2067.097412	2013-08-21T08:14:04Z	1121
-0.80297	36.83622	2068.918945	2013-08-21T08:14:28Z	1122
-0.803	36.83632	2069.288086	2013-08-21T08:14:51Z	1123
-0.80304	36.83641	2070.405518	2013-08-21T08:15:25Z	1124
-0.80307	36.83645	2069.612061	2013-08-21T08:15:41Z	1125
-0.8031	36.83654	2068.206055	2013-08-21T08:16:02Z	1126
-0.80311	36.83663	2067.687256	2013-08-21T08:16:15Z	1127
-0.80314	36.83668	2067.995117	2013-08-21T08:16:28Z	1128
-0.8032	36.8368	2065.98584	2013-08-21T08:16:42Z	1129
-0.80325	36.83688	2064.196777	2013-08-21T08:16:56Z	1130
-0.80329	36.83699	2062.408936	2013-08-21T08:17:11Z	1131
-0.80331	36.83706	2060.92749	2013-08-21T08:17:27Z	1132
-0.80333	36.83712	2060.569336	2013-08-21T08:18:41Z	1133
-0.80335	36.83721	2061.096924	2013-08-21T08:18:57Z	1134
-0.80337	36.8373	2064.052734	2013-08-21T08:19:15Z	1135
-0.8034	36.83736	2068.848145	2013-08-21T08:21:00Z	1136
-0.80343	36.83744	2071.473877	2013-08-21T08:21:34Z	1137
-0.80345	36.83752	2073.99585	2013-08-21T08:21:55Z	1138
-0.8035	36.8376	2079.072998	2013-08-21T08:22:34Z	1139
-0.80353	36.83768	2082.881592	2013-08-21T08:23:18Z	1140
-0.80356	36.83776	2085.20874	2013-08-21T08:25:27Z	1141
-0.8036	36.83783	2087.183594	2013-08-21T08:26:57Z	1142
-0.80362	36.8379	2095.575928	2013-08-21T08:28:56Z	1143

-0.80365	36.83798	2096.956543	2013-08-21T08:32:18Z	1144
-0.80367	36.83805	2104.55835	2013-08-21T08:34:18Z	1145
-0.8037	36.83812	2111.830078	2013-08-21T08:36:09Z	1146
-0.80373	36.83819	2115.582275	2013-08-21T08:37:47Z	1147
-0.80376	36.83828	2119.510742	2013-08-21T08:38:34Z	1148
-0.8038	36.83836	2120.87793	2013-08-21T08:38:55Z	1149
-0.80381	36.83843	2124.295898	2013-08-21T08:39:15Z	1150
-0.80385	36.83851	2126.325684	2013-08-21T08:39:37Z	1151
-0.80386	36.8386	2128.566406	2013-08-21T08:39:55Z	1152

KAANJA LINE 800M: Electrode Coordinates of the entire profile

lat	lon	ns1:ele	ns1:time2	ns1:name
-0.76837	36.83433	2122.4	2013-08-23T07:10:43Z	1391
-0.76837	36.83439	2116.6	2013-08-23T07:12:36Z	1392
-0.76839	36.83447	2115.7	2013-08-23T07:13:35Z	1393
-0.76847	36.83454	2119.2	2013-08-23T07:14:40Z	1394
-0.76847	36.83463	2112.9	2013-08-23T07:15:17Z	1395
-0.76851	36.83471	2115.5	2013-08-23T07:16:18Z	1396
-0.76853	36.83479	2116.3	2013-08-23T07:16:56Z	1397
-0.76852	36.83488	2125.2	2013-08-23T07:20:39Z	1398
-0.76855	36.83497	2127.7	2013-08-23T07:22:23Z	1399
-0.76858	36.83504	2129	2013-08-23T07:23:55Z	1400
-0.76862	36.83513	2130.1	2013-08-23T07:24:37Z	1401
-0.76864	36.83521	2131.2	2013-08-23T07:24:58Z	1402
-0.76865	36.8353	2130.2	2013-08-23T07:25:18Z	1403
-0.76867	36.83539	2130	2013-08-23T07:25:45Z	1404
-0.76867	36.83547	2132.5	2013-08-23T07:27:00Z	1405
-0.7687	36.83556	2133.4	2013-08-23T07:28:49Z	1406
-0.76872	36.83565	2133.1	2013-08-23T07:29:23Z	1407
-0.76872	36.83574	2134.6	2013-08-23T07:30:51Z	1408
-0.76873	36.83584	2133.1	2013-08-23T07:32:05Z	1409
-0.76878	36.83588	2128.3	2013-08-23T07:37:59Z	1410
-0.76876	36.83597	2126.1	2013-08-23T07:38:29Z	1411
-0.76879	36.83606	2123.4	2013-08-23T07:38:50Z	1412
-0.76883	36.83616	2123.3	2013-08-23T07:39:46Z	1413
-0.76881	36.83623	2127.3	2013-08-23T07:43:34Z	1414

-0.76879	36.83632	2131	2013-08-23T07:44:43Z	1415
-0.76883	36.83641	2131.8	2013-08-23T07:45:21Z	1416
-0.76883	36.83649	2136.4	2013-08-23T07:46:32Z	1417
-0.76882	36.83659	2135.8	2013-08-23T07:47:32Z	1418
-0.76883	36.83667	2137.1	2013-08-23T07:48:50Z	1419
-0.76884	36.83674	2136.3	2013-08-23T07:51:44Z	1420
-0.76885	36.83684	2141.6	2013-08-23T07:54:17Z	1421
-0.76885	36.8369	2144.6	2013-08-23T07:54:46Z	1422
-0.76887	36.837	2145.5	2013-08-23T07:55:12Z	1423
-0.76888	36.83708	2145.8	2013-08-23T07:55:48Z	1424
-0.76889	36.83716	2147.7	2013-08-23T07:56:35Z	1425
-0.7689	36.83725	2150	2013-08-23T07:57:05Z	1426
-0.76892	36.83734	2148	2013-08-23T07:58:20Z	1427
-0.76893	36.83741	2151.3	2013-08-23T07:59:05Z	1428
-0.76897	36.83751	2149.9	2013-08-23T07:59:34Z	1429
-0.76901	36.8376	2153	2013-08-23T08:00:08Z	1430
-0.76904	36.83768	2154.9	2013-08-23T08:01:04Z	1431
-0.7691	36.83774	2152.6	2013-08-23T08:02:39Z	1432
-0.76914	36.83782	2153.9	2013-08-23T08:02:57Z	1433
-0.7692	36.8379	2154.1	2013-08-23T08:03:25Z	1434
-0.76927	36.83796	2154.4	2013-08-23T08:05:46Z	1435
-0.76932	36.83804	2155.9	2013-08-23T08:06:51Z	1436
-0.76937	36.8381	2155.7	2013-08-23T08:11:50Z	1437
-0.76941	36.83817	2154.5	2013-08-23T08:12:37Z	1438
-0.76948	36.83825	2156.3	2013-08-23T08:13:46Z	1439
-0.76952	36.83831	2160.4	2013-08-23T08:15:46Z	1440
-0.76958	36.83837	2156.8	2013-08-23T08:17:01Z	1441
-0.76962	36.83845	2154	2013-08-23T08:17:22Z	1442
-0.7697	36.8385	2151	2013-08-23T08:17:42Z	1443
-0.76979	36.83856	2152.7	2013-08-23T08:18:08Z	1444
-0.76987	36.83859	2151.4	2013-08-23T08:18:40Z	1445
-0.76993	36.83864	2149.7	2013-08-23T08:19:06Z	1446
-0.77003	36.83868	2153.3	2013-08-23T08:20:42Z	1447
-0.77008	36.83873	2152.7	2013-08-23T08:21:13Z	1448
-0.77014	36.8388	2154.4	2013-08-23T08:21:41Z	1449
-0.77021	36.83888	2158.5	2013-08-23T08:22:05Z	1450

-0.77027	36.83893	2160.1	2013-08-23T08:22:31Z	1451
-0.77032	36.839	2160.2	2013-08-23T08:23:02Z	1452
-0.77038	36.83906	2161.8	2013-08-23T08:23:25Z	1453
-0.77043	36.83913	2162.9	2013-08-23T08:24:56Z	1454
-0.77051	36.83919	2162.3	2013-08-23T08:25:18Z	1455
-0.77057	36.83925	2163.2	2013-08-23T08:25:58Z	1456
-0.77064	36.83929	2165.2	2013-08-23T08:26:23Z	1457
-0.7707	36.83936	2168	2013-08-23T08:26:52Z	1458
-0.7708	36.83941	2170.4	2013-08-23T08:27:33Z	1459
-0.77083	36.83946	2169.6	2013-08-23T08:28:02Z	1460
-0.77093	36.83952	2169.1	2013-08-23T08:28:27Z	1461
-0.77099	36.83954	2168.6	2013-08-23T08:29:19Z	1462
-0.77107	36.8396	2169.7	2013-08-23T08:29:42Z	1463
-0.77117	36.83965	2170	2013-08-23T08:30:12Z	1464
-0.77123	36.83968	2167.2	2013-08-23T08:30:43Z	1465
-0.77131	36.83973	2168.1	2013-08-23T08:31:21Z	1466
-0.7714	36.83976	2169.4	2013-08-23T08:32:23Z	1467
-0.77149	36.83978	2164.8	2013-08-23T08:35:12Z	1468
-0.77157	36.83981	2166.2	2013-08-23T08:35:31Z	1469
-0.77165	36.83984	2166.9	2013-08-23T08:36:05Z	1470
-0.77173	36.83985	2165.8	2013-08-23T08:36:22Z	1471

KAANJA LINE 1: Electrode Coordinates of the entire profile

lat	lon	ns1:ele	ns1:time2	ns1:name
-0.76587	36.8349	2167.668	2013-08-22T11:24:39Z	1324
-0.76596	36.83491	2166.689	2013-08-22T11:27:07Z	1325
-0.76605	36.83495	2169.013	2013-08-22T11:29:51Z	1326
-0.76613	36.83497	2166.091	2013-08-22T11:30:22Z	1327
-0.76617	36.83497	2158.73	2013-08-22T11:31:07Z	1328
-0.76628	36.83498	2157.321	2013-08-22T11:31:25Z	1329
-0.76637	36.83496	2154.65	2013-08-22T11:31:49Z	1330
-0.76646	36.83499	2154.844	2013-08-22T11:32:07Z	1331
-0.76655	36.83498	2152.628	2013-08-22T11:32:24Z	1332
-0.76664	36.83497	2151.014	2013-08-22T11:33:03Z	1333
-0.76671	36.83496	2149.999	2013-08-22T11:33:18Z	1334

-0.76681	36.83497	2147.907	2013-08-22T11:33:32Z	1335
-0.76689	36.83497	2142.151	2013-08-22T11:33:44Z	1336
-0.76699	36.83495	2138.62	2013-08-22T11:34:06Z	1337
-0.76701	36.83506	2137.21	2013-08-22T11:34:40Z	1338
-0.76705	36.83493	2139.242	2013-08-22T11:35:43Z	1339
-0.76717	36.83495	2136.949	2013-08-22T11:36:20Z	1340
-0.76725	36.83497	2133.669	2013-08-22T11:36:31Z	1341
-0.76735	36.83494	2130.579	2013-08-22T11:36:44Z	1342
-0.76743	36.83494	2130.429	2013-08-22T11:36:59Z	1343
-0.76752	36.83493	2126.856	2013-08-22T11:37:15Z	1344
-0.76763	36.83495	2127.274	2013-08-22T11:41:21Z	1345
-0.76769	36.83493	2126.33	2013-08-22T11:43:36Z	1346
-0.7677	36.83493	2125.382	2013-08-22T11:43:43Z	1347
-0.76779	36.83492	2122.776	2013-08-22T11:44:03Z	1348
-0.76787	36.8349	2122.181	2013-08-22T11:44:21Z	1349
-0.76796	36.83491	2118.553	2013-08-22T11:44:43Z	1350
-0.76803	36.83488	2115.598	2013-08-22T11:45:24Z	1351
-0.76812	36.83488	2115.041	2013-08-22T11:45:51Z	1352
-0.76821	36.83489	2112.112	2013-08-22T11:46:09Z	1353
-0.76828	36.83488	2111.464	2013-08-22T11:47:31Z	1354
-0.76838	36.83488	2112.573	2013-08-22T11:48:01Z	1355
-0.76846	36.83487	2116.217	2013-08-22T11:50:44Z	1356
-0.76857	36.83484	2125.346	2013-08-22T11:52:27Z	1357
-0.76863	36.83487	2127.492	2013-08-22T11:53:08Z	1358
-0.7687	36.83488	2127.351	2013-08-22T11:54:13Z	1359
-0.76869	36.83486	2127.557	2013-08-22T11:54:52Z	1360
-0.76884	36.83487	2133.598	2013-08-22T11:57:13Z	1361
-0.76889	36.83487	2134.075	2013-08-22T11:57:27Z	1362
-0.76895	36.83486	2136.096	2013-08-22T11:57:55Z	1363
-0.76904	36.83486	2136.931	2013-08-22T11:58:22Z	1364
-0.76913	36.83485	2139.613	2013-08-22T11:58:56Z	1365
-0.76921	36.83484	2142.446	2013-08-22T11:59:25Z	1366
-0.7693	36.83485	2146.004	2013-08-22T12:00:35Z	1367
-0.76938	36.83483	2146.862	2013-08-22T12:08:53Z	1368
-0.76945	36.83483	2150.379	2013-08-22T12:09:37Z	1369
-0.76954	36.83482	2155.939	2013-08-22T12:10:46Z	1370

-0.76962	36.83481	2160.139	2013-08-22T12:11:39Z	1371
-0.76971	36.83481	2164.913	2013-08-22T12:12:38Z	1372
-0.76978	36.83481	2166.338	2013-08-22T12:13:08Z	1373
-0.76988	36.83481	2168.208	2013-08-22T12:13:26Z	1374
-0.76997	36.83481	2170.169	2013-08-22T12:13:45Z	1375
-0.77006	36.8348	2173.453	2013-08-22T12:14:01Z	1376
-0.77014	36.8348	2174.117	2013-08-22T12:14:18Z	1377
-0.77022	36.8348	2175.866	2013-08-22T12:14:45Z	1378
-0.77031	36.83481	2176.805	2013-08-22T12:15:05Z	1379
-0.7704	36.83481	2175.246	2013-08-22T12:15:40Z	1380
-0.77057	36.83476	2178.73	2013-08-22T12:17:09Z	1381
-0.77067	36.83476	2176.366	2013-08-22T12:18:16Z	1382
-0.77078	36.83474	2174.545	2013-08-22T12:19:09Z	1383
-0.77085	36.83472	2176.057	2013-08-22T12:19:44Z	1384
-0.77093	36.83472	2173.594	2013-08-22T12:20:00Z	1385
-0.77102	36.83471	2172.026	2013-08-22T12:20:17Z	1386
-0.7711	36.83469	2169.489	2013-08-22T12:20:34Z	1387

APPENDIX 4

Temperature Conditions in Muranga (source Wrma sub-station)

Mean Max (°C)	26.8	28	27.4	24.6	24.1	23.1	22.3	22.7	25.3	26.2	23.6	25.1	24.9
Mean min (°C)	**13.1**	**13.4**	**14.4**	**14.3**	**14.2**	**12.6**	**11.5**	**11.8**	**12.2**	**13.7**	**14.4**	**13.8**	**13.3**
Mean range (°C)	13.7	14.6	13	10.3	9.9	10.5	10.8	10.9	13.1	12.5	9.2	11.6	11.6

APPENDEX 5

Borehole Logs (Maragua Site)

CONTRACTOR: _Turn-O_Metal Engrs___ INCLINATION: ___0°_____ PROJECT NAME: ___NORTHERN COLLECTOR TUNNEL____ X-COORD: _ 260129.120___
MACHINE: __BBS 56_____ BOREHOLE SIZE: _____4”_____ BOREHOLE No.: _____BH1A_____ Y-COORD: __ 9923139.118____
DRILLER: ___David Orao_____ DATE DRILLED: ___7/10/12_____ WATER LEVEL: _____2m_____ ELEVATION: __ 2083.549__m
PROFILED BY: ___E. Githogori_____ DATE LOGGED: _26/11/12_____

	SPT “N”	Mat. Recov. %	Core Recov. %	RQD %	Rock Hardness	Grain Size	Rock Fabric	Weathering	Discontinuity Spacing	Joint incl (deg)	Joint Roughness	Joint filling	Filling Thickness (mm)	Depth (m)		Notes: e.g., rock type, color, weathering, structure, hardness
5		95	77	77	VHR	MG	MF	SW	SF	15	RJ	-	-	5		Basalt boulders, greenish-grey
10		0												10		No material recovered
15		0												15		No material recovered
20		0 0 0	94	28	VSR	MG	MF	HW	HF	15	RJ	-	-	20		No material recovered Highly weathered agglomeratic basalts, mottled yellow
25		0 0	96 95	56 75	SR SR	MG MG	MF MF	M W M W	HF HF	23 12	RJ RJ			25		Weathered vesicular agglomeratic basalt No material recovered

ROCK HARDNESS
EHR – Extremely hard rock (UCS>200MPa)
VHR – Very hard rock (UCS 70-200MPa)
HR – Hard rock (UCS 25-70MPa)
SR – Soft rock (UCS 3-10Mpa)
VSR – Very soft rock (UCS 1-3MPa)

GRAIN SIZE
FG – Fine grained
MG – Medium grained
CG – Coarse grained

ROCK FABRIC
MF – Massive
BF – Bedded
FF – Foliated
CF – Cleaved
SF – Schistose
GF – Gneissose
LF - Laminated

WEATHERING
CW – Completely weathered
HW – Highly weathered
MW – Moderately weathered
SW – Slightly weathered
UW – Unweathered

DISCONTINUITY SPACING
VSF – Very slightly fractured (1 per m)
SF – Slightly fractured (1 per m)
MF – Moderately fractured (1-5 per m)
HF – Highly fractured (5-50 per m)

JOINT ROUGHNESS
SLJ – Slickensided
SJ – Smooth
RJ – Rough

APPENDEX 6

Borehole Logs (Irate Site)

CONTRACTOR: _Turn-O-Metal Engrs___ INCLINATION: ___0°_____ PROJECT NAME: ___NORTHERN COLLECTOR TUNNEL____ X-COORD: _ 259676.343m___
MACHINE: __BBS 56_____ BOREHOLE SIZE: _____4”_____ BOREHOLE No.: _____BH4A_____ Y-COORD: __ 9917893.848m____
DRILLER: ___David Orao_____ DATE DRILLED: ___18/09/2012_____ WATER LEVEL: _____8.0m_____ ELEVATION: __ 2131.343m
PROFILED BY: ___E. Githogori_____ DATE LOGGED: _24/11/12_____

epth (m)	SPT “N”	Mat. Recov. %	Core Recov.	RQD %	Rock Hardness	Grain Size	Rock Fabric	Weathering	Discontinuity Spacin	Joint incl (deg)	Joint Roughness	Joint filling	Filling Thickness	Depth (m)		Notes: e.g., rock type, color, weathering, structure, hardness
		80	70	75	HR	CG	MF	MW	HF	20,45	RJ	-	-			Buff-grey weathered agglomeratic basalt
		95	95	80	HR	CG	MF	MW	HF	20	RJ	-	-			Buff-grey weathered agglomeratic basalt
		90	80	75	SR	CG	MF	MW	HF	20,33	RJ	-	-			Buff-grey weathered , fractured agglomeratic basalt
		60	30	90	HR	CG	MF	MW	HF	15	RJ	-	-			Grey to buff-grey fractured agglomeratic basalt
55		75	75	80	HR	CG	MF	MW	HF	10,15	RJ	-	-	55		Grey fractured agglomeratic basalt
		99	99	100	HR	CG	MF	MW	MF	21,60	RJ	-	-			Grey fractured agglomeratic basalt
		99	99	100	HR	CG	MF	MW	MF	21, 34	RJ	-	-			Grey agglomerates
		95	95	85	SR	CG	MF	HW	HF	10,15	RJ	-	-			Buff weathered agglomeratic basalt
		60	20	30	SR	CG	MF	HW	HF	10,15	RJ	-	-			Buff highly fractured agglomeratic basalt
60		90	85	50	SR	CG	MF	HW	HF	10	RJ	-	-	60		Buff weathered agglomeratic basalt
		33	33	95	HR	CG	MF	MW	MF	10	RJ	-	-			Buff weathered agglomeratic basalt
		0														No material recovered
		80	80	85	HR	CG	MF	MW	HF	10	RJ	-	-			Buff weathered agglomeratic basalt
		40	40	55	SR	CG	MF	MW	HF	10	RJ	-	-			Buff weathered agglomeratic basalt
65		0												65		No recovered material
		10	10	0	SR	CG	MF	MW	HF	15	RJ	-	-			Grey agglomeratic basalt
		98	98	100	HR	CG	MF	MW	MF	33	RJ	-	-			Grey agglomeratic basalt
		20	20	0	SR	CG	MF	MW	HF	33	RJ	-	-			Grey agglomeratic basalt
		0														No recovered material
70		0												70		No recovered material
		0														No recovered material
		0														No recovered material
		10	0	0	SR	CG	MF	HW	HF	-	-	-	-			Weathered grey agglomeratic basalt
		95	90	80	HR	CG	MF	MW	MF	10,15	RJ	-	-			Greyish agglomerate, large lapilli
75		25	25	50	HR	CG	MF	MW	HF	43	RJ	-	-	75		Greyish agglomerate, large lapilli

ROCK HARDNESS
EHR – Extremely hard rock (UCS>200MPa)
VHR – Very hard rock (UCS 70-200MPa)
HR – Hard rock (UCS 25-70MPa)
SR – Soft rock (UCS 3-10Mpa)
VSR – Very soft rock (UCS 1-3MPa)

GRAIN SIZE
FG – Fine grained
MG – Medium grained
CG – Coarse grained

ROCK FABRIC
MF – Massive
BF – Bedded
FF – Foliated
CF – Cleaved
SF – Schistose
GF – Gneissose
LF - Laminated

WEATHERING
CW – Completely weathered
HW – Highly weathered
MW – Moderately weathered
SW – Slightly weathered
UW – Unweathered

DISCONTINUITY SPACING
VSF – Very slightly fractured (1 per m)
SF – Slightly fractured (1 per m)
MF – Moderately fractured (1-5 per m)
HF – Highly fractured (5-50 per m)

JOINT ROUGHNESS
SLJ – Slickensided
SJ – Smooth
RJ – Rough

APPENDEX 7

Borehole Logs (Makomboki Site)

CONTRACTOR: _Turn-O-Metal Engrs___ INCLINATION: ___0°_____ PROJECT NAME: ___NORTHERN COLLECTOR TUNNEL____ X-COORD: _ 259215.871m___
MACHINE: __BBS 56_____ BOREHOLE SIZE: _____4”_____ BOREHOLE No.: _____BH6A_____ Y-COORD: 9911538.809m____
DRILLER: ___David Orao_____ DATE DRILLED: ___11/12/2012_____ WATER LEVEL: _____None_____ ELEVATION: __ 2078.159m
PROFILED BY: ___E. Githogori_____ DATE LOGGED: _14/12/12_____

Depth (m)	SPT “N”	Mat. Recov. %	Core Recov. %	RQD %	Rock Hardness	Grain Size	Rock Fabri	Weatherin	Discontinuity	Joint incl (deg)	Joint Roughness	Joint filling	Filling Thick	Depth (m)		Notes: e.g., rock type, color, weathering, structure, hardness
		0														No material recovered
		0														
		0														
		0														
5		0												5		
		0														No material recovered
		0														
		0														
		0														
10		10	0	0	VSR	MG	MF	CW	HF	-	-	-	-	10		Completely weathered agglomeratic basalt
		15	0	0	VSR	MG	MF	CW	HF	-	-	-	-			Completely weathered agglomeratic basalt
15		100	70	70	SR	MG	MF	HW	HF	-	-	-	-	15		Reddish vesicular basalt
		100	100	100	SR	MG	MF	HW	HF	-	-	-	-			Weathered grey basalt
20														20		
		47	45	60	SR	MG	MF	SW	MF	-	-	-	-			Yellowish nearly fresh (slightly weathered) agglomeratic basalt
25		50	44	40	SR	MG	MF	SW	MF	-	-	-	-	25		Yellowish-grey agglomeratic basalt

ROCK HARDNESS
EHR – Extremely hard rock (UCS>200MPa)
VHR – Very hard rock (UCS 70-200MPa)
HR – Hard rock (UCS 25-70MPa)
SR – Soft rock (UCS 3-10Mpa)
VSR – Very soft rock (UCS 1-3MPa)

GRAIN SIZE
FG – Fine grained
MG – Medium grained
CG – Coarse grained

ROCK FABRIC
MF – Massive
BF – Bedded
FF – Foliated
CF – Cleaved
SF – Schistose
GF – Gneissose
LF - Laminated

WEATHERING
CW – Completely weathered
HW – Highly weathered
MW – Moderately weathered
SW – Slightly weathered
UW – Unweathered

DISCONTINUITY SPACING
VSF – Very slightly fractured (1 per m)
SF – Slightly fractured (1 per m)
MF – Moderately fractured (1-5 per m)
HF – Highly fractured (5-50 per m)

JOINT ROUGHNESS
SLJ – Slickensided
SJ – Smooth
RJ – Rough